MECHANISM OF OCHRATOXIN A-STIMULATED LIPID PEROXIDATION

RABEEA FAHMY OMAR, B.Sc. Honours

MECHANISM OF OCHRATOXIN A-STIMULATED LIPID PEROXIDATION

by

© Rabeea Fahmy Omar, B.Sc., Honours

A thesis submitted to the School of Graduate
Studies in partial fulfillment of the
requirements for the degree of
Master of Science
Toxicology

Memorial University of Newfoundland
St. John's, Newfoundland
May, 1990

ISBN 0-315-61836-1

ABSTRACT

Ochratoxin A (OTA) is a mycotoxin and a nephrotoxic carcinogen. The mechanism by which it stimulates lipid peroxidation was investigated in a reconstituted system consisting of phospholipid vesicles (liposomes), flavoprotein NADPH-cytochrome P-450 reductase, EDTA, Fe^{3+} ions, and NADPH. Lipid peroxidation, measured either as malondialdehyde formed or by oxygen uptake, was greatly stimulated in the presence of OTA. Omission of EDTA lowered the extent of lipid peroxidation but did not eliminate it. Fluorometric and spectrophotometric studies demonstrated the formation of a 1:1 Fe^{3+}-OTA complex. The rate of reduction of Fe^{3+} to Fe^{2+} was greatly enhanced in the presence of OTA and there was a further increase in the rate when EDTA was also included. Cytochrome P-450 (an enzyme normally present in microsomes) was found to effectively replace EDTA in the reconstituted system and its role in microsomal lipid peroxidation was also implicated suggesting that this hemoprotein could play an important role in OTA-stimulated lipid peroxidation in vivo.

ESR studies showed that the Fe^{3+}-OTA complex produced hydroxyl radicals in the presence of NADPH and NADPH-cytochrome P-450 reductase. The lack of any diminution of lipid peroxidation by catalase and several hydroxyl radical scavengers suggests that hydroxyl radical production by the Fe^{3+}-OTA complex may not be a significant factor in the lipid

peroxidation *in vitro*, but these results do not preclude hydroxyl radicals produced by the Fe^{3+}-OTA complex from playing an important role in the toxicity of OTA.

Structure-activity relationship studies indicated that the presence of a free carboxyl group and chlorine atom as well as the L-Phe moiety on OTA contributed significantly to the stimulatory effect on lipid peroxidation. Earlier studies had shown an absolute requirement for a free phenolic hydroxyl group on OTA.

My results indicate that OTA stimulates lipid peroxidation by complexing with Fe^{3+} and facilitating its reduction. Subsequent to oxygen binding, an iron-oxygen complex of undetermined nature initiates lipid peroxidation. The extent of OTA-dependent lipid peroxidation *in vivo* and its role in the toxicity of OTA remain to be determined.

To

My Parents

ACKNOWLEDGEMENTS

I would like to thank Dr. A.D. Rahimtula for his supervision and his valuable guidance throughout this work. I thank Dr. C. Sharpe for his kind support. I am grateful to Dr. B. Hasinoff for devoting a considerable amount of time and effort towards the ESR studies. I also thank the members of my supervisory committee, Dr. E. Barnsley and Dr. F. Shahidi for their constructive suggestions. A special thanks to Ms. Marie Codner for technical assistance and helping to make bench work a more enjoyable experience. I thank Dr. Phil Davis for demonstrating the operation of GC and giving me access to it. I am also grateful to the members of Biochemistry Department and its head Dr. K. Keough for their generosity. I am indebted to the Kidney Foundation of Canada for generous financial support.

I wish to extend special thanks to my parents for their kind blessings.

TABLE OF CONTENTS

LIST OF TABLES

LIST OF FIGURES

LIST OF ABBREVIATIONS

BPS	bathophenanthrolinedisulfonic acid
BHA	butylated hydroxyanisole
BHT	butylated hydroxytoluene
CHAPS	(3-[(cholamidopropyl)-dimethylammonio]-1-propanesulfonate)
DMPO	5,5-dimethyl-1-pyrroline-1-oxide
DTT	dithiothreitol
ESR	electron spin resonance
Fp	the flavoprotein NADPH cytochrome P-450 reductase
FMN	flavin mononucleotide
Glu-Oα	glutamic acid ochratoxin α
MDA	malondialdehyde
OTA	ochratoxin A
Oα	ochratoxin α
OB	ochratoxin B
OC	ochratoxin C
Pro-Oα	proline ochratoxin α
PB	sodium phenobarbital
Ser-Oα	serine ochratoxin α
SOD	superoxide dismutase

TBA	2-thiobarbituric acid
TCA	trichloroacetic acid.

CHAPTER 1

INTRODUCTION

1.1 OCHRATOXIN A

1.1.1 Occurrence and human exposure

Ochratoxin A (OTA) is a mycotoxin produced by Aspergillus ochraceus, Penicillium viridicatum and other fungal species. It was discovered in 1965 by De Scott (1) as the toxic metabolite in a culture medium of Aspergillus ochraceus Wilh, and chemically characterized by Van der Merwe et al. (2) and Steyn and Holzapfel (3,4). Its chemical structure consists of a 5-chloro-8-hydroxy-3,4-dihydro-3-methyl isocoumarin moiety linked by an amide bond to L-β-phenylalanine (Fig. 1). The toxigenic molds known to produce the tox · (5) are the following species:

Aspergillus ochraceus	Penicillium viridicatum
A. ostianus	P. cyclopium
A. melleus	P. commune
A. petrakii	P. palitans
A. sclerotiorum	P. purpurescens
A. sulphureus	P. variabile

The occurrence of OTA in food and feed is widespread.

Figure 1. Chemical structure of ochratoxin A.

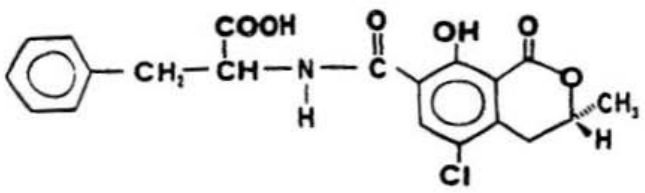
COOH
O
OH
O
CH2
CH
N
C
O
CH3
H
H
Cl

It is present as a contaminant in plant products, especially cereals, beans and peanuts (5). OTA is also found in meats, dried fish and nuts (6) as well as in the kidney, liver, and blood of slaughtered pigs (7). In a recent analysis of 1200 blood samples obtained from pigs slaughtered in Western Canada, Marquardt et al. (8) found that 76% had detectable levels of OTA, 11.3% had OTA levels > 10 ng/ml with the highest being 229 ng/ml. Scott et al. (9) detected OTA in concentrations of up to 27 μg/ml in 18 out of 29 samples of heated grain from Saskatchewan farms (Canada), whereas the highest observed concentration of residues in animal products (bacon from pigs) is 0.067 μg/ml (10). The potential for human exposure exists because of the direct consumption of contaminated cereals and the consumption of animals that retain OTA in their tissues after being fed contaminated feed (Fig. 2).

Ochratoxin A is suspected of being the main etiological agent responsible for Balkan endemic nephropathy (BEN) and associated urinary tract tumors, diseases which affect multiple members of families residing in particular areas of Bulgaria, Romania and Yugoslavia (11). BEN and porcine nephropathy (a disease with morphological and clinical symptoms similar to those of BEN) are found in areas where home-grown cereals are contaminated with OTA (12,13). Galtier et al. (14) have shown that OTA persists longer in pigs than in other species, which suggests that problems of

Figure 2. Factors influencing the occurrence of mycotoxins in human food and animal feed (175).

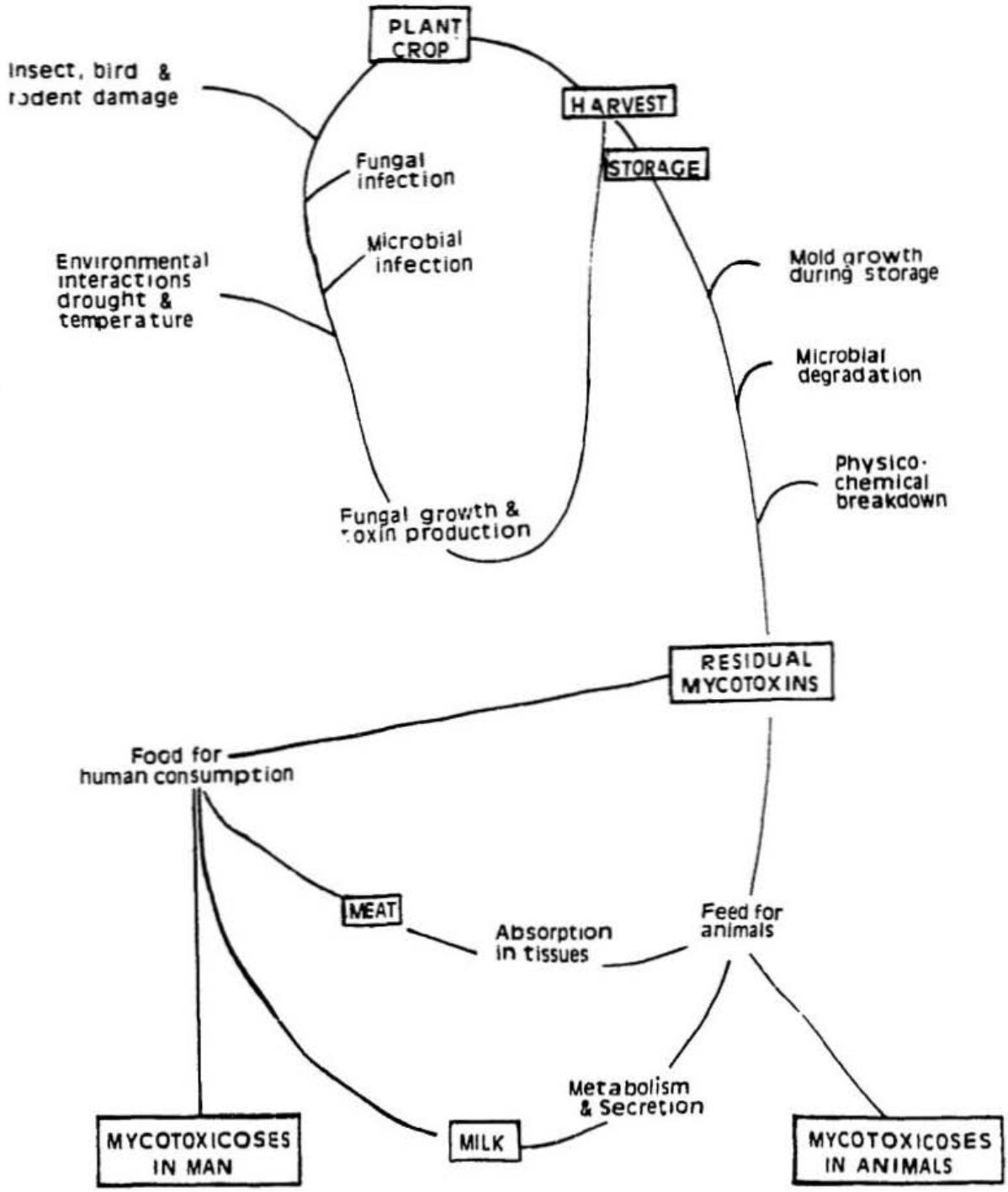
PLANT CROP
HARVEST
STORAGE
Insect, bird & rodent damage
Fungal infection
Microbial infection
Environmental interactions drought & temperature
Fungal growth & toxin production
Mold growth during storage
Microbial degradation
Physico-chemical breakdown
RESIDUAL MYCOTOXINS
Food for human consumption
MEAT
Absorption in tissues
Feed for animals
Metabolism & Secretion
MILK
MYCOTOXICOSES IN MAN
MYCOTOXICOSES IN ANIMALS

OTA residues in the human food chain may be greater when pork rather than other meats is consumed.

1.1.2 Toxicity

Ochratoxin-A is toxic to many test animals including chickens, dogs, ducklings, mice, rats, hens, sheep, swine and rainbow trout (15,16). The toxic effect of OTA is displayed initially on the nephron, and the proximal tubule is the primary target site (6). Later, the glomeruli as well as the interstitia may be involved. The changes of renal function in OTA-exposed rats and pigs are characterized by an increase in polyuria, glucosuria, proteinuria and blood urea nitrogen, and a decrease in urine osmolarity, glomerular filtration rate (GFR) and inulin clearance (17). The changes in renal structure in pigs are characterized by degeneration of the proximal tubules, leading to tubular atropy accompanied by interstitial fibrosis. Later, hyalinization of the glomeruli may occur (26,27). In rats oral doses of OTA led to reduced plasma fibrinogen, factors II, VII and X and thrombocyte and megakaryocyte counts (28). In chickens lymphocytopenia developed at every dose level tested (29), and concentrations of serum immunoglobulins (IgA, IgG and IgM) were reduced to 57-66% of normal values in the toxin-exposed groups (30). In mice, myelotoxicity was observed resulting

in bone marrow hypocellularity, decreased marrow pluripotent stem cells, and granulocyte-macrophage progenitors (31). The treatment of pregnant mice and rats i.p. with OTA resulted in increased prenatal mortality, decreased fetal weight, and various fetal malformations (32). In chickens fed diets containing 0, 1, 5 and 10 mg OTA/kg over a four-week period, the rate of growth and relative weight of the bursa of Fabricius were depressed, and the relative weights of the liver, kidney, pancreas and various sections of the gastrointestinal tract were increased, but there was no effect on the heart and spleen (33). The transport of p-aminohippurate (PAH) and tetraethyl ammonium (TEA) by renal slices was also found to be inhibited by OTA (18).

Kane et al. (19) observed a particularly good correlation between the increase in urinary excretion and a decrease in renal activities of γ-glutamyl transferase (γ-GT), alkaline phosphatase (ALP) and leucine aminopeptidase (LAP) within a week of the oral administration of 145 μg OTA/kg body weight/day for 12 weeks. An inhibition of gluconeogenesis was also observed in kidney slices from rats which had been fed with 2 mg/kg body weight for 2 days (20), and renal phosphoenol pyruvate carboxykinase (PEPCK) was selectively lowered by 50%. Suzuki et al. (21) observed a 60% decrease in hepatic glycogen levels and a concomitant increase in serum glucose and blood and liver lactate levels in the rat after daily administration of OTA (5 mg/kg) for 3

days. Administration of OTA to mice inhibited protein synthesis (22). The degree of inhibition of protein synthesis 5 hr after administration of 1 mg OTA/kg was 26% in liver, 68% in kidney and 75% in spleen. Phenylalanine (100 mg/kg) injected together with OTA (10 mg/kg) prevented the inhibition of protein synthesis in all of these organs. OTA is thought to inhibit protein synthesis through competition with phenylalanine in the reaction catalyzed by phenylalanyl t-RNA synthetase.

In vitro studies showed that OTA inhibited liver mitochondrial respiration primarily by altering the membrane permeability (23,24). Recently, Rahimtula and associates (25) reported that OTA disrupted microsomal calcium homeostasis by impairment of the endoplasmic reticulum membrane, probably via enhanced lipid peroxidation.

The LD50 values of OTA in various species are listed below (material safety data sheet (MSDS), Sigma Chemical Co., 1989):

Species	Route of Administration	LD50
Rat	Oral	20.0 mg/Kg
Rat	i.p.	12.6 mg/Kg
Rat	i.v.	12.7 mg/Kg
Mouse	Oral	46.0 mg/Kg
Mouse	i.p.	22.0 mg/Kg
Mouse	i.v.	25.7 mg/Kg
Dog	Oral	0.2 mg/Kg
Pig	Oral	1.0 mg/Kg
Chicken	Oral	3.3 mg/Kg

1.1.3 Carcinogenicity and mutagenicity

Bendele et al. (34) found that 40 ppm OTA fed to (C57BL/6J x C3H)F1 mice for up to 24 months induced renal neoplasms in males only. Female mice had a slight increase in hepatocellular neoplasms. Earlier, Kanesawa and Suzuki (35) had observed an increased incidence of both hepatic and renal tumors in male DDY mice fed 40 ppm OTA. In a recent study conducted by the U.S. National Toxicology Program (NTP) (186), OTA in corn oil was administered by gavage to group of male and female F344/N rats for up to 2 years. There was clear evidence of an increased incidence of uncommon tubular cell adenomas and carcinomas of the kidney in both sexes. In addition, female rats had an increased incidence and multiplicity of fibroadenomas of the mammary gland. Other non-neoplastic renal changes observed included tubular cell hyperplasia, tubular cell proliferation, cytoplasmic alterations, karyomegaly, and degeneration of the renal tubular epithelium.

OTA did not produce genetic or related effects in a variety of short term tests (36,37). From the same NTP study, OTA was not mutagenic in four strains of Salmonella typhimurium (TA 97, TA 98, TA 100, or TA 1535) when tested both with and without exogenous metabolic activation. Also, OTA did not significantly increase the number of chromosomal aberrations in cultured chinese hamster ovary cells. OTA

induced sister chromatid exchanges in the presence, but not in the absence, of metabolic activation (186). OTA has also been shown to cause single-strand breaks in DNA isolated from livers and kidneys of rats that had been fed the equivalent of 4 ppm OTA for 12 weeks (38).

1.1.4 Absorption and metabolism

The primary site of OTA absorption is thought to be in the small intestine. When OTA was injected into the lumen of the stomach, small intestine, caecum, or colon of male Wistar rats, the highest absorption was in the proximal jejunum (39). In mice, when OTA was given orally, the site of highest absorption was the duodenum (40). In the latter study, immunohistochemical staining revealed that the highest concentration of OTA was in the intestine, with decreasing levels in the kidney and liver (40).

Many environmental carcinogens and toxins require oxidative metabolism, most often by the cytochrome P-450-dependent monoxygenase system, in order to exert their toxic or carcinogenic effects (41). OTA is known to be metabolized by rat liver microsomes to (4S)-4-hydroxy-OTA and (4R)-4-hydroxy-OTA (42), while with rabbit liver microsomes an additional metabolite, 10-hydroxy-OTA, is formed (43). In vivo, OTA metabolites detected in the urine of rats include ochratoxin α and 4-hydroxy-OTA (44). In

rats intubated with labelled OTA (^{3}H in Phe), three other metabolites have been detected in liver extracts, but these have not been identified (38).

1.2 LIPID PEROXIDATION

1.2.1 Definition

In eukaryotes, membrane fluidity is maintained by the incorporation of polyunsaturated fatty acid (PUFA) chains into membrane lipids. Most of these PUFA chains occur on the 2-C position of the glycerol moiety of phospholipids, particularly phosphatidyl choline and phosphatidyl ethanolamine, although some also occur in neutral lipids. In the membranes of rat liver microsomes, the most abundant PUFAs (expressed as percentage of total fatty acids) are shown in Fig. 3. The presence of an adjacent double bond weakens the carbon-allylic hydrogen bonds. These allylic hydrogens, especially those on the carbon atom between double bonds, can be abstracted by reactive species containing one or more unpaired electrons (free radicals). The lipid radical thus formed will then react with molecular oxygen, and the ensuing chain reaction results in the breakdown of the PUFA. This reaction sequence is known as **lipid peroxidation**. Lipid peroxidation propagates by collision of a radical molecule with a non-radical molecule and

Figure 3. The major polyunsaturated fatty acids in rat liver microsomes (176).

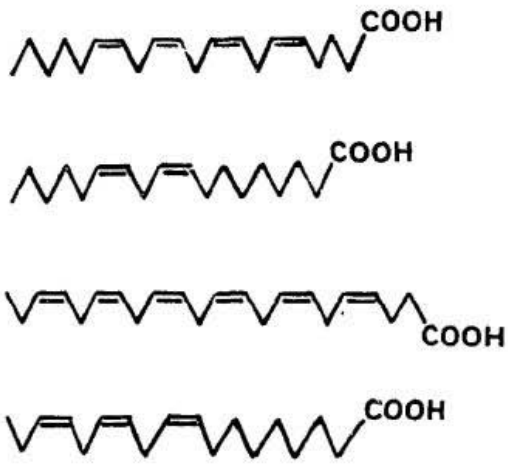

17% arachidonic acid

10% linoleic acid

5% docosahexaenoic acid

5% linolenic acid

terminates when two radicals collide each other. The reactions of lipid peroxidation may be classified into three main steps: 1) initiation, 2) propagation and 3) termination (Fig. 4).

1.2.2 Measurement

The products of lipid peroxidation include lipid epoxides, hydroperoxides, epoxy alcohols, and the short-chain compounds such as malondialdehyde (MDA), ethane, pentane, and 4-hydroxy alkenals (45-48). Lipid peroxidation has been measured by the detection of conjugated dienes formed during the early phase of the peroxidation reaction sequence (49-51), and less commonly by measurement of lipid hydroperoxides (52,53). The most common procedures are based on the measurement of the products of lipid hydroperoxide breakdown such as MDA (Fig. 5). This is the most widely used method because of its simplicity and sensitivity. This substance (MDA) has been commonly detected by the thiobarbituric acid (TBA) reaction (54-57). In addition, lipid peroxidation has been assayed recently by the evolution of short-chain alkanes (ethane and pentane) both <u>in vivo</u> and <u>in vitro</u> (58-61).

In my studies, different parameters were measured as indices of lipid peroxidation to study the role of OTA in stimulating lipid peroxidation. The classic TBA reaction to

Figure 4. Simplified reactions of the process of lipid peroxidation (177).

Lipid peroxidation

(1) $LH + R^{\bullet} \longrightarrow L^{\bullet} + RH$ — Initiation

(2) $L^{\bullet} + O_2 \longrightarrow LOO^{\bullet}$
$LH + LOO^{\bullet} \longrightarrow LOOH + L^{\bullet}$ — Propagation

(3) $L^{\bullet} + L^{\bullet} \longrightarrow LL$
$LOO^{\bullet} + LOO^{\bullet} \longrightarrow LOOL + O_2$
$LOO^{\bullet} + L^{\bullet} \longrightarrow LOOL$ — Termination

$R^{\bullet}$ = a free radical

LH = lipid undergoing lipid peroxidation

$L^{\bullet}$ = lipid radical

$LOO^{\bullet}$ = lipid peroxy radical

Figure 5. Scheme demonstrating the formation of malondialdehyde (MDA) during lipid peroxidation induced by ferrous-oxygen complexes or by hydroxyl radicals (134).

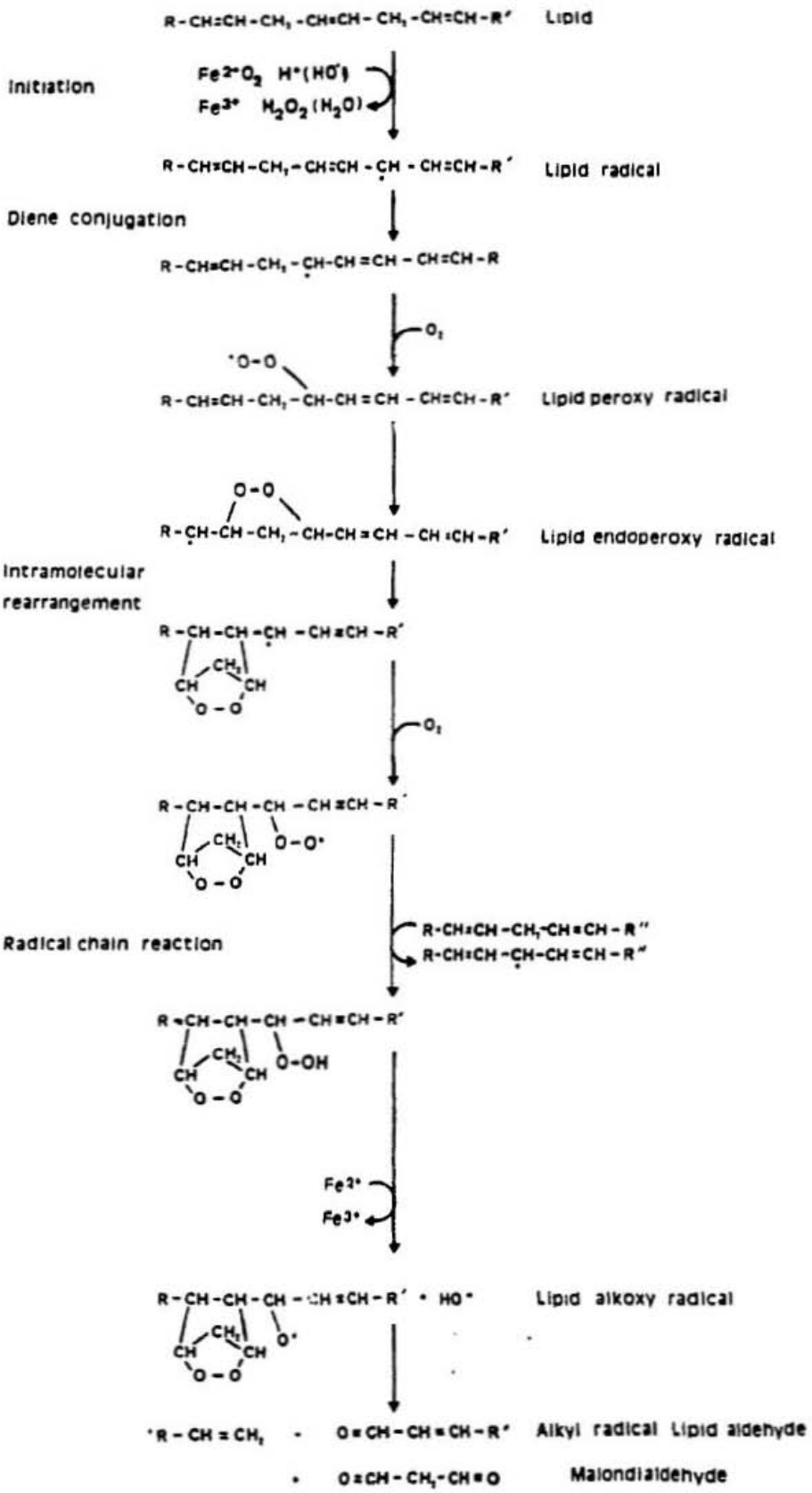
Lipid
Initiation
Lipid radical
Diene conjugation
Lipid peroxy radical
Lipid endoperoxy radical
Intramolecular rearrangement
Radical chain reaction
Lipid alkoxy radical
Alkyl radical
Lipid aldehyde
Malondialdehyde

Figure 6. The complex formed between thiobarbituric acid (TBA) and malondialdehyde (MDA). The complex can be measured at 535 nm as an index of lipid peroxidation.

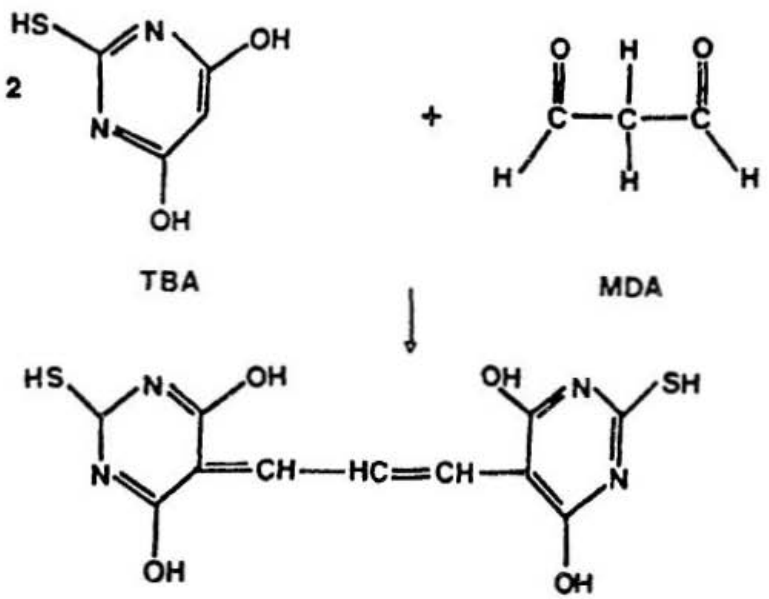

TBA—MDA Complex

measure MDA as an MDA-TBA adduct (Fig. 6) was the first index to be measured (as described in the Methods section). It has been reported that MDA itself is reactive and forms Schiff bases with amino groups of various biomolecules, e.g. amino acids and proteins, nucleic acids and amino sugars (62-65), and such reactions would decrease the MDA available for reaction with TBA. On the other hand, the acidic conditions used during the TBA reaction may hydrolyse the Schiff bases and maximize MDA measurement. Recently, Pompella et al. (66) investigated whether some of the commonly used methods to detect lipid peroxidation in vivo correlate with each other. They tested and compared the following methods: i) measurement of MDA formation; ii) detection of diene conjugation; iii) measurement of the loss of PUFA; and iv) determination of carbonyl functions formed in acyl residues of membrane phospholipds. Correlations among the values they obtained with these methods showed high statistical significance, indicating that the procedures measure lipid peroxidation in vivo with comparable reliability. Analogously, the four methods also appeared to correlate when applied to in vitro microsomal lipid peroxidation, reaffirming confidence in these procedures.

Oxygen uptake was the second method to be used as a measure of lipid peroxidation (described in the methods section). It is also an acceptable method but it is not as

widely used as the MDA-TBA reaction. It is known that lipid peroxidation is accompanied by uptake of oxygen in the formation of peroxy radicals and in subsequent decomposition reactions. It is worth mentioning that (from my results) the amount of oxygen uptake is about 60 fold the amount of MDA formed over the same period of time. That is because oxygen uptake represents a measure for the whole lipid peroxidation process plus a direct reduction of oxygen to superoxide anions and H_2O_2, while MDA is only one of several components resulting from the breakdown of the peroxidized lipid. In addition, measurement of MDA formation cannot account for peroxidized lipids that have not yet been broken down, whereas oxygen uptake does include this amount.

It is generally accepted that iron plays an important role in lipid peroxidation. Ferrous iron is able to produce hydroxyl radicals via the Fenton reaction, and it can also participate in the initiation of lipid peroxidation by interacting with unsaturated lipid (LH) undergoing lipid peroxidation to form lipid radical (L·). The rate of reduction of ferric to ferrous iron is a useful measurement (described in the Methods section) which was also used to confirm the role of OTA in facilitating ferric reduction subsequent to forming a complex with it.

1.2.3 Enzymatic lipid peroxidation systems

Enzymatically induced microsomal lipid peroxidation was first described by Hochstein and Ernster in 1963, who demonstrated the requirement for nicotinamide adenine dinucleotide phosphate, reduced form (NADPH) and adenosine 5'-diphosphate (ADP) and the enzymatic nature of the process (67). In a subsequent study they showed the necessity for iron (68) which had been a contaminant of their original ADP solutions. Later, Pederson and Aust (69) characterized the enzymatic nature of lipid peroxidation further by demonstrating that NADPH-cytochrome P-450 reductase (Fp) was the enzyme linking NADPH oxidation to the ADP-Fe^{3+}-dependent peroxidation of microsomal membranes (69). They also developed a reconstituted lipid peroxidation system consisting of phospholipid vesicles (liposomes), purified Fp, ferric chelates and NADPH. In their reconstituted system, a second ferric chelate, EDTA-Fe^{3+} (in addition to ADP-Fe^{3+}) was also required (69). Therefore, Aust et al. (69) suggested that there may be a microsomal component(s) that directly reduces ADP-Fe^{3+} (for which EDTA-Fe^{3+} can substitute) in the reconstituted lipid peroxidation system. In support of this, Hochstein and Ernster (70) suggested that cytochrome P-450 may be involved. Later, Aust et al. (71) demonstrated that when cytochrome P-450 was incorporated into phospholipid vesicles, EDTA-Fe^{3+} was not

required.

1.2.4 Physiological sources of iron

Because of the important role of iron in promoting lipid peroxidation, it is worth giving a brief description of its physiological sources. Iron is transported in the plasma and extracellular fluids by transferrin, a glycoprotein with two Fe^{3+} binding sites per molecule. Intracellularly iron is stored in ferritin (72). This is the major physiological store of iron. It is a large protein of 440000 molecular weight which can store up to 4500 mol of iron per mol of protein, although it is usually not saturated (73). In aerated aqueous solutions iron exists predominantly as Fe^{3+}. At physiological pH values, the chemistry of ferric ion is mainly that of hydrolysis to yield insoluble ferric hydroxides and oxyhydroxides (74). For this reason, low molecular weight chelators of iron are required to exchange iron in both directions between transferrin and ferritin and between ferritin and intracellular iron-containing compounds (75). Heme proteins, mostly hemoglobin and myoglobin, can also serve as other sources of intracellular iron (76).

1.2.5 Initiation

Lipid peroxidation is sometimes a major mechanism of cellular injury in organisms subjected to oxidative stress (reviewed 77-79). Surprisingly little is known, however, about the chemistry of initiation of peroxidation in membrane systems such as liposomes or microsomes. The nature of the free radical species ultimately responsible for the initiation of iron-dependent lipid peroxidation has been the subject of considerable debate. The principal candidates suggested for this role are the hydroxyl radical ($OH^{\cdot}$) and the ferrous dioxygen complex (perferryl ion). The hydroxyl radical is an extremely reactive species, reacting very rapidly with most organic molecules (80). Hydroxyl radicals can be formed via the Fenton reaction as follows:

$$Fe^{2+} + H_2O_2 \dashrightarrow Fe^{3+} + OH^- + OH^{\cdot}$$

The superoxide radical ($O_2^{\cdot -}$) is produced at a number of intracellular sites (81-83) and H_2O_2 can then be formed readily from the nonenzymic or superoxide dismutase-catalyzed dismutation of $O_2^{\cdot -}$ (83). Subsequently, chelated iron can yield $OH^{\cdot}$ in the Fenton reaction as above. An alternative hypothesis for the initiating species is that ferrous ion, in undergoing autoxidation to ferric ion, passes through an intermediate ($Fe^{2+}\text{---}O_2 \dashleftarrow\dashrightarrow Fe^{3+}\text{---}O_2^{\cdot -}$)

state (ferrous dioxygen complex). Upon the discovery of ADP-Fe^{3+}-initiated microsomal lipid peroxidation, Hochstein and Ernster (68) postulated the involvement of an ADP-Fe^{2+}---O_2 complex. Furthermore, Aust's group has pursued the idea that an ADP-ferrous dioxygen complex initiates lipid peroxidation (84,85). The concept of a ferrous dioxygen complex has been criticized on the grounds that the complex is insufficiently reactive towards PUFA (86). The highly-reactive hydroxyl radical can often be detected in microsomal or liposomal lipid peroxidation systems (87-90). The hydroxyl radical is known to be capable of initiating lipid peroxidation by abstracting a hydrogen atom from fatty acid side chains (91,92). H_2O_2-degrading enzymes or scavengers of $OH^{\cdot}$, however, rarely inhibit iron-dependent peroxidation in microsomal or liposomal systems (87-90). It has been proposed that the ferryl ion (see below) is the true Fenton reagent rather than $OH^{\cdot}$, and this would not be available for scavenging by conventional $OH^{\cdot}$ scavengers (95,96).

$$Fe^{2+} + H_2O_2 \xrightarrow{\quad} Fe^{3+}\text{-}OH \xrightarrow{\quad} [Fe^{3+}\text{-}O^{-} \longleftrightarrow Fe^{2+}\text{-}O] \dashrightarrow Fe^{2+} + OH^{\cdot}$$

OH^{-} H^{+} ferryl ion

Superoxide radicals may play a minor role in initiating lipid peroxidation under conditions in which they act to reduce Fe^{3+} to Fe^{2+} (97,98). Recently, Aust et al. (99-100)

have proposed that a specific Fe^{2+}-O_2-Fe^{3+} complex, or at least a 1:1 ratio of Fe^{2+} to Fe^{3+}, acts as an initiator of peroxidation in liposomal and microsomal systems, but some doubts have been raised about this complex as a specific initiator of peroxidation. Attempts to isolate such a complex have failed (99,101). The Fe^{2+}/Fe^{3+} ratios required for maximal stimulation of peroxidation have been reported to vary from 1:1 to 1:7 in different experiments (102), perhaps suggesting that a specific stoichiometric complex is not required. It must be concluded that the identity of the initiating species of lipid peroxidation produced by ferrous iron is still an open question.

1.2.6 Cellular toxicity

The peroxidative breakdown of PUFA has been implicated in the pathogenesis of many types of injury and especially in the hepatic damage induced by several toxic substances. Among these toxic substances are the haloalkanes, carbon tetrachloride (103-105), trichlorobromomethane (103,106), chloroform (107), 1,2-dibromoethane (108) and halothane (109). In addition, paracetamol (110), bromobenzene (111), iron (112), bipyridyl compounds (113), allyl alcohol (114) and in some instances, ethanol (79,115,116) have been shown to stimulate lipid peroxidation. The peroxidation of PUFA within biological membranes results in a complex series of

biochemical and biophysical events which lead to inactivation of enzymatic functions in several subcellular organelles (103,104,117-119). These alterations include changes in the physical properties of the lipid bilayer, reactions between acylperoxyl radicals and membrane proteins and formation of reactive products originating from the degradation of peroxidized fatty acids (117-119).

The stimulation of lipid peroxidation in either artificial membranes of liposomes or in subcellular organelles has been shown to increase membrane rigidity (120,121). Such a loss of fluidity does not seem to be dependent upon an increase in the ratio between cholesterol and phospholipids (120), but is rather an effect of the formation of cross-linking between acyl chains (122) and of the depletion of long chain PUFA (120). In addition to the changes in fluidity, lipid peroxidation causes an increase in the ionic permeability and affects the surface potentials of the membranes (118). In the liver, the membranes of the mitochondria and endoplasmic reticulum contain unsaturated fatty acids in high proportion and therefore are vulnerable to peroxidative attack. At the same time they contain enzymes of the electron transport systems which make them capable of producing free radical species (103,104,118,119). The consequences for the cell of lipid peroxidation reactions and products are many. Microsomal membranes undergoing peroxidation <u>in vitro</u> show fragmentation and

turbidity changes, destruction of cytochrome P-450 (123), and loss of latency and activity of glucose-6-phosphate and UDP-glucuronyl transferase (123-125). The plasma membrane Ca^{2+}-ATPase is inactivated because of oxidation of essential sulfhydryl groups in the enzyme (126), resulting in defective control of cytosolic calcium. Ribosomes become detached from the endoplasmic reticulum during lipid peroxidation (127). In mitochondria, peroxidation causes membrane swelling, deterioration of electron transport, and organelle lysis (128,129). Lipid peroxidation of lysosomes causes lysis and enzyme release (130,131), and the erythrocyte plasma membrane responds in a similar manner (132).

Cephaloridine, a beta-lactam antibiotic of the cephalosporin type, causes renal injury in humans and in laboratory animals. Like OTA, its main toxic effect is considered to be on the proximal tubules (178,179). Several biochemical mechanisms have been proposed to explain the nephrotoxic effects of cephaloridine (182,180,181). The most recent hypothesis suggests an involvement of lipid peroxidation initiated by reactive oxygen species (181,183). Recent studies showed that the formation of cephaloridine-induced reactive oxygen species and peroxidation of renal cortical membrane lipids was inhibited by radical scavengers and antioxidants (182,184).

1.3 Objective of the thesis

Lipid peroxidation has been proposed as the mechanism of toxicity of a wide and ever-increasing range of compounds (134,135). Recently, Rahimtula et al. (133) reported that the addition of OTA to rat liver or kidney microsomes, or the administration of OTA to rats enhanced lipid peroxidation.

The major objective of my studies was to investigate the mechanism by which ochratoxin A stimulated lipid peroxidation. For this purpose, I used a reconstituted system consisting of phospholipid vesicles (liposomes), the flavoprotein NADPH-cytochrome P-450 reductase, OTA, EDTA, Fe^{3+} and NADPH.

The role of purified cytochrome P-450 as a possible substitute *in vivo* for EDTA was also examined in the reconstituted system.

Using ESR I attempted to characterize the free radicals formed in the reconstituted system in the presence or OTA.

Finally, I examined several OTA analogues in a study of structure-activity relationships to characterize the components effectively contributing to the stimulatory effect of OTA on lipid peroxidation.

C H A P T E R 2

BIOSYNTHESIS OF OCHRATOXIN A

OTA is available commercially from a few chemical companies, but it is very expensive (100 mg cost about $ 2,000). I therefore considered the production of the toxin in our laboratory. The OTA produced was characterized by thin layer chromatography (TLC), high pressure liquid chromatography (HPLC), UV absorption and fluorescence spectroscopy, and was found to be identical to that purchased from Sigma Chemical Co. The early part of my research (lipid peroxidation) was done with OTA purchased from Sigma Chemical Co. In most of the later work I used OTA produced in our laboratory.

2.1 Organism

Aspergillus ochraceus NRRL-3174, obtained from Dr. S.W. Peterson, Northern Regional Research Center, U.S. Dept. of Agriculture, Peoria, Illinois, was used for OTA production. Cultures were maintained at 5°C on modified Czapek agar* (see section 2.2) with 20% sucrose supplemented with 0.7% yeast extract.

2.2 Culture

Flasks (250 ml) containing 100 ml of modified Czapek liquid medium** with 4% sucrose and 2% yeast extract, were stoppered with cotton plugs and autoclaved at 121°C for 15 min (136). Media were inoculated with a spore suspension of A. ochraceus and incubated at 25°C for 12 days without agitation. The initial pH of the media was about 6.7, and the final pH was about 6.4.

*Modified Czapek agar medium (for fungus preservation)

Sucrose	200	gm
$NaNO_3$	3	gm
K_2HPO_4	1	gm
$MgSO_4.7H_2O$	500	mg
KCl	500	mg
$FeSO_4.7H_2O$	10	mg
Yeast extract (Difco)	7	gm
Agar	15	gm
Dist.H_2O	1	L

**Modified Czapek liquid medium (for OTA production)

Sucrose	40	gm
$NaNO_3$	3	gm
K_2HPO_4	1	gm
$MgSO_4.7H_2O$	500	mg
KCl	500	mg
$FeSO_4.7H_2O$	10	mg
Yeast extract (Difco)	20	gm
Dist.H_2O	1	L

Since OTA contains a chlorine atom, the effect of different Cl^- concentrations in the culture medium on OTA

production was investigated. Chloride concentrations of 0, 25, 100, 250 and 500 mg/L were tried, and it was found that the maximum toxin yield was achieved at 100 mg/L Cl^-. Hence, this concentration was used in the regular medium for OTA production instead of 500 mg/L that was used before. An added advantage of lower Cl^- concentration is that it can be used to produce ^{36}Cl-labelled OTA of higher specific activity. Others have also recommended that a lower Cl^- concentration be used (137).

Because OTA contains a phenylalanine (Phe) moiety, the effect of adding exogenous Phe to the regular medium was investigated. It was found that the yield of OTA increased by about 25% when Phe (10 mM) was included in the culture medium.

Cultures were incubated for different periods of time (from 3 days up to 30 days prior to harvesting). The highest toxin production was found to be between 10 and 12 days of incubation, and so this time period was used for all further experiments. It was also of interest to determine the toxin concentration in the fungal mycelium and in the culture filtrate. Twelve point seven percent of the total toxin yield was found in the culture filtrate which is in good agreement with values in the literature (10-12%). The remaining toxin (87.3%) was in the mycelium.

2.3 Ochratoxin A extraction

After measuring the final pH, the culture medium was acidified to pH 2.0 with conc. HCl and then thoroughly homogenized using a Polytron homogenizer (Brinkman Instruments) for 3-5 min at 30,000 rpm to break all fungal hyphae. To 1 L of homogenate about 10 ml of saturated NaCl solution was added, and the mixture was extracted with 1L of chloroform. After vigorous shaking, the mixture was centrifuged at 2000 rpm for 5 min. Three separate layers were obtained : an upper aqueous layer, a lower chloroform layer and a fluffy layer in between containing cell debris. Both the chloroform layer and the aqueous layer were chromatographed by TLC (K5F silica gel, layer thickness 250 μ, Whatman) and chromatograms were examined under UV. OTA purchased from Sigma Chemical Co. was used as a standard. The solvent systems used were: benzene, methanol, acetic acid (95:5:5 v/v) (solvent A); benzene, acetic acid (8:1 v/v) (solvent B); benzene, acetic acid (4:1 v/v) (solvent C). OTA was not detected in the extracted aqueous solution after a sample (50 μl) had been chromatographed, and so the aqueous layer was discarded. The chloroform layer contained material chromatographically identical with OTA. The chloroform layer (about 800 ml) was dried over anhydrous sodium sulfate (30-40 gm) and then reduced under vacuum to about 25 ml.

2.4 Ochratoxin A purification

To the reduced volume of OTA in chloroform, an equal volume of $NaHCO_3$ solution (0.5 M) was added (138). After vigorous shaking the mixture was centrifuged at 4000 rpm for 10 min. The chloroform layer was extracted again with an equal volume of fresh bicarbonate solution. The combined bicarbonate extracts and the residual chloroform layer were tested for OTA by TLC as previously described, and OTA was not detected in the chloroform layer. The combined bicarbonate layers were acidified cautiously to pH 2.0 with conc. HCl and then the toxin was re-extracted with chloroform (3 x 70 ml). Again, the chloroform extracts and the residual bicarbonate layer were tested for OTA by TLC, and no toxin was detected in the bicarbonate layer. The chloroform layer that contai d the OTA (about 200 ml) was dried over anhydrous sodium sulfate (20-25 gm) and the volume was reduced to about 10 ml.

For further purification, a silica gel column was used (138). Silica gel 60 (mesh 230-400) was dried at 110°C for 1 hr, suspended in benzene and packed into a 500 x 38 mm column. Some of the benzene was allowed to drain to aid settling of the silica gel. When the silica gel had settled, a thin layer of anhydrous sodium sulfate was added to the top of the column. The benzene was then drained just to the top of the sodium sulfate layer. The reduced volume

of OTA in chloroform was applied to the column which was then eluted with the solvent benzene:acetic acid, 94:6 (v/v) at a flow rate of 1.5 ml/min. Fractions of 15 ml each were collected. Progress of OTA through the column could be observed by shining a UV light at the column. OTA was eluted between fractions 31-54. Only those fractions that showed a single spot of OTA on TLC were combined. Fungal pigments and other contaminants of OTA stayed behind while OTA was eluted as a separate band. The collected OTA was pure (judged by TLC at this step), colourless and had a blue fluorescence under a UV lamp.

2.5 Ochratoxin A crystallization

From 6 L of culture medium, 380 mg of pure OTA was obtained. The purified OTA was dissolved in hot benzene (ca 25 ml) and filtered. The filtrate was evaporated in a steam bath until crystals started to form and then cooled to room temperature (138). The crystals were collected by filtration, washed with cold benzene and dried (yield 359 mg). According to Nesheim (138), the crystalline OTA contains 1 mol of benzene of crystallization, and so after subtraction of 1 mol of benzene of crystallization, the net toxin yield was about 302 mg.

2.6 Determination of OTA purity

TLC on silica gel plates containing a UV fluorescent indicator was used as a simple, rapid and reliable method for checking the purity of the toxin especially during the isolation procedure. The produced toxin gave a single spot on TLC which had the same R_f value as commercial OTA in 3 solvent systems A , B and C (Table 1). HPLC was also used to determine the purity of the produced OTA. The toxin gave a sharp clean peak that came out in the same position as that of standard OTA and both peak area percentages were comparable (Fig. 7).

OTA was further characterized spectrophotometrically between 400 and 200 nm. It showed 2 main peaks at 332 and 214 nm identical to the maxima for standard OTA (Fig. 8). The molar absorption coefficient of OTA at 332 nm (6330 cm^{-1} M^{-1}) was used to calculate the OTA concentration (139). The produced OTA was also scanned fluorometrically using an excitation wavelength of 340 nm and scanning the fluorescence between 500 and 300 nm (Fig. 9).

Using the above techniques, it was clear that the produced toxin was comparable in purity and spectral characteristics to standard OTA purchased from Sigma Chemical Co.

Table 1: The R_f values of ochratoxin A.

Solvent system	Sigma OTA*	Isolated OTA*
Benzene, acetic acid (4:1, v/v)	0.68	0.68
Benzene, acetic acid (8:1, v/v)	0.41	0.41
Benzene, acetic acid, methanol (95:5:5, v/v/v)	0.45	0.45

*3µl of 25 mM were spotted on TLC plates with fluorescent indicator.

Figure 7. The HPLC profile of OTA.

A. OTA preparation

B. Standard OTA from Sigma Chemical Co.

Both samples were injected in methanol (10 µl of a 2.5 mM solution) into a Perkin Elmer Series 4 Liquid Chromatograph. The column used was Partisil 10 ODS-2. The solvent system consisted of a mixture of a) acetonitrile:methanol (500:500, v/v) 65% and b) 5 mM sodium acetate:acetic acid (500:14, v/v) 35%. The flow rate was 1.5 ml/min and the photometric detection was performed at 332 nm.

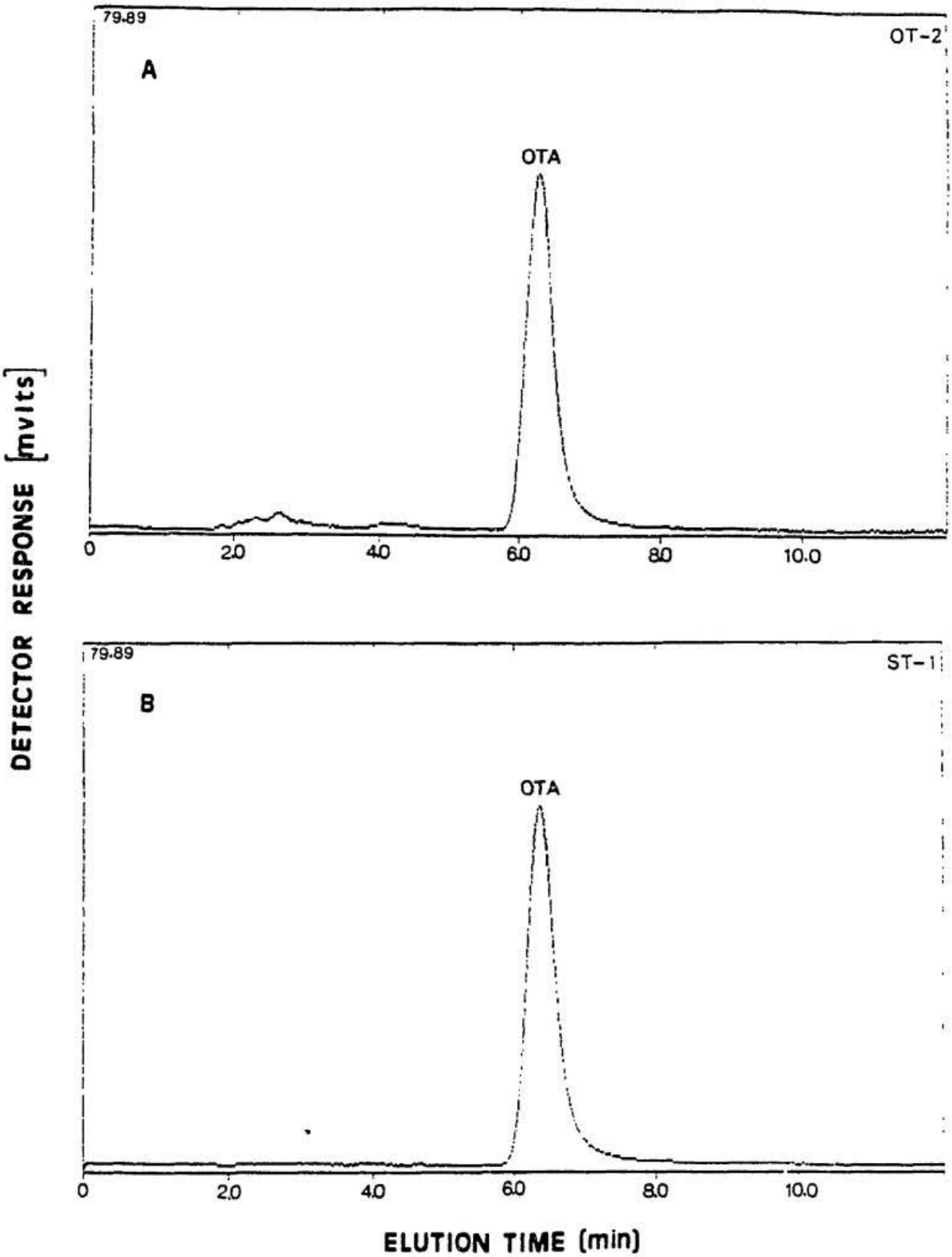
79.89
OT-2
A
OTA
0
2.0
4.0
6.0
8.0
10.0
79.89
ST-1
B
OTA
0
2.0
4.0
6.0
8.0
10.0
DETECTOR RESPONSE [mvlts]
ELUTION TIME (min)

Figure 8. The UV spectrum of OTA.

The continuous line represents standard OTA from Sigma Chemical Co. (—), while the broken line represents my OTA preparation (--). Both samples are at a concentration of 25 μM OTA in 3 ml methanol. The instrument (Perkin Elmer Lambda 3B spectrophotometer) settings were: wavelength scan 400-200 nm, chart speed 60 mm/min and scan speed 60 nm/min.

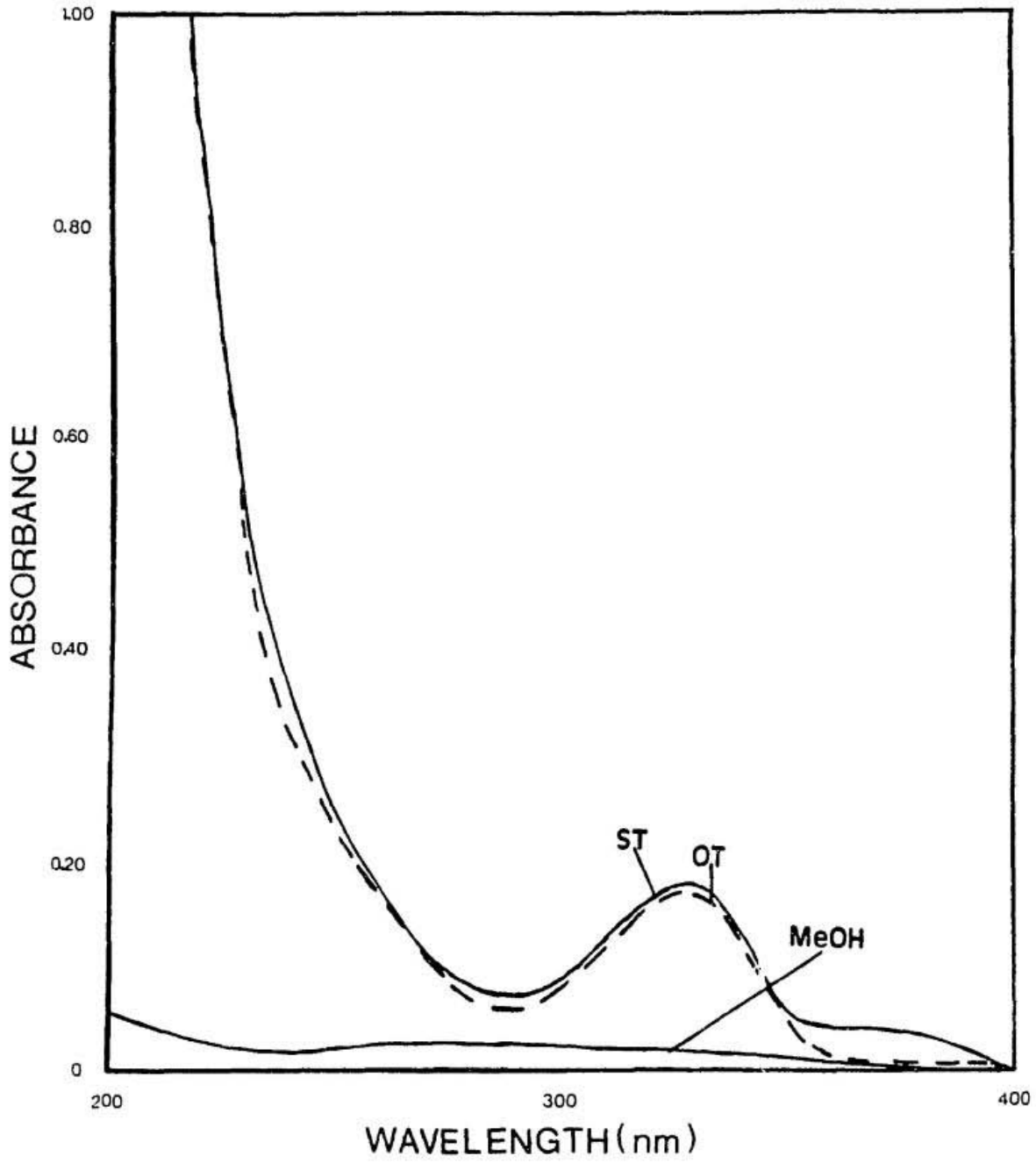
1.00
0.80
0.60
0.40
0.20
0
ABSORBANCE
ST
OT
MeOH
200
300
400
WAVELENGTH(nm)

Figure 9. The fluorescence spectrum of OTA.

The continuous line represents standard OTA from Sigma Chemical Co. (—), while the broken line represents my OTA preparation (--). Both samples are at a concentration of 50 μM OTA in 3 ml methanol. The instrument (Perkin Elmer LS-5 spectrofluorimeter) settings were as follows: Excitation wavelength 340 nm, while emission was scanned from 300 to 500 nm. The Ex/Em slits were set at 5/3 nm, chart speed 60 mm/min and scan speed 120 nm/min.

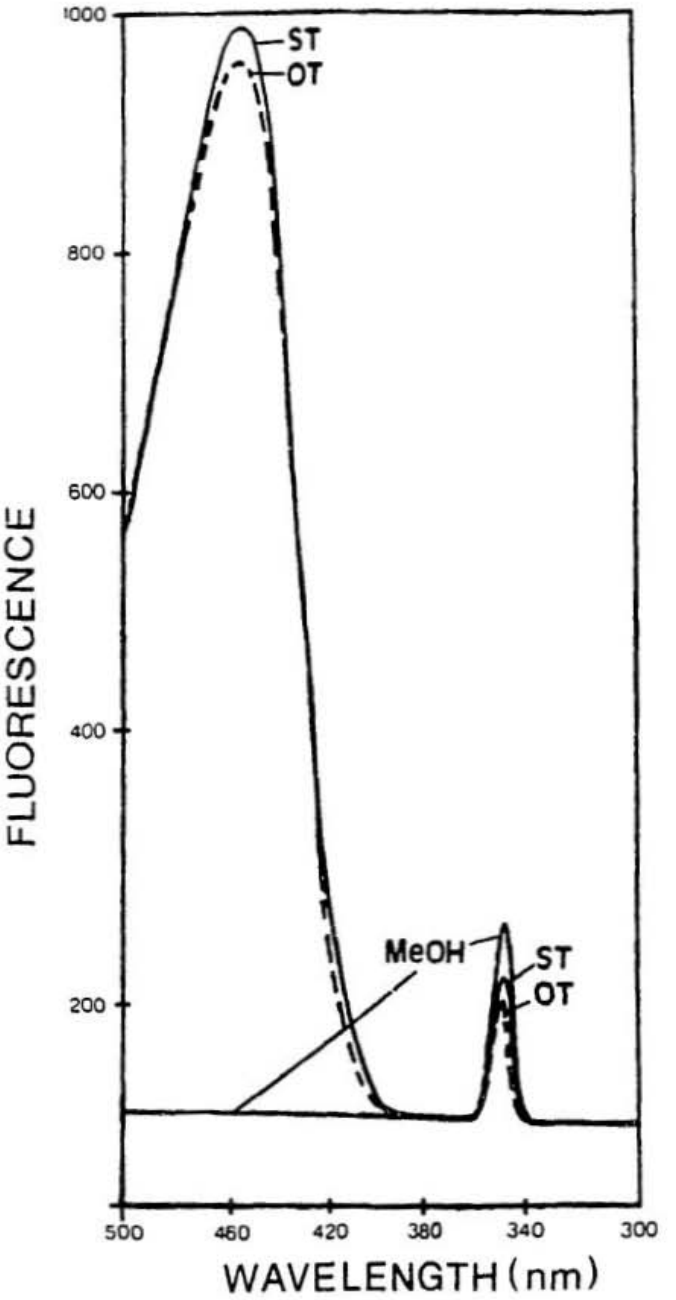
1000
800
600
400
200
FLUORESCENCE
ST
OT
MeOH
ST
OT
500
460
420
380
340
300
WAVELENGTH (nm)

C H A P T E R 3

MATERIALS AND METHODS

3.1 Materials

3.1.1 Chemicals

2',5'-ADP agarose, bathophenanthroline disulfonic acid (BPS), butylated hydroxyanisole (BHA), butylated hydroxytoluene (BHT), catalase, Chaps (3-[cholamidopropyl)-dimethyl ammonio]-1-propanesulfonate), cholic acid, cytochrome *c*, DMPO (5,5-dimethyl-1-pyrroline-1-oxide), EDTA (ethylenediamine tetracetic acid-disodium salt), glycerol, Lubrol PX, NADPH, OTA, Renex 690, superoxide dismutase and 2-thiobarbituric acid (TBA) were purchased from Sigma Chemical Co. (St. Louis, MO, U.S.A). Anhydrous ferric chloride, ferric nitrate and ferrous chloride were obtained from BDH Chemicals, Dartmouth, Nova Scotia, Canada. DEAE-Sephacel was purchased from Pharmacia, Dorval, Quebec, Canada. All other chemicals were of the highest grade commercially available.

3.2 Methods

3.2.1 Preparation of microsomes

Male Sprague-Dawley rats (200-220 g) were obtained from Charles River Canada, La Prairie, Quebec and were allowed free access to standard laboratory rat chow and water. Untreated rats or rats pretreated with sodium phenobarbital (PB) (0.1% PB in drinking water for 5 days) were fasted overnight prior to use. Liver microsomes were isolated by differential centrifugation as described earlier (140). Livers were excised and pooled (6 livers = ~100 gm wet weight) in ice-cold 50 mM Tris-HCl buffer (pH 7.4) containing 1.0 mM EDTA, 1.15% KCl, and 20 μM BHT. The livers were chopped into pieces, homogenized in 3 parts (300 ml) of the above buffer to one part liver (wet wt) using a Teflon/glass homogenizer, and then centrifuged at 10,000 x g for 15 min. Following filtration through cheesecloth, microsomes were isolated from the 10,000 x g supernatant by centrifugation at 110,000 x g for 60 min. The microsomal pellets were resuspended in 100 mM sodium pyrophosphate (pH 7.4) (about 200 ml) containing 1.0 mM EDTA and 20 μM BHT and again centrifuged at 110,000 x g for 60 min. The final microsomal pellets were suspended in 10 mM phosphate buffer (pH 7.4) (35 ml) containing 0.25 M sucrose at a protein concentration of 50 mg/ml and stored at -80°C until used.

Protein was determined by the method of Lowry et al. (141). Microsomes prepared as described above were used for the purification of the flavoprotein NADPH-cytochrome P-450 reductase. When microsomes were prepared for lipid extraction, BHT was excluded from the buffers and the final microsomal pellets were suspended in 10 mM Tris-HCl buffer (pH 7.4) (16 ml from 2 rats) at a protein concentration of 40 mg/ml.

3.2.2 NADPH-cytochrome P-450 reductase (Fp)

3.2.2.1 Fp Purification

The flavoprotein NADPH-cytochrome P-450 reductase (Fp) was purified from liver microsomes isolated from PB-pretreated rats essentially as described by Murray Ardies et al. for hamster microsomes (140) . The following procedures were all performed at 4°C. Microsomes (50 mg protein/ml) were diluted to 10 mg protein/ml with 100 mM Tris-HCl buffer (pH 7.7) containing 1.0 mM EDTA, 1.0 mM dithiothreitol (DTT), 20 μM BHT, 5 μM flavin mononucleotide (FMN), and 30% glycerol (buffer A). Immediately prior to use, CHAPS (3-[(cholamidopropyl)-dimethylammonio]-1-propanesulfonate) was diluted 1:1 (v/v) with buffer A. A solution of 10% CHAPS (in buffer A) was added slowly dropwise with stirring to a final concentration of 1% (w/v; 1.1 mg CHAPS/mg protein) and

the mixture was stirred for 30 min. Then, a 1.5% solution of protamine sulfate was added dropwise to a final concentration of 0.07% (w/v). After stirring for an additional 20 min, the mixture was centrifuged at 110,000 x g for 60 min. The supernatant was removed and the resulting gray-colored, tightly packed pellet was resuspended in buffer A with the aid of a Teflon/glass homogenizer to a protein concentration of 50 mg/ml. A 10% (w/v) solution of sodium cholate in water was then added dropwise with stirring to a final detergent:protein ratio of 3 mg/mg. Ten minutes later, a 20% (v/v) solution of Lubrol PX (ethylene oxide condensate of fatty alcohols, Sigma Chemical Co., MO, USA) in water was added dropwise to a final concentration of 0.5% (w/v) and the mixture was stirred for an additional 30 min. The detergent-treated fraction was again centrifuged at 110,000 x g for 60 min and the resulting supernatant was applied directly to a 2',5'-ADP agarose column (2.5 x 4.0 cm) at a flow rate of 1 ml/min. The affinity column had been equilibrated previously with 100 mM phosphate buffer (pH 7.7) containing 0.4% cholate, 0.1 mM EDTA, 0.1 mM DTT, 20 μM BHT, 5 μM FMN, and 20% glycerol. Once loaded, the resin was washed with 15 column volumes of equilibration buffer, 12 column volumes of 100 mM phosphate buffer (pH 7.7) containing 1.0% Chaps, 0.5% Lubrol PX, 0.1 mM EDTA, 0.1 mM DTT, 20 μM BHT, 5 μM FMN, and 20% glycerol, and again with 15 column volumes of equilibration buffer. All washes

were performed at a flow rate of a 1 ml/min. Fp was then eluted from the affinity resin with a small volume (about 25 ml) of equilibration buffer to which 10 mM $NADP^+$ had been added (flow rate = 0.5 ml/min). The peak Fp-containing fractions were pooled and dialyzed twice with 2 liters of 50 mM phosphate buffer (pH 7.4) containing 0.1 mM DTT and 20% glycerol for a total of 28 hr. The purified Fp was then stored in small aliquots (0.5 ml each) at -80°C. The purified Fp showed a single band on sodium dodecyl sulfate-polyacrylamide gel electrophoresis (Fig. 10).

3.2.2.2 Fp assay

The enzyme was assayed as described by Lake (142) using cytochrome *c* as the electron acceptor. Briefly, 1 ml of 0.125 mM cytochrome *c* solution in 0.1 M phosphate buffer, pH 7.0, and 0.2 ml of 15 mM KCN in water were pipetted into each of a two matched 3 ml spectrophotometer cuvettes. Ten microliters of Fp were pipetted into each cuvette and phosphate buffer was added to the test and reference cuvette contents to bring the volumes up to 2.4 and 2.5 ml, respectively. After mixing, the cuvettes were placed in their cell compartments of the spectrophotometer (thermostatted to 22°C), and after 3 min the reaction was

Figure 10. **Gel electrophoresis analysis of the purified native NADPH-cytochrome P-450 reductase (Fp)** (0.177 μg protein, lanes 2-4) along with Pharmacia low molecular weight standard (lanes 1,5). The Fp was judged to be electrophoretically homogeneous and its molecular weight was determined to be 76000.

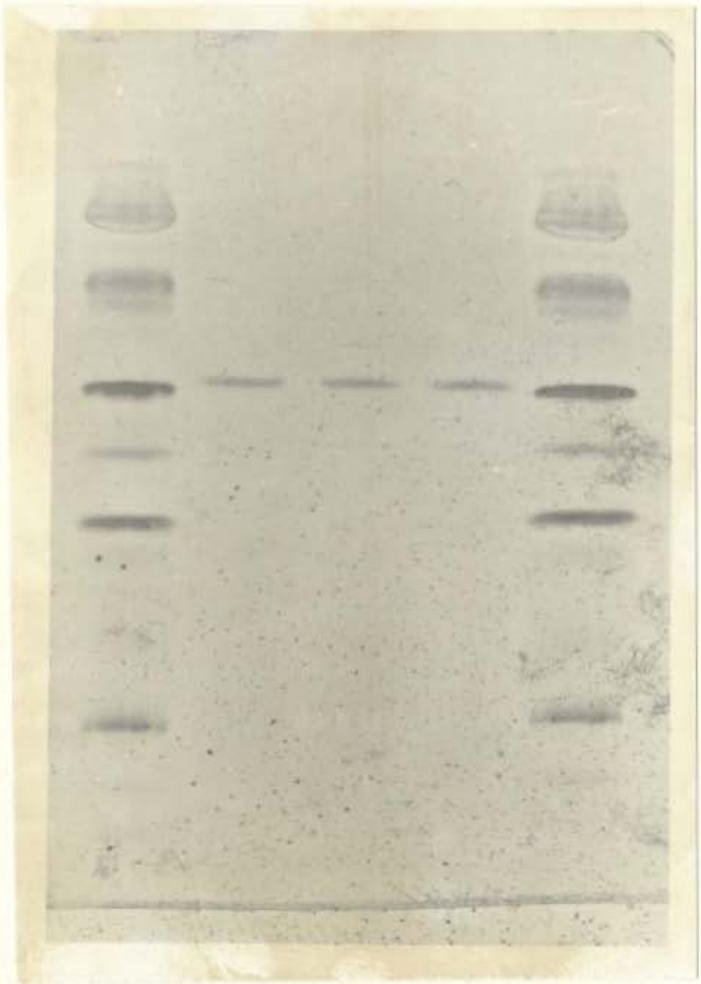

initiated by adding 0.1 ml of 10 mM NADPH to the test cuvette only. The contents were again mixed and the increase in absorbance with time was recorded at 550 nm. Using an extinction coefficient for the reduced cytochrome *c* at 550 nm of 0.021 cm^{-1} μM^{-1}, the specific activity of the flavoprotein was calculated to be 18,000 units/mg protein (142). One unit of enzyme activity is defined as that amount which catalyzes the reduction of 1 nmol cytochrome *c*/min.

3.2.3 Cytochrome P-450

3.2.3.1 Cytochrome P-450 purification

Cytochrome P-450 was purified from liver microsomes isolated from PB-pretreated rats as described by Guengerich (143). Microsomes were suspended to 2 mg protein/ml in 0.1 M potassium phosphate buffer (pH 7.25) containing 20% glycerol, 1mM EDTA, and 20 μM BHT. Sodium cholate (recrystallized from 50% aqueous ethanol) was added dropwise (from a separatory funnel) to the stirring suspension over 20 min to give a final concentration of 0.6% (wt/vol). After stirring for an additional 30 min, the clarified solution was centrifuged at 100,000 x g for 1 hr. An amount of the supernatant equivalent to 2,000 nmoles of cytochrome

P-450 was applied to an w-amino-octyl agarose column (2.5 x 50 cm) previously equilibrated with 300 ml of 0.1 M potassium phosphate buffer (pH 7.25) containing 1 mM EDTA, 20% glycerol, and 0.6% (wt/vol) sodium cholate at a flow rate of 1 ml/min. The cytochrome P-450, a reddish brown protein, was bound to the top one-third of the column. For the first column, all steps were carried out at 4°C and the sodium cholate used was recrystallized. The column was washed with 800 ml of 0.1 M potassium phosphate buffer (pH 7.25) containing 1 mM EDTA, 20% glycerol, and 0.42% (wt/vol) sodium cholate. Cytochrome P-450 was eluted using about 1,500 ml of 0.1 M potassium phosphate buffer containing 1 mM EDTA, 20% glycerol, 0.33% (wt/vol) sodium cholate, and 0.06% (wt/vol) Renex 690 (polyoxyethylene (10) nonyl phenol ether, ICI Americas Inc., WA, USA). The eluted fractions were monitored for cytochrome P-450 (A_{417}). The A_{417} peak fractions were pooled and concentrated to about 50 ml using an Amicon ultrafiltration apparatus and a PM-30 membrane. The concentrated solution was dialyzed against 1 L of a 20% glycerol-0.1% mM EDTA solution (about 3 hr) and then versus 1 L of 10 mM potassium phosphate buffer (pH 7.7) containing 0.1 mM EDTA, 20% glycerol, 0.1% (wt/vol) Lubrol PX, and 0.2% (wt/vol) sodium cholate (not recrystallized) (about 3 hr).

The cytochrome P-450 was further purified by DEAE-cellulose chromatography at room temperature (about 22°C). The dialyzed cytochrome P-450 solution was applied to a 2.5

x 50 cm column of Pharmacia DEAE-Sephacel previously equilibrated with 1 L of 10 mM potassium phosphate buffer (pH 7.7) containing 0.1 mM EDTA, 20% glycerol, 0.1% (wt/vol) Lubrol PX, and 0.2% (wt/vol) sodium cholate (not recrystallized). The column was washed with 700 ml of the equilibration buffer and then eluted with 2 L of the equilibration buffer in which the concentration of NaCl increased linearly to 0.25 M. The last major A_{417} peak contains the bulk of the cytochrome P-450. The peak fractions were pooled and concentrated to about 20 ml with an Amicon ultrafiltration apparatus using a PM-30 membrane. The concentrated solution was stirred with Bio-Beads SM-2 (Bio-Rad Labs; 0.2 gm/mg protein) for 3 hr to remove excess detergent and then filtered through glass wool. Finally, the enzyme preparation was dialyzed overnight against 50 volumes of 10 mM Tris-acetate buffer (pH 7.4) containing 0.1 mM EDTA and 20% glycerol. The dialyzed enzyme was stored in aliquots (0.25 ml each) at - 80°C. SDS-gel electrophoresis revealed the presence of a single protein band (Fig. 11).

3.2.3.2 Cytochrome P-450 assay

Cytochrome P-450 was assayed as described by Guengerich (143) using an extinction coefficient of 91 cm^{-1} mM^{-1}. Briefly, 6 mg microsomal protein or 0.6 mg protein of the

Figure 11. **SDS-gel electrophoretic analysis of the purified cytochrome P-450** (lanes 3, 4 and 5; 0.25, 0.5 and 1.0 μg protein, respectively) along with Pharmacia low molecular weight standards (lanes 6,7) (from top to bottom 94000, 67000, 43000,30000,20000 and 14000) and microsome standard (lanes 1 and 2; 2 μg protein). The cytochrome P-450 molecular weight was determined to be 54000.

cytochrome preparation was suspended in 6 ml of 0.1 M potassium phosphate buffer (pH 7.4) and a few small crystals of sodium dithionite were added to it. After mixing, the contents were divided between 2 matched cuvettes (3 ml in each) and scanned from 500-400 nm (scan speed 120 nm/min, chart speed 30 mm/min) to obtain a baseline. The sample cuvette was bubbled for about 30 sec to 1 min with CO gas and then re-scanned to get the characteristic peak for the cytochrome P-450 at 450 nm.

The specific activity of my cytochrome P-450 (8.25 nmol/mg protein) was lower than expected, but it showed a complete absence of NADPH cytochrome P-450 reductase activity (Fp). Aust and his group (71) satisfactorily used cytochrome P-450 preparations with specific activities between 10 and 14 nmol/mg protein.

3.2.4 Preparation of microsomes from cobalt protoporphyrin IX-treated rats

Treated rats recieved 2 doses (50 μmol/Kg each) of cobalt protoporphyrin IX 9 days and 2 days prior to killing, while control rats received the vehicle saline at the same time as the treated rats. Cobalt protoporphyrin IX (24.8 mg) was dissolved in 0.4 ml of 0.1 M NaOH, the pH was adjusted to 7.4 and the solution was made up to 4 ml with normal saline (final concentration of cobalt protoporphyrin

IX, 10 mM). The freshly prepared cobalt protoporphyrin solution was administered subcutaneously to rats at a dose of 0.5 ml/100 gm body weight. After the time period for treatment had elapsed, microsomes were prepared from the rat livers as described under 3.2.1.

Cobalt protoporphyrin pretreatment has been shown to drastically reduce both cytochrome P-450 and NADPH-cytochrom P-450 reductase (Fp), by 80% and 75%, respectively. To avoid the possible effect of reduced Fp, these microsomes were fortified by incubating them with purified Fp. Microsomes (2 mg protein) were incubated with Fp (640 nmol) for 1 hr at 22°C and then centrifuged at 110,000g as in section 3.2.1. The microsomes were resuspended in buffer and assayed for Fp content as described in section 3.2.2.2. Fortified microsomes were found to have an Fp content of 70 nmol/mg protein as compared to 20 nmol/mg protein in non-fortified microsomes.

3.2.5 Synthesis of OTA analogues

3.2.5.1 Ochratoxin α

Ochratoxin α (Oα) (see page 115 for structure) was obtained by refluxing OTA with 6N HCl for 30 hr as described by Van Der Merwe et al. (2). Briefly, OTA (210 mg) was suspended in 6N HCl (100 ml) and heated under reflux for 30

hr. After cooling, the mixture was extracted with chloroform (2x20 ml). The combined chloroform extracts were dried over anhydrous sodium sulfate and then evaporated under reduced pressure to yield Oα. The Oα thus obtained was dried to a constant weight in a freeze dryer. Yield = 120 mg (~90%). Oα thus obtained was judged to be pure on TLC and HPLC.

3.2.5.2 Ochratoxin B

Ochratoxin B (OB) (see page 115 for structure) was a gift from Dr. M. Castegnaro, International Agency for Research on Cancer, Lyon, France.

3.2.5.3 Ochratoxin C

Ochratoxin C (OC) (see page 115 for structure) was prepared by estrification of the carboxyl group of OTA in the presence of 14% boron trifluoride (BF_3) in metha ol according to a method described by Nesheim (138). Briefly, OTA (45 mg) was dissolved in 5 ml of 14% BF_3 in methanol (w/v). The solution was heated in a steam bath for 5 min. After 15 ml of water was added, the solution was extracted three times with chloroform (5 ml each). The combined chloroform extracts were washed once with 5 ml and twice with 2.5 ml of 0.5 N $NaHCO_3$, and four times with 2.5 ml

water. The chloroform was evaporated in the steam bath and the residue was dried to constant weight under reduced pressure. Yield = 43 mg (89.4%).

3.2.5.4 Replacement of L-Phe moiety in OTA by different amino acids

To replace the L-Phe moiety in OTA by other amino acids, the method described by Steyn and Holzapfel (144) was followed. Briefly, Oα (14 mg) was heated under reflux (anhydrous conditions) with thionyl chloride ($SOCl_2$) (4.0 ml) for 2 hr. The $SOCl_2$ was evaporated under reduced pressure and the acid chloride was taken up in dry pyridine (0.35 ml), cooled to 0°C, and then dimethyl formamide (0.2 ml) was added. Sodium azide (5 mg) was slowly added to the solution at 0°C and the mixture was shaken for 30 min. Water (0.1 ml) was then added and the mixture shaken for an additional 30 min. The solution was extracted twice with ethyl acetate (1.5 ml) and the organic phase was added to a solution of either L-Ser, L-Pro or L-Glu (10.5, 11.5 or 14.7 mg, respectively) in water (0.5 ml) containing triethylamine (15 μl). The solution was shaken at 5°C for 55 hr and subsequently treated with 1 N NaOH (0.5 ml). The mixture was separated into two layers; the aqueous phase was extracted with ethyl acetate, acidified with acetic acid, and extracted with chloroform. The chloroform solution was

concentrated under reduced pressure and the product was separated by TLC with 4:1 (v/v) benzene-acetic acid as mobile phase. The R_f values (Table A1) for the new compounds (see page 115 for structure) were comparable to those reported by Steyn et al. (145). HPLC profiles for these new compounds in comparison to OTA and Oα are also given in Fig. A1.

3.2.6 Lipid extraction and preparation of phospholipid vesicles

Total lipid was extracted from untreated rat liver microsomes by the method of Folch et al. (146), with care being taken to flush all solvents with nitrogen and to perform all operations under nitrogen at 0-4°C to minimize autoxidation of polyunsaturated lipids. Microsomes (11 ml; 40 mg protein/ml) were homogenized using 220 ml of chloroform:methanol (2:1, v/v). The homogenate was filtered through a number 1 filter paper (Whatman) into a glass stoppered bottle. The crude lipid extract was vigorously mixed with 32 ml of salt solution (upper phase of the mixture chloroform:methanol:0.58 % NaCl solution, 8:4:3, v/v/v). The mixture was allowed to separate (by standing) into two layers (2 phases). As much of the upper phase as possible was removed by siphoning and removal of the upper phase solutes was completed by rinsing the surface of the

lower phase three times with small amounts (about 5 ml each time) of pure solvents upper phase without disturbing the lower phase. Lower phase and the remaining rinsing solution were made into one phase by adding few drops of methanol. The extracted lipid in chloroform:methanol (2:1) was stored under nitrogen in 10 ml aliquots at -80°C.

Total lipid phosphorus was determined as described by Bartlett (147) and modified by Marinetti (148). Different sample volumes (25, 50 and 100 µl) of extracted lipid were placed in digestion test tubes and evaporated to dryness. Appropriate blanks were set up without lipid. To each tube, 1 ml perchloric acid (70 %) and 3-5 boiling stones were added and all samples were digested in an electron digestor for 12 min. After the tubes had cooled, 8 ml of distilled water, 0.5 ml of 5 % ammonium molybdate and 0.5 ml of ANSA (1-amino-2-naphthol-4-sulfonic acid) (1 gm/6.3 ml H_2O, Sigma Chemical Co.) were added to each tube which was then vortexed. All tubes were placed in a boiling water bath for 12 min and then allowed to cool before measuring the absorbance at 815 nm. A standard curve was constructed using different concentrations of inorganic phosphorus P (as phosphate) from 0 up to 5 µg P/ml. The same procedures were followed as above except for the digestion step. A linear relation between absorbance at 815 nm and the amount of Pi was observed. This standard curve was used to determine the unknown sample phosphorous concentration. The lipid extract

had a phosphorus concentration of 2.0 μmol/ml.

Phospholipid vesicles were prepared fresh daily by sonication of the extracted lipid under anaerobic conditions as described in (149). Briefly, an aliquot of the phospholipid solution was evaporated to dryness in a plastic tube under nitrogen, and nitrogen-saturated Tris-HCl buffer (0.25 M; pH 6.8) was added to give a final lipid phosphorus concentration of 10 μmol/ml. The tube was flushed with nitrogen, capped and placed in a glass beaker filled with a mixture of ice and water. Phospholipid vesicles were obtained by placing the probe of a Branson sonifier (model W185) in the beaker and applying a power of 50 watts for 5 min.

3.2.7 Lipid peroxidation assays

Incubations were carried out in triplicate at 37°C in 0.25 M Tris-HCl buffer (pH 6.8)/0.25 M NaCl. The complete system contained phospholipid vesicles, Fp, OTA, EDTA, Fe^{3+} and NADPH. Final concentrations of the various components are given in the figure and table legends. Lipid peroxidation was initiated by addition of NADPH, and terminated by transferring 0.5 ml aliquots of the reaction mix into tubes containing 50 μl of 2% BHT in ethanol and 500 μl of 30% trichloroacetic acid (TCA). The tubes were covered with marbles and heated in a boiling water bath for

15 min, cooled, centrifuged and the absorbance of the MDA-TBA adduct (Fig. 6) was read at 535 nm (150). Various agents, when included in the incubation mix, were added before initiation of lipid peroxidation.

3.2.8 Spectrophotometric measurements

Spectrophotometric measurements were conducted at 25°C using either a Shimadzu UV-260 or a Perkin-Elmer Lambda 3B double beam spectrophotometer in 1 cm cells. Fluorescence measurements were carried out in a Perkin-Elmer LS-5 spectrofluorimeter in 1 cm cells. The fluorimeter settings were (unless otherwise specified) as follows: Ex./Em. slits of 5/3 nm and $\lambda_{Ex.}/\lambda_{Em.}$ of 355/465 nm .

3.2.9 Reduction of Fe^{3+} to Fe^{2+}

Reduction of Fe^{3+} to Fe^{2+} was measured spectrophotometrically by recording the time-dependent increase in absorbance at 535 nm (E = 22.14 $mM^{-1}cm^{-1}$) due to formation of the colored water soluble bathophenanthroline disulfonic acid-Fe^{2+} complex (151). The reaction mixture contained per ml: 110 μM Fe^{3+}, 250 μM OTA, 10 μM EDTA, 3.2 units Fp, 400 μM BPS and 200 μM NADPH. The reaction was started by addition of NADPH.

3.2.10 Oxygen uptake studies

Oxygen uptake was measured polarographically with a Clark electrode (152). The reaction mixture (total volume of 1.5 ml) contained: 0.25 M Tris-HCl (pH 6.8), phospholipid vesicles (1.5 μmoles lipid P), 4.8 units Fp, varying concentrations of OTA (0-1000 μM), 110 μM Fe^{3+}, 25 μM EDTA and 200 μM NADPH. Appropriate controls were performed omitting one or the other of the various components. Rates of oxygen consumption showed significant variation from day to day presumably due to the free radical nature of the reaction. However, the relative rates of oxygen uptake under the various conditions were always consistent although the absolute values differed.

3.2.11 Fatty acid analysis in microsomes

Total lipids were extracted from both control microsomes as well as microsomes from cobalt protoporphyrin IX-pretreated rats according to the method of Bligh and Dyer (185). Briefly, 400 μg microsomal protein were suspended in 250 μl of 0.1 M potassium phosphate buffer, pH 7.4 and a mixture of methanol:chloroform (2:1 v/v) (750 μl) was added to it. The mixture was vortexed and left for 1 hr at 4°C before centrifugation in an Eppendorf centrifuge for 2 min to get rid of the protein precipitate. The clear

supernatant was washed with 500 µl of a chloroform:water mixture (1:1, v/v), and then the supernatant was centrifuged again. The chloroform layer was taken (lipid extract), dried under nitrogen and resuspended in 100 µl of chloroform. Different lipid fractions were separated by TLC on Silica Gel G (layer thickness 250 µ, Whatman), using a solvent system of n-hexane:ether:acetic acid (170:30:4, v/v/v). The various fractions were identified with the aid of known standards, exposed to iodine vapor and the phospholipid band was scraped off.

Fatty acid methyl esters were prepared by refluxing the phospholipid fraction with 2 ml of a mixture of methanol:conc H_2SO_4 (23.5:1.5, v/v) overnight at 70°C. The mixture also contained a few crystals of the antioxidant hydroquinone, and 5 µg of C17 fatty acid as standard. After the addition of 1 ml water, the methyl esters were extracted twice with n-hexane (1.5 ml each). The hexane extract was dried with anhydrous sodium sulfate, evaporated under nitrogen and the residue was dissolved in carbon disulfide (25 µl). Gas chromatography was performed with a Hewlett Packard apparatus equipped with 30 m Supelcowax 10 wide bore capillary column (0.75 mm i.d., Supelco Canada, Ltd., Oakville, Ontario), and a flame ionization detector. The following separation protocol was used: carrier gas, helium at 15 ml/min, isothermal at 195°C. Quantitative analysis of chromatograms were completed using Hewlett Packard 3365 Chem-Station software.

3.2.12 ESR studies

The spin trap DMPO was purified over charcoal and assayed as described in (153). The ESR spectra were measured (by Dr. Brian B. Hasinoff, Chemistry Dept., Memorial University of Newfoundland) in 20 mM Tris-HCl buffer (pH 8.5). The reddish-brown Fe^{3+}-OTA complex was pre-formed by adding $FeCl_3$ dissolved in methanol to OTA also in methanol. To this was added aqueous air-saturated buffer, 2 mol of NaOH per mol of OTA (to react with the two dissociable protons on OTA), catalase (when included), Fp, NADPH and DMPO. Due to the high concentrations of OTA and Fe^{3+} present, a small amount of the reddish-brown precipitate was present in the ESR tube. Methanol from $FeCl_3$ and OTA stock solutions was also present, generally in the order of 5% (v/v) and was shown to have no significant effect on the ESR spectra. The ESR spectra were recorded at room temperature in identical quartz capillary tubes on an X-band Bruker ESP-300 spectrometer using a 100 kHz modulation frequency. The spectra shown are the arithmetic sum of 5 consecutive spectra collected over a total time of 3.5 min.

CHAPTER 4

RESULTS

4.1 Role of various components in lipid peroxidation

Inclusion of OTA in a reconstituted enzyme system significantly enhanced the rate of lipid peroxidation. Figure 12 shows the time course of this lipid peroxidation. The rate of MDA formation was approximately linear, but showed a slight lag phase. About 9 nmol of MDA were formed at the end of 60 min when the complete system contained phospholipid, Fp, OTA, EDTA, Fe^{3+}, and NADPH (Fig. 12). Fe^{3+} was essential since its absence led to no MDA formation (Fig. 12B). Very little MDA was formed (< 1 nmol) at the end of 1 hr in the absence of OTA (Fig. 12B). Deletion of either EDTA, Fp or NADPH from the incubation system resulted in lower rates of MDA formation (about 3.5-5.0 nmol/hr). The rate of MDA formation increased with increasing OTA concentration (Fig. 13). Concentrations higher than 1 mM OTA were not tested due to insolubility. Results essentially similar to those in Figs. 12 and 13 were obtained when oxygen uptake instead of MDA formation was measured as an index of lipid peroxidation (Figs. 14 and 15).

Figure 12. **Effect of various components of the reconstituted system on OTA stimulated MDA formation.**

Incubations were carried out at 37°C for 0, 20, 40 and 60 min in 0.25 M Tris-HCl buffer (pH 6.8)/0.25 M NaCl. The complete system contained per ml: phospholipid vesicles (1 μmole P), 177 ng Fp (3.2 units), 500 nmol OTA, 50 nmol EDTA, 110 nmol Fe^{3+} and 200 nmol NADPH. Other details are as described in section 3.2.7. The effect of omitting Fp or NADPH is shown in A while the omission of OTA, EDTA or Fe^{3}+ is shown in B. Experiments in A and B were carried out separately. Each point represents the mean ± SD of triplicate incubations from one experiment typical of two.

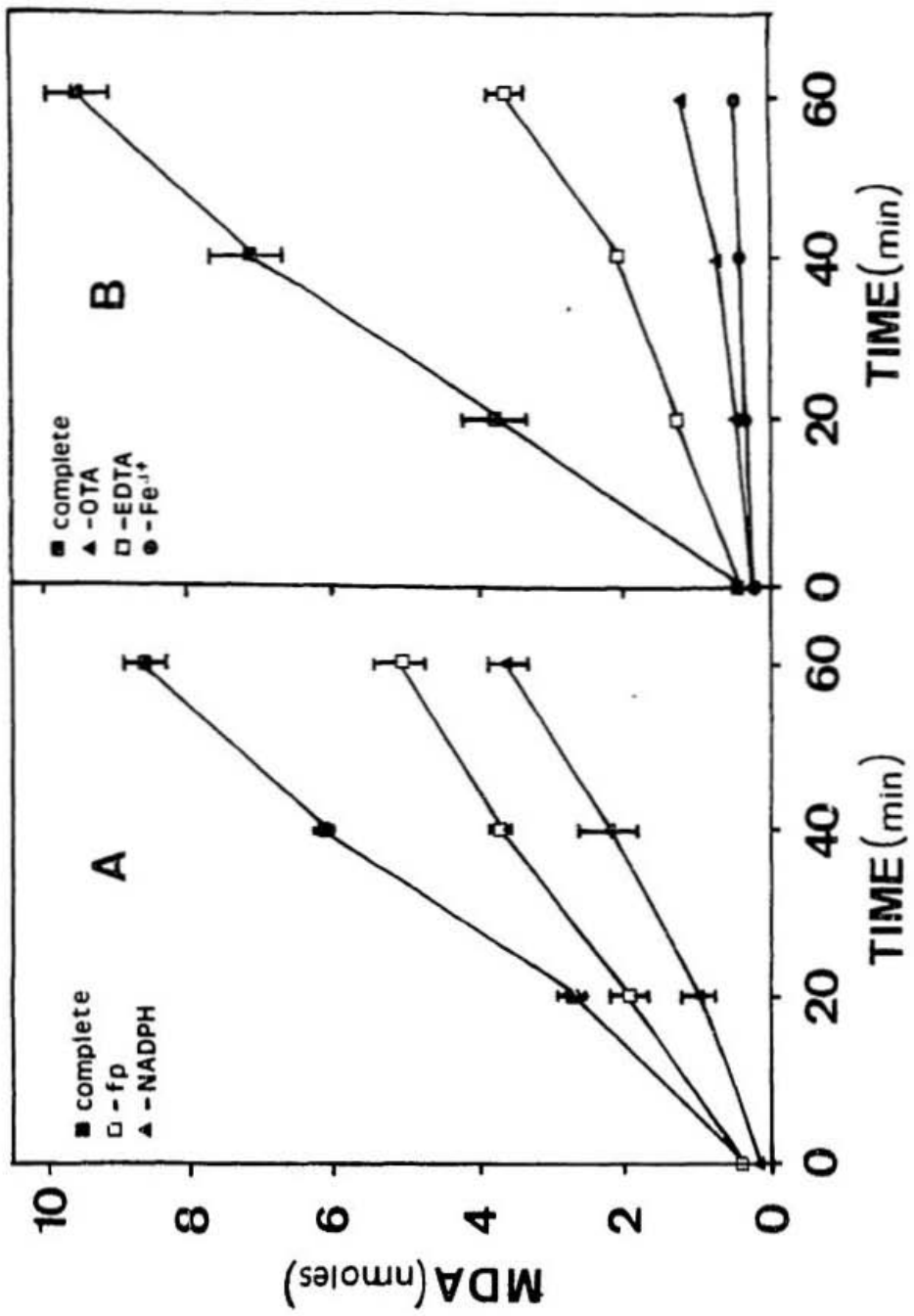
MDA (nmoles)
10
8
6
4
2
0
A
B
■ complete
□ - fp
▲ - NADPH
■ complete
▲ - OTA
□ - EDTA
● - Fe++
0
20
40
60
TIME (min)

Figure 13. **Effect of OTA concentration on MDA formation.** Incubations were carried out at 37°C for 0, 20, 40 & 60 min in 0.25 M Tris-HCl buffer, pH 6.8/0.25 M NaCl and contained per ml: phospholipid vesicles (1 μmol P), 177 ng Fp (3.2 units), varying amounts of OTA (0-1000 μM), 25 nmol EDTA, 110 nmol Fe^{3+} and 200 nmol NADPH. Each point represents the mean ± SD of triplicate incubations from one experiment typical of three.

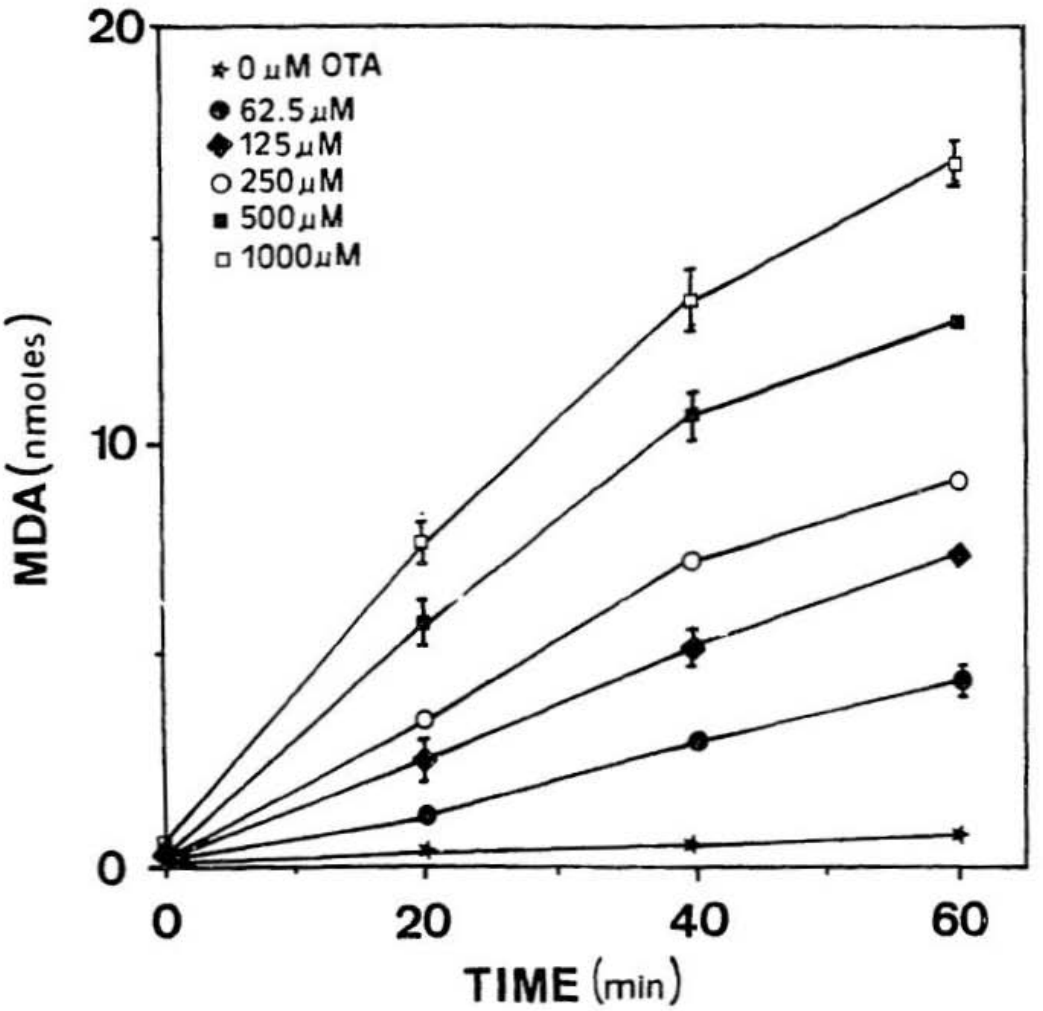
20
10
0
MDA (nmoles)
0 µM OTA
62.5 µM
125 µM
250 µM
500 µM
1000 µM
0
20
40
60
TIME (min)

Figure 14. **Effect of various components on OTA stimulated oxygen uptake.**

Oxygen consumption was measured polarographically with a Clark electrode as described in section 3.2.10. The reaction was carried out at 37°C in 0.25 M Tris-HCl buffer, pH 6.8/0.25 M NaCl and contained per ml: phospholipid vesicles (1 μmol P), 177 ng Fp (3.2 units), 250 nmol OTA, 25 nmol EDTA, 110 nmol Fe^{3+} and 200 nmol NADPH. B represents a control in which NADPH was omitted. Two experiments gave essentially identical results, one set of which is given.

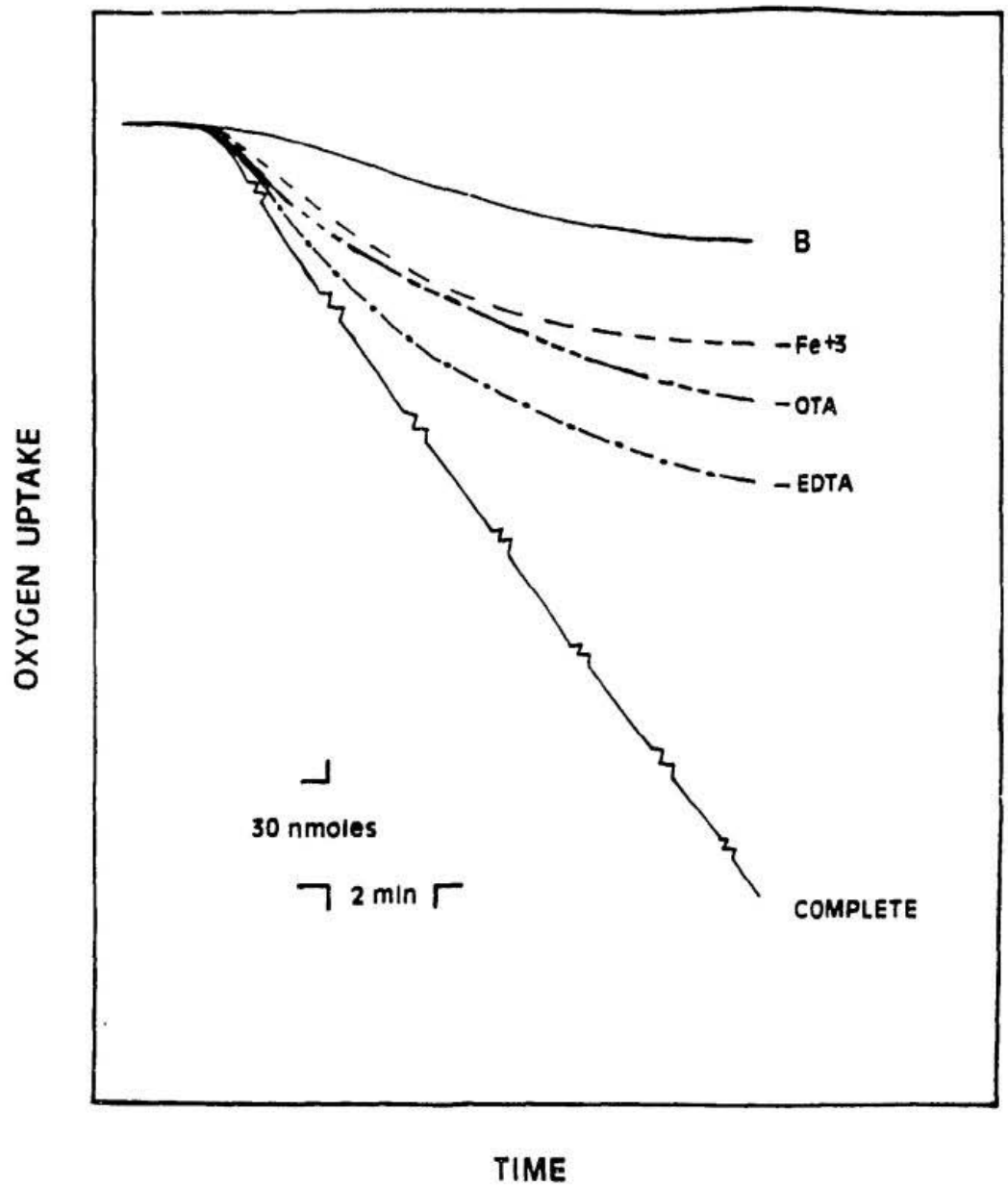
OXYGEN UPTAKE
B
-Fe+3
-OTA
-EDTA
30 nmoles
2 min
COMPLETE
TIME

Figure 15. **Effect of OTA concentration on oxygen uptake.** Oxygen consumption was measured polarographically with a Clark electrode. The reaction was carried out at 37°C in 0.25 M Tris-HCl buffer, pH 6.8/0.25 M NaCl and contained per ml: phospholipid vesicles (1 μmol P), 177 ng Fp (3.2 units), varying amounts of OTA (0-1000 μM), 25 nmol EDTA, 110 nmol Fe^{3+} and 200 nmol NADPH. B represents a control in which NADPH was omitted. The results represent one experiment typical of two.

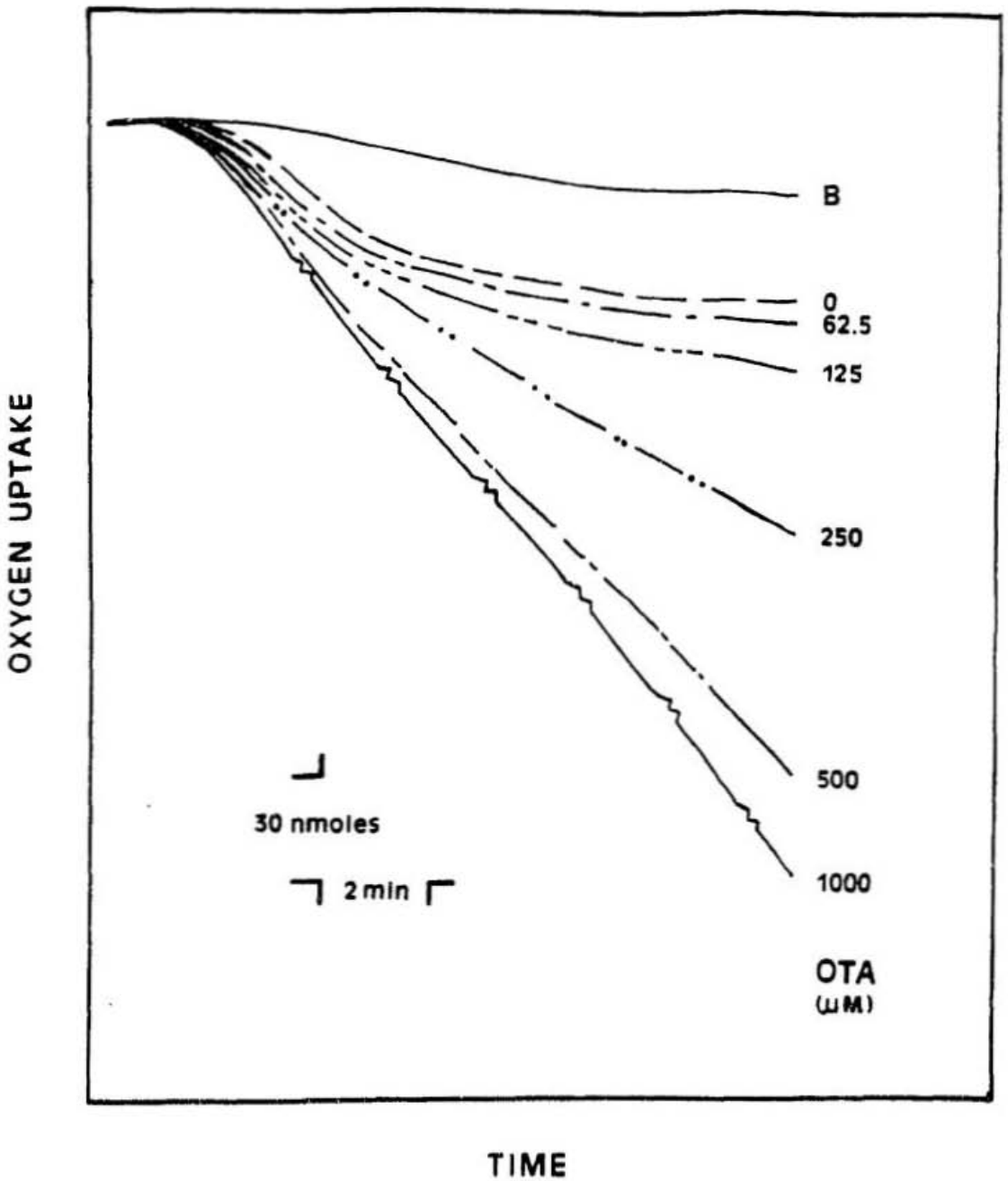
OXYGEN UPTAKE
B
0
62.5
125
250
500
1000
30 nmoles
2 min
OTA
(μM)
TIME

Table 2. Effect of various agents on OTA-stimulated lipid peroxidation.

addition to system	MDA-formed* (nmoles)
None	10.47 ± 0.71 (100)
SOD (6 μg/ml)	8.10 ± 0.42 (77)
Catalase (36 μg/ml)	11.20 ± 0.70 (108)
Sodium formate (11 mM)	11.81 ± 0.81 (113)
Mannitol (11 mM)	13.74 ± 0.94 (131)
BHA (50 μg/ml)	0.73 ± 0.01 (7)

*Incubations were carried out in triplicate for 40 min at 37°C in 0.25 M Tris-HCl buffer, pH 6.8/0.25 M NaCl and contained (per ml): phospholipid vesicles (1 μmole P), 177 ng Fp (3.2 units), 25 nmol EDTA, 110 nmol Fe^{+3}, 200 nmol NADPH and 500 nmol OTA. All concentrations indicated are final concentrations in the reaction medium. MDA values obtained are means ± SD of triplicate incubations from one experiment typical of three. The numbers in parenthesis represent percentage activity relative to "None" as 100%.

4.2 Effect of free radical scavengers on lipid peroxidation

As expected, the antioxidant BHA completely inhibited lipid peroxidation (Table 2). But, the hydroxyl radical scavengers mannitol and sodium formate, as well as catalase, which decomposes hydrogen peroxide, showed no protective effect against lipid peroxidation. A slight inhibition (23%) was observed in the presence of superoxide dismutase. These results are consistent with earlier studies (87-90).

4.3 Effect of varying the concentration of individual components on lipid peroxidation

4.3.1 Varying the EDTA concentration

Since EDTA was required for maximum lipid peroxidation (Figs. 12B and 14), I examined the effect of varying the EDTA concentration on MDA levels keeping the concentration of Fe^{3+} fixed at 110 μM. A broad bell-shaped curve was obtained with maximum stimulation of 4 to 5-fold at an EDTA concentration of 25 μM (Fig. 16). However, the amount of EDTA required appeared not to be critical since 5 μM EDTA was almost as effective. Increasing the EDTA concentration to 75 μM and beyond led to a total inhibition of lipid peroxidation presumably due to excessive Fe^{3+} chelation.

Figure 16. **Effect of EDTA concentration on OTA stimulated lipid peroxidation.**
Incubations were carried out at 37°C for 20 and 60 min in 0.25 M Tris-HCl buffer, pH 6.8/0.25 M NaCl and contained per ml: phospholipid vesicles (1 μmol P), 177 ng Fp (3.2 units), 500 nmol OTA, varying amounts of EDTA (0-75 μM), 110 nmol Fe^{3+} and 200 nmol NADPH. Each point represents the mean ± SD of triplicate incubations from one experiment typical of three.

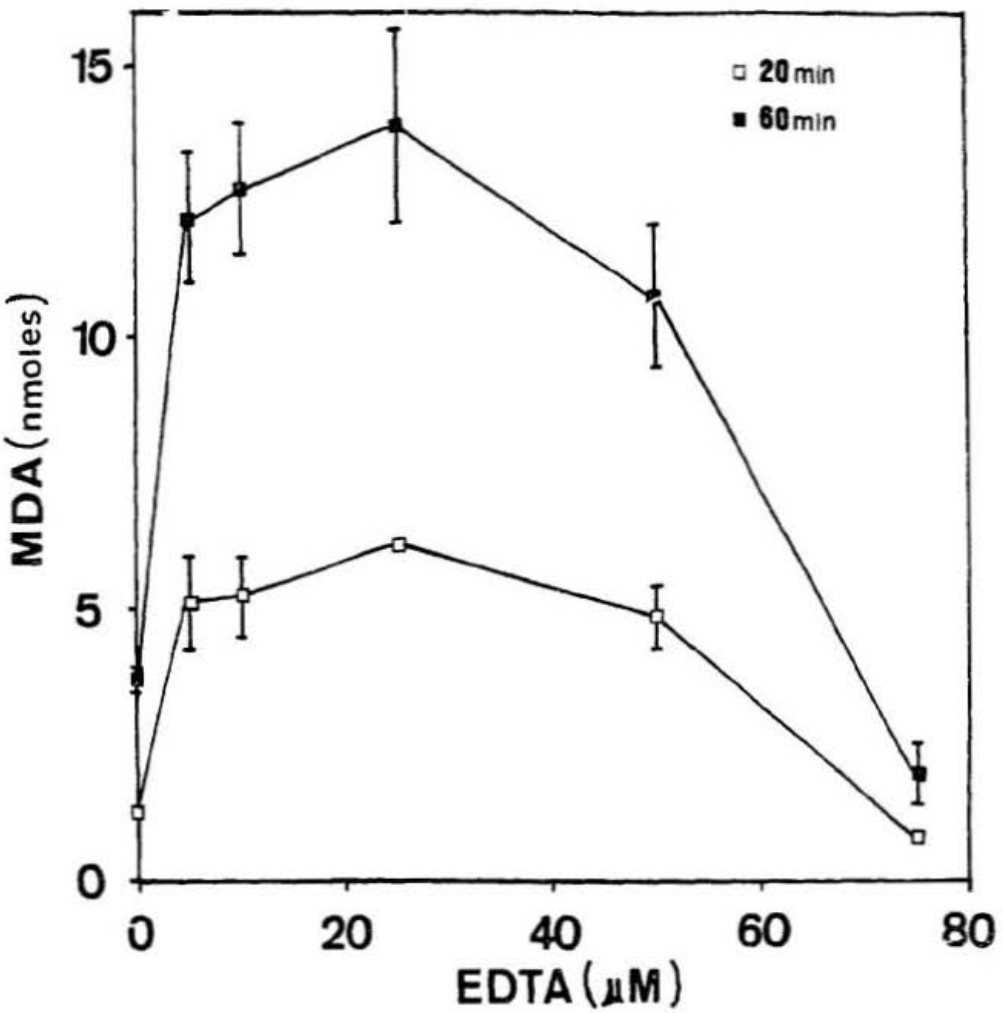
20 min
60 min
MDA (nmoles)
EDTA (μM)
0
5
10
15
0
20
40
60
80

4.3.2 Varying Fp concentration

The effect of Fp concentration on the rate of MDA formation is shown in Fig. 17. In the absence of Fp, a lower rate of MDA formation was observed indicating that NADPH is directly able to reduce Fe^{3+} to Fe^{2+}. However, addition of Fp substantially increased the rate of MDA formation especially at earlier time points. Thus, after 5 min, the MDA level in the absence of Fp was 0.22 nmol and this increased 3-fold (0.60 nmol), 4.5-fold (0.99 nmol) and 11-fold (2.52 nmol) in the presence of 3.2 units, 6.4 units and 16.0 units of Fp respectively (Fig. 17). After 60 min, the relative differences were much less and increases of 42%, 73% and 110% over the basal rate were observed in the presence of 3.2 units, 6.4 units and 16.0 units of Fp respectively (Fig. 17).

4.3.3 varying the pH

The pH optimum for the lipid peroxidation was found to be around neutrality, and slightly acidic (pH 6.0) or alkaline (pH 9.0) conditions were substantially inhibitory (Fig. 18). Thus, all incubations were carried out at a pH of 6.8.

Figure 17. **Effect of Fp concentration on OTA stimulated lipid peroxidation.**

Incubations were carried out at 37°C for 5, 20 & 60 min in 0.25 M Tris-HCl buffer, pH 6.8/0.25 M NaCl and contained per ml: Phospholipid vesicles (1 μmol P), varying amounts of Fp (0-16 units; 0-885 ng), 250 nmol OTA, 25 nmol EDTA, 110 nmol Fe^{3+} and 200 nmol NADPH. Each bar represents the mean ± SD of triplicate incubations from one experiment typical of two.

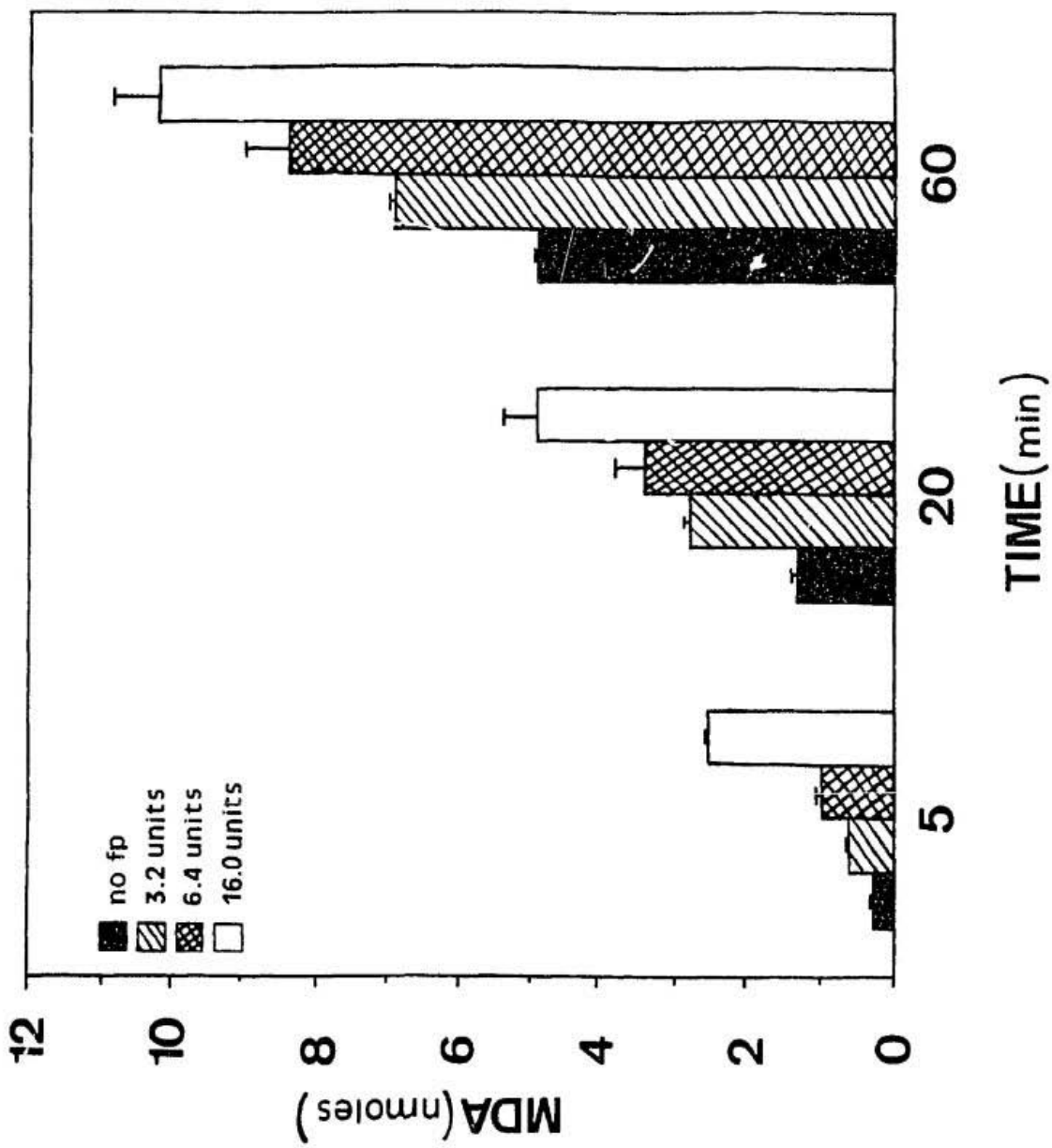
MDA (nmoles)
12
10
8
6
4
2
0
5
20
60
TIME (min)
no fp
3.2 units
6.4 units
16.0 units

Figure 18. **Effect of pH on OTA stimulated lipid peroxidation.**

Incubations were carried out at 37°C for 15 & 60 min in 0.25 M Tris-HCl buffer of different pH (6.0 - 9.0)/0.25 M NaCl in the presence of (per ml): phospholipid vesicles (1 μmol P), 177 ng Fp (3.2 units), 250 nmol OTA, 25 nmol EDTA, 110 nmol Fe^{3+} and 200 nmol NADPH. Each point represents the mean ± SD of triplicate incubations from one experiment typical of two.

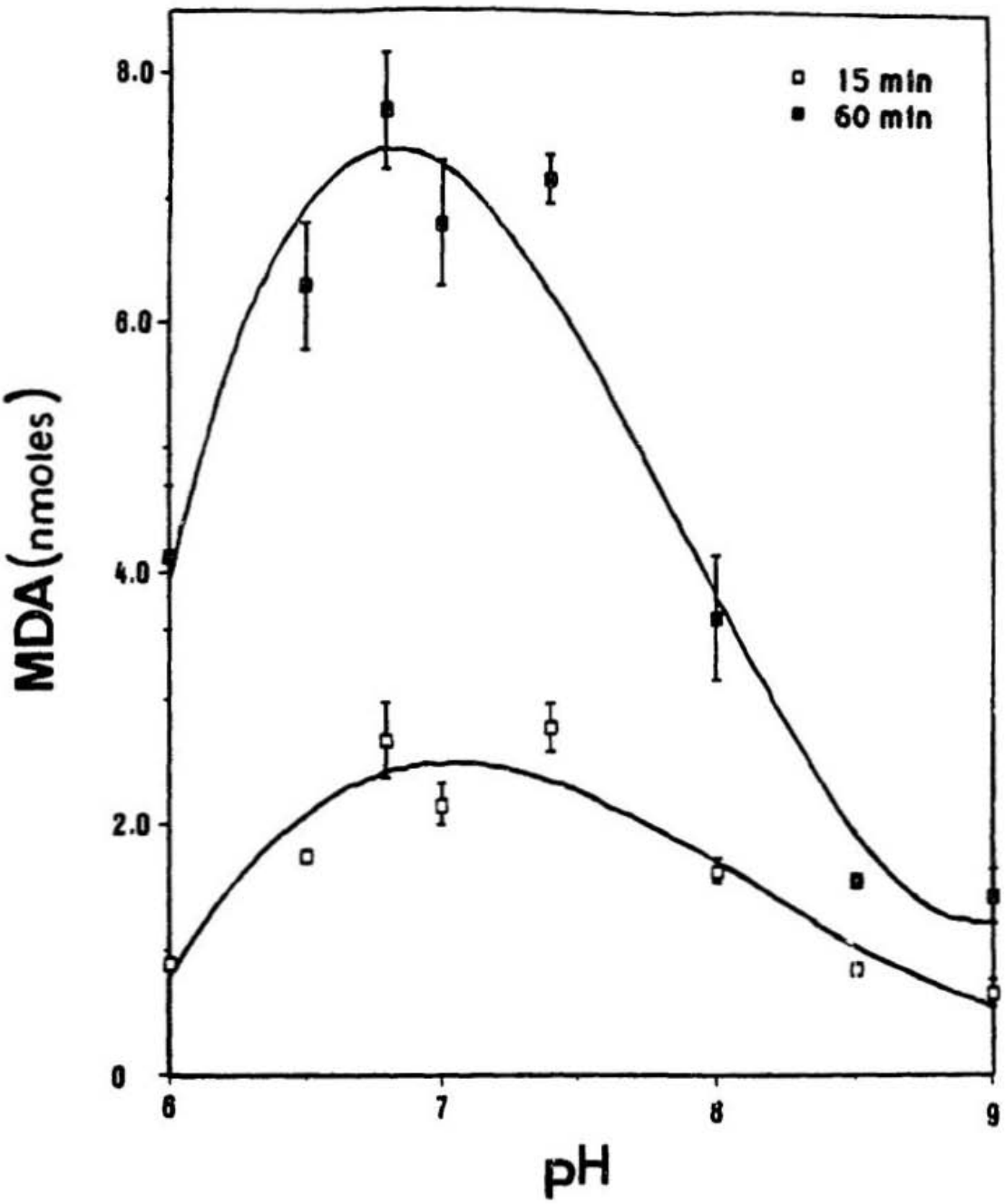
15 min
60 min
MDA (nmoles)
8.0
6.0
4.0
2.0
0
6
7
8
9
pH

4.4 Involvement of cytochrome P-450 in lipid peroxidation

4.4.1 Effect of varying cytochrome P-450 concentration

It was suggested by Ernster and Hochstein (70) as well as by Aust (69) that there may be a microsomal component that replaces EDTA *in vivo*. Later this microsomal component was suggested to be cytochrome P-450 (normally present in liver endoplasmic reticulum). Recently, Aust (71) demonstrated that when cytochrome P-450 was incorporated into phospholipid vesicles, EDTA-Fe^{3+} was not required. For the above mentioned reasons, I purified cytochrome P-450 from liver microsomes to investigate its involvement in the OTA-stimulated liposomal lipid peroxidation system. Concentrations up to 1.0 nmol cytochrome P-450/ml were tested for their effect on lipid peroxidation in a reconstituted system consisting of phospholipid vesicles, Fp, OTA, cytochrome P-450, Fe^{3+}, and NADPH (no EDTA). The rate of MDA formation increased with increasing cytochrome P-450 concentration up to 0.20 nmol/ml (Fig. 19). Above this level, the rate of MDA formation decreased. The reason for decreased MDA formation at high concentrations of cytochrome P-450 is not clear at the moment.

Figure 19. **Effect of cytochrome P-450 concentration on OTA stimulated lipid peroxidation.** Incubations were carried out at 37°C for 20 and 40 min in 0.25 M Tris-HCl buffer, pH 6.8/0.25 M NaCl and contained per ml: phospholipid vesicles (1 μmol P), 177 ng Fp (3.2 units), 500 nmol OTA, varying amounts of cytochrome P-450 (0-1 nmol), 110 nmol Fe^{3+} and 200 nmol NADPH. Each point represents the mean ± SD of duplicate incubations from one experiment typical of two.

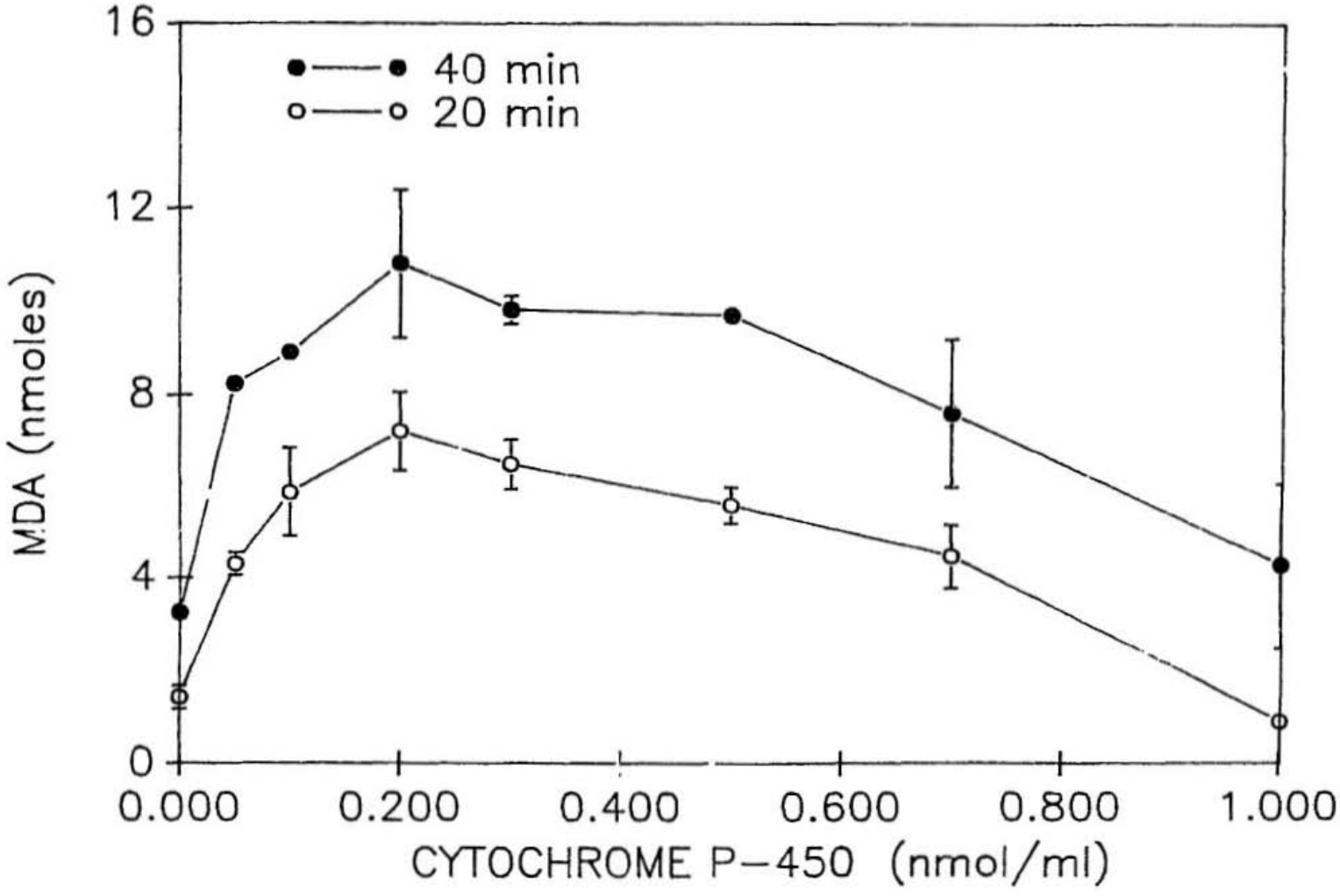
16
12
8
4
0
40 min
20 min
MDA (nmoles)
0.000
0.200
0.400
0.600
0.800
1.000
CYTOCHROME P-450 (nmol/ml)

4.4.2 Effect of inhibiting cytochrome P-450

Cobalt protoporphyrin IX pretreatment of rats has been shown to dramatically lower hepatic cytochrome P-450 levels (187). I thus compared liver microsomes from untreated rats and Co-protoporphyrin IX-pretreated rats for their ability to promote OTA-induced lipid peroxidation. Cobalt protoporphyrin IX drastically inhibited both cytochrome P-450 and cytochrome P-450 reductase (Fp), by 80% and 75% respectively. To avoid the possible effect of a lowered Fp content, microsomes from cobalt protoporphyrin-treated rats were fortified by incubating them with purified Fp. Fatty acid analysis of both kinds of microsomes using gas chromatography (GC) showed no significant differences (Fig. 20A and B). These precautions substantially reduced the possibility of other factors being involved and strongly suggested that the limiting factor in the lipid peroxidation reaction was cytochrome P-450. The results indicated that Co-protoporphyrin microsomes were only 50% as efficient as control microsomes in promoting OTA-stimulated lipid peroxidation (Fig. 21).

4.5 Role of OTA and EDTA in reduction of Fe^{3+} to Fe^{2+}

The reduction of Fe^{3+} to Fe^{2+} was followed over a 15 min period by recording the increase in absorbance at 535 nm due

Figure 20. **Fatty acid analysis of microsomal lipids extracted from: A) control and B) cobalt protoporphyrin IX pretreated rats.** Individual fatty acid methyl esters were separated by a Hewlett Packard Gas Chromatograph equipped with 30 m Supelcowax 10 wide bore capillary column, 0.75 mm i.d. (Supelco Canada Ltd., Oakville Ontario), and a flame ionization detector. The following separation protocol was used: carrier gas, He at 15 ml/min., isothermal at 195 °C. Individual fatty acids are indicated on the chromatograms.

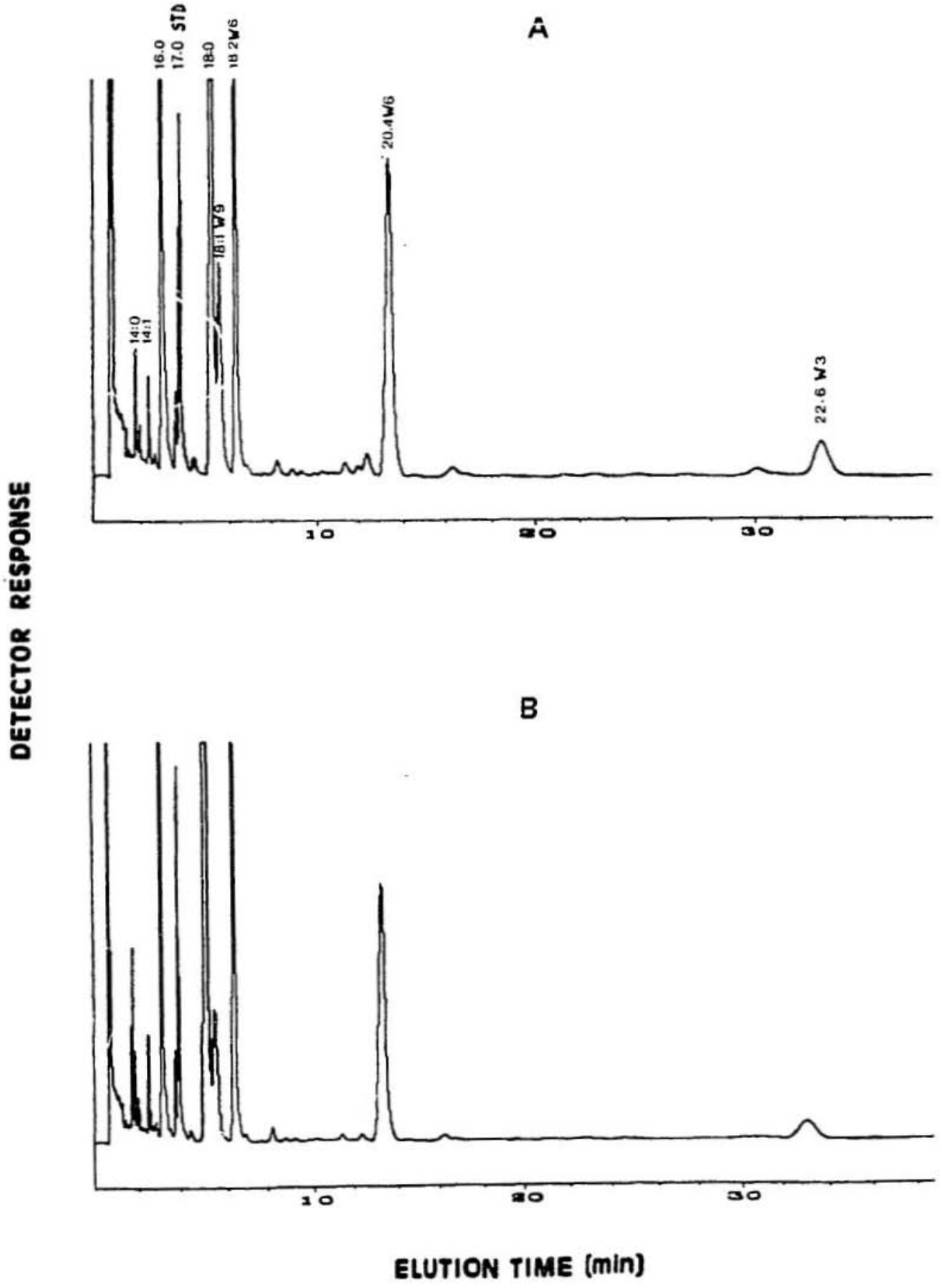
A
B
16.0
17.0 STD
18:0
18:2W6
18:1 W9
20:4W6
14:0
14:1
22:6 W3
10
20
30
DETECTOR RESPONSE
ELUTION TIME (min)

Figure 21. **The effect of reducing cytochrome P-450 content on OTA stimulated lipid peroxidation.** Incubations were carried out at 37°C for 0, 5, 20 and 40 min in 100 mM phosphate buffer, pH 7.4 and contained per ml: 2 mg microsomal protein (control or treated, 2.9 & 0.6 nmol cytochrome P-450/mg protein, respectively) and 125 nmol OTA. The reaction was initiated with 1 mM NADPH (final concentration). Microsomes from rats pretreated with cobalt protoporphyrin (before use in lipid peroxidation) were first fortified for Fp by incubating them with the purified enzyme preparation (as described in section 3.2.4. The results represent one experiment typical of two.

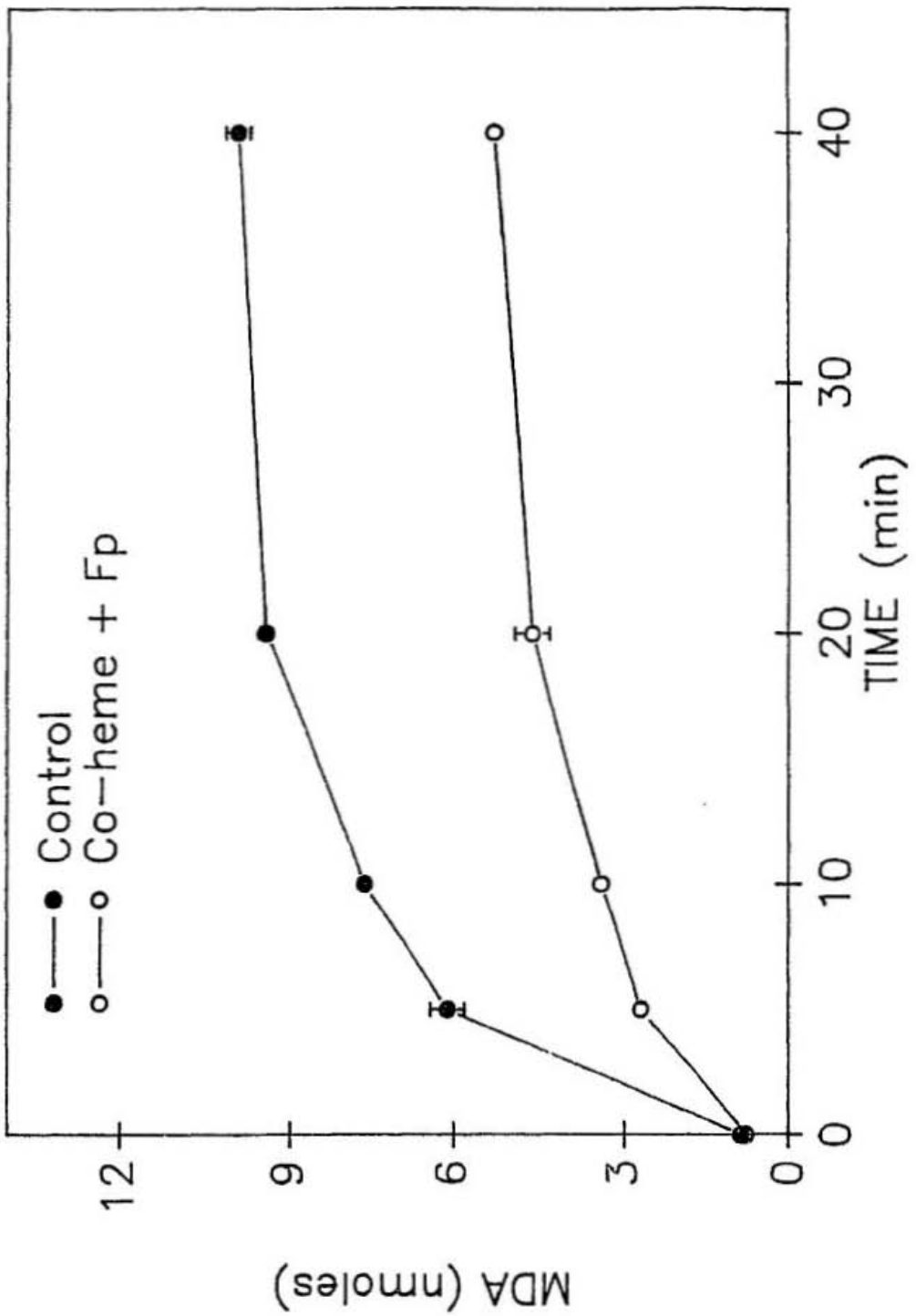
MDA (nmoles)
12
9
6
3
0
0
10
20
30
40
TIME (min)
Control
Co-heme + Fp

to formation of the Fe^{2+}-BPS complex (Fig. 22). No reduction of Fe^{3+} was observed in the absence of NADPH while the maximum rate of reduction was observed in the complete system which included both OTA and EDTA (11.7 nmol/min). Omission of EDTA led to a 21% reduction in the rate of Fe^{2+} formation (9.2 nmol/min), while deletion of OTA reduced the rate by 70% (3.5 nmol/min). In the absence of both EDTA and OTA the rate of Fe^{2+} formation was only 2.7 nmol/min (Fig. 22). The data clearly show that OTA by itself substantially increases the rate of Fe^{3+} reduction, and that addition of EDTA further enhances this effect.

4.6 Formation of Fe^{3+}-OTA complex

When anhydrous $FeCl_3$, dissolved in methanol, is added to OTA in methanol, a reddish-brown complex is formed with a λ_{max} at 342 and 483 nm (Fig. 23A). The spectrum of the Fe^{3+}-OTA complex in aqueous pH 8.6 Tris buffer (Fig. 23B) was similar to that found in methanol except that the peak at 483 nm was converted into a shoulder. The spectrophotometric titration of 190 μM OTA with $FeCl_3$ (Fig. 24) indicated that in methanol a 1:1 Fe^{3+}-OTA complex was formed, though formation of the complex may not be complete even with five fold molar excess of Fe^{3+}. Attempts to perform similar spectrophotometric titrations in either pH 7.0 or 8.6 aqueous Tris buffers were unsuccessful due to

Figure 22. Effect of various components on iron reduction.

The rate of Fe^{3+} reduction was followed spectrophotometrically by measuring the rate of Fe^{2+}-bathophenanthroline-disulfonic acid formation at 535 nm. The reaction was carried out at 37°C in 0.25 M Tris-HCl buffer, pH 6.8/0.25 M NaCl in a 3 ml spectrophotometer cuvette and contained per ml: 110 nmol Fe^{3+}, 250 nmol OTA, 177 ng Fp (3.2 units), 10 nmol EDTA, 400 nmol bathophenanthroline-disulfonic acid and 200 nmol NADPH. Details are as described in section 3.2.9. The results represent one experiment typical of two.

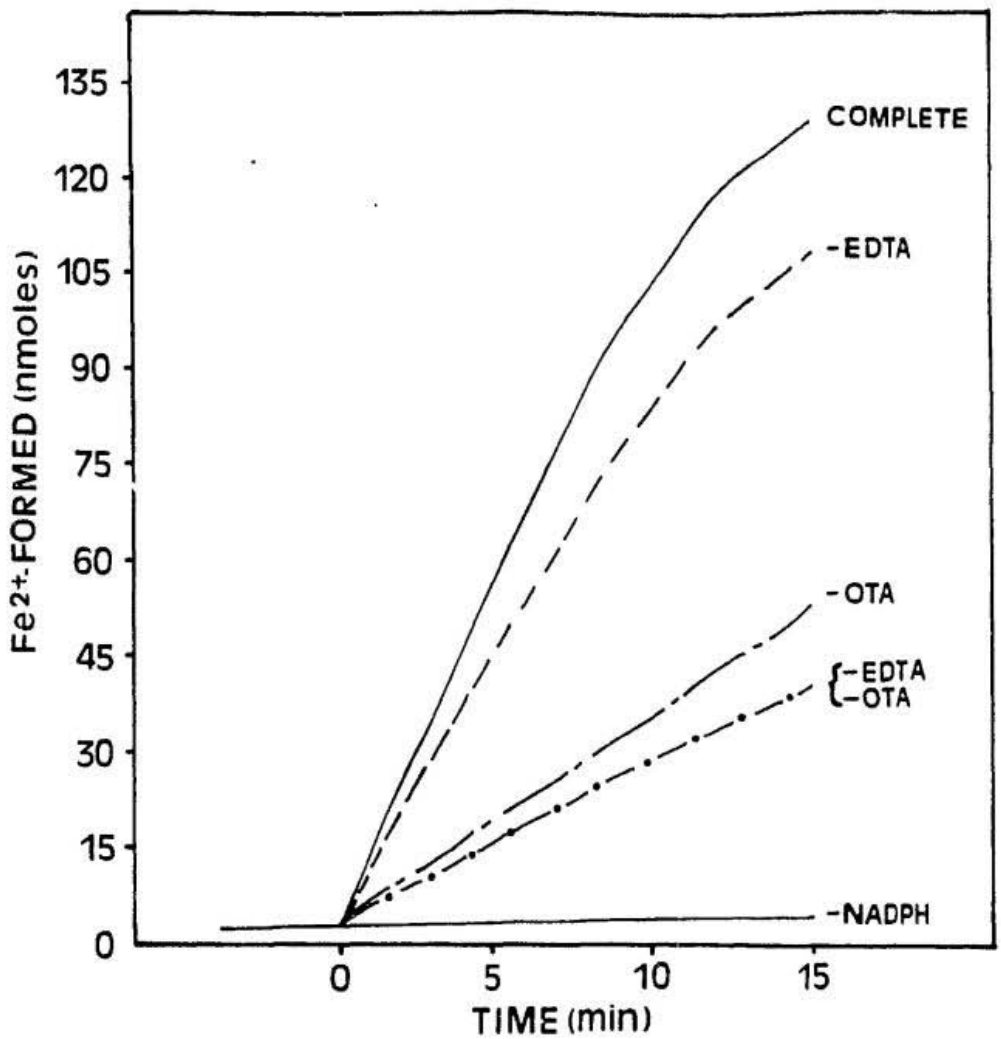
135
120
105
90
75
60
45
30
15
0
Fe2+-FORMED (nmoles)
0
5
10
15
TIME (min)
COMPLETE
-EDTA
-OTA
-EDTA
-OTA
-NADPH

Figure 23. **A: Spectrum of the Fe^{3+}-OTA complex formed in methanol.**

The concentrations of Fe^{3+} and OTA were both 200 μM. Arrows point at the corresponding absorbance scales.

B: Spectrum of Fe^{3+}-OTA complex in Tris buffer.

$FeCl_3$ and OTA, both dissolved in methanol, were mixed together and then diluted into the buffer (pH 8.6). The Fe^{3+} and the OTA concentrations were, after dilution, 330 and 1000 μM, respectively. A small amount of precipitate was observed in the cell after dilution of Fe^{3+}-OTA complex into the buffer. The broken line (---) is the spectrum of OTA alone and the continuous line (——) that of the Fe^{3+}-OTA complex.

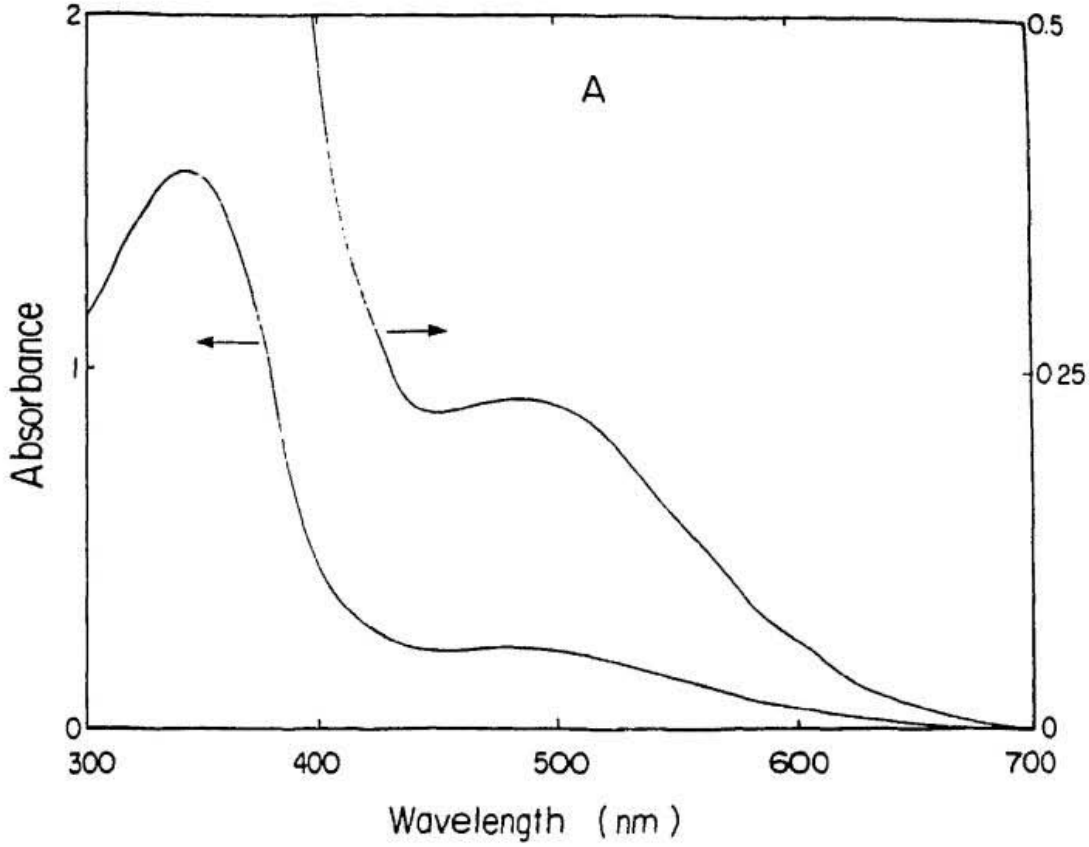
A
Absorbance
2
1
0
0.5
0.25
0
300
400
500
600
700
Wavelength (nm)

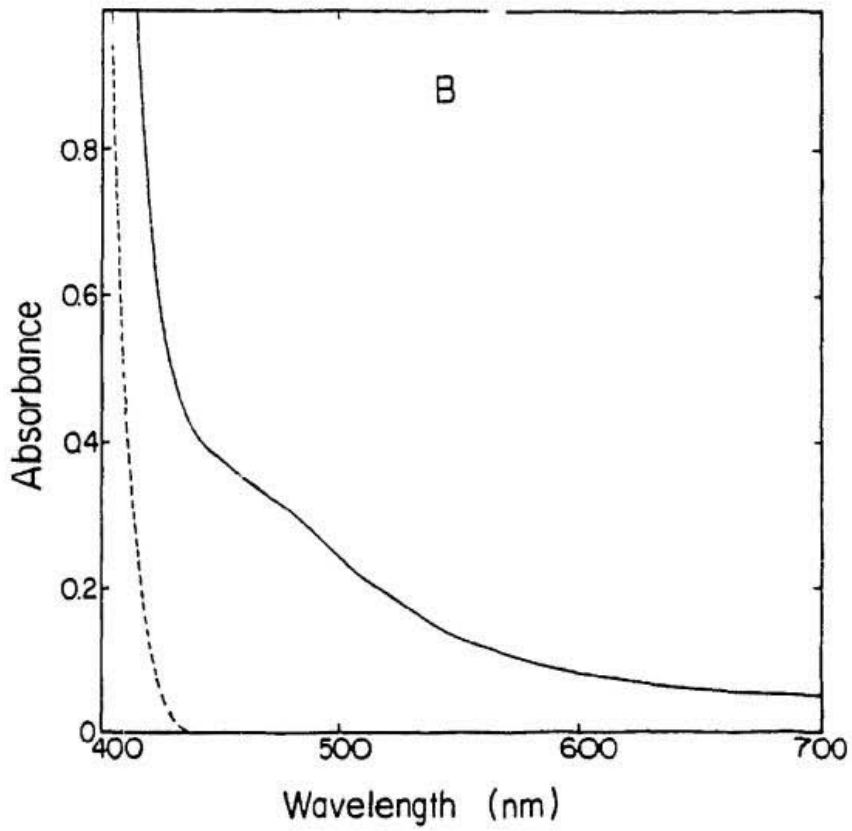
B
Absorbance
0.8
0.6
0.4
0.2
0
400
500
600
700
Wavelength (nm)

Figure 24. **Titration of OTA by $FeCl_3$.**

Spectrophotometric titration at 490 nm of 190 μM OTA by $FeCl_3$. The solvent used was methanol. The intersection of the two least squares calculated straight lines (through the lowest 5 and the highest 3 data points, respectively) intersect at a mole ratio of 1.0 indicating that a 1:1 complex is formed under these conditions.

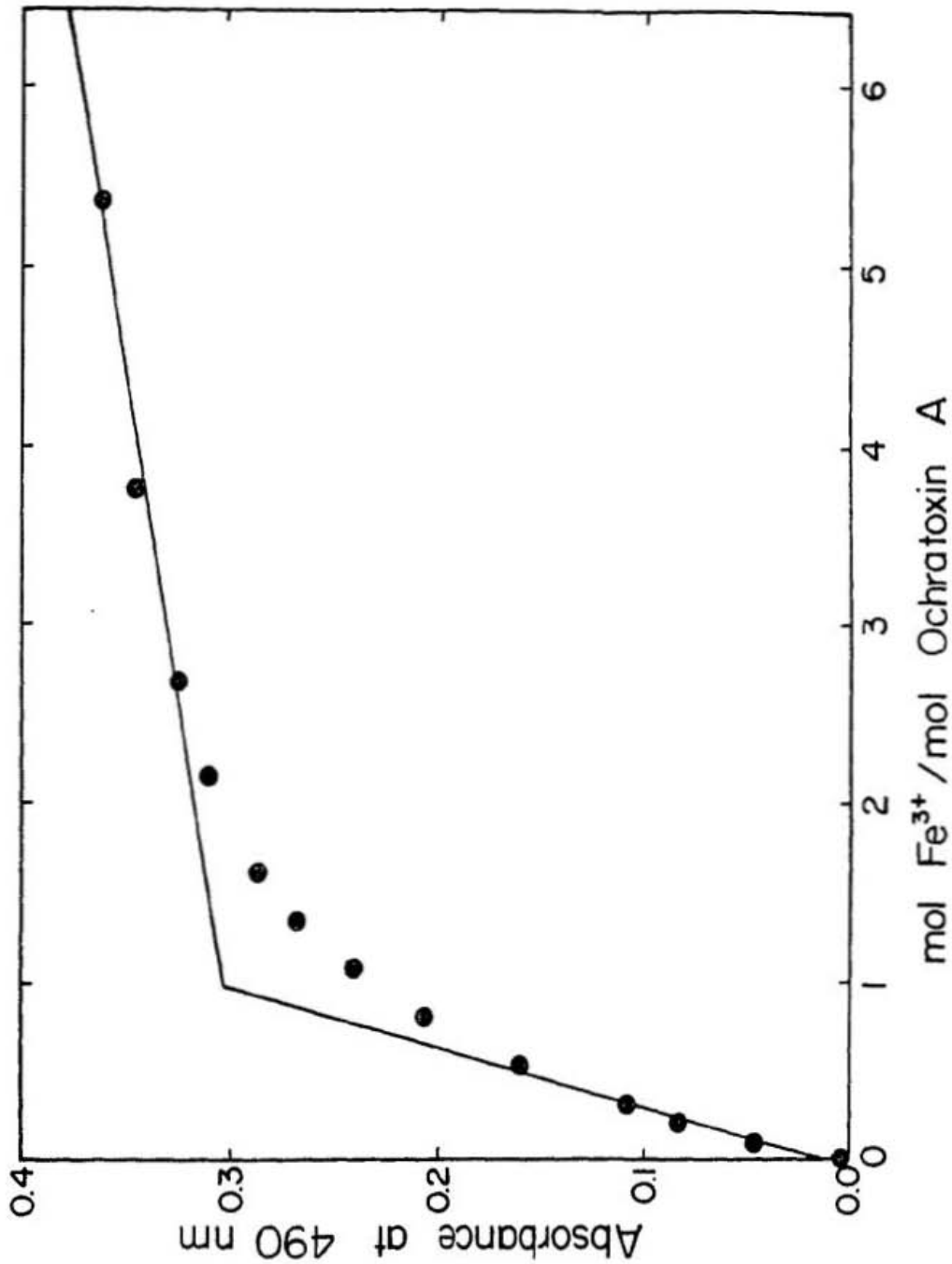
Absorbance at 490 nm
0.0
0.1
0.2
0.3
0.4
0
1
2
3
4
5
6
mol Fe3+/mol Ochratoxin A

insolubility problems with both OTA and the Fe^{3+}-OTA complex.

The binding of Fe^{3+} to OTA in methanol was also followed fluorometrically (Ex_{max} 340 nm; Em_{max} 465 nm) (Fig. 25A and B). Experiments at a constant OTA concentration of 5 μM and in the presence of increasing amounts of $FeCl_3$, showed that the fluorescence was about one-half quenched at a 6-fold excess of $FeCl_3$ (Fig. 25B) and completely quenched at a 40-fold excess of $FeCl_3$. Assuming an equilibrium of the type:

$$Fe^{3+} + HL \rightleftharpoons FeL^{2+} + H^+$$

$$K = \frac{[FeL^{2+}]\,[H^+]}{[Fe^{3+}][HL]}$$

it can be calculated from the titration data of Fig. 25A, which was carried out in the presence of 100 μM HCl, and from an additional titration conducted under the same conditions but at a constant $FeCl_3$ concentration of 1 μM, that K has a value of 19±6 (n = 11) (L^- and HL are the phenolate anion and phenol forms of OTA, respectively). In order to calculate the related association constant, K_{ass} for

$$Fe^{3+} + L^- \rightleftharpoons FeL^{2+}$$

$$K_{ass} = \frac{[FeL^{2+}]}{[Fe^{3+}][L^-]}$$

Figure 25. **Quenching of OTA fluorescence by Fe^{3+}.**

A: Change in fluorescence when OTA is added to a solution containing no (0) and 5 μM $FeCl_3$ (●), respectively. The solvent was methanolic HCl (100 μM).

B: Change in fluorescence when $FeCl_3$ (in 10 mM HCl) is added to 5 μM OTA in methanol.

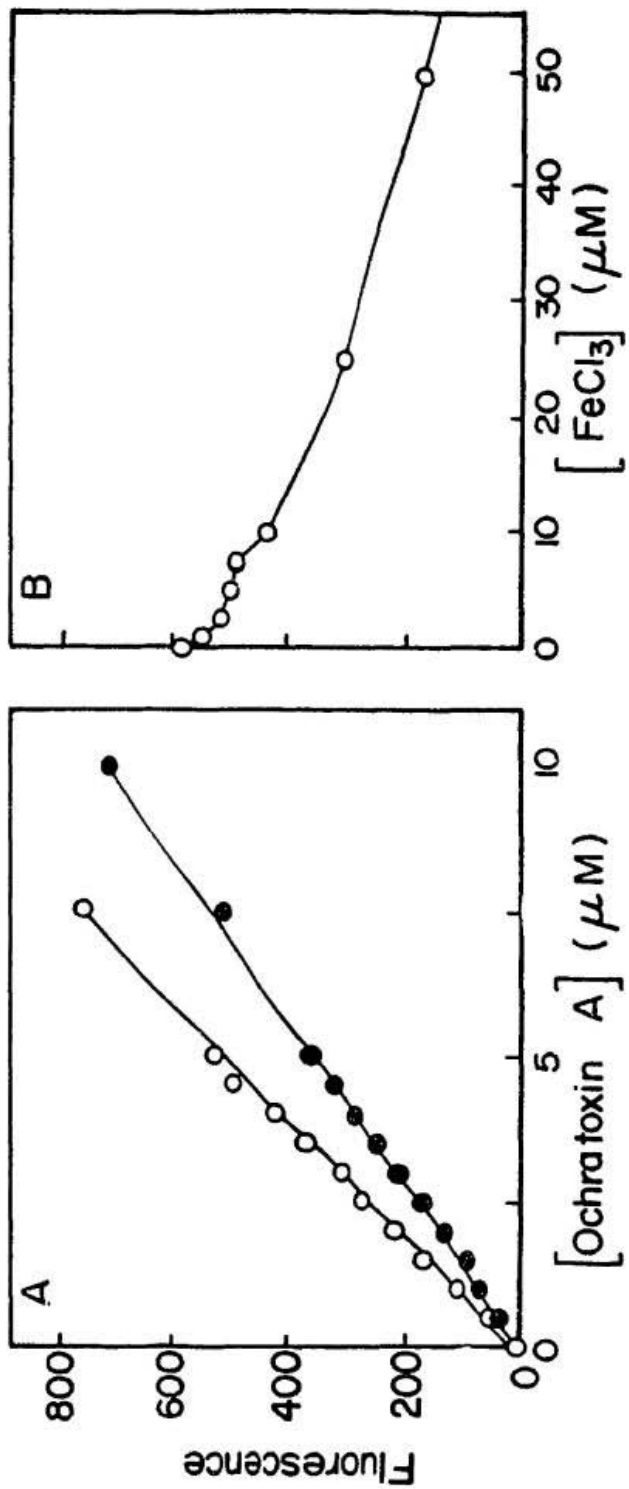
A
B
Fluorescence
800
600
400
200
0
0
5
10
[Ochratoxin A] (μM)
0
10
20
30
40
50
[FeCl3] (μM)

it is necessary to know the pK_a of HL (assumed to be that of the phenolic group). While this value is unknown in methanol, assuming that it is the same as it is in water (pK_a 7.05 [159]), K_{ass} can then be calculated to be approximately 2×10^8 M^{-1}. While this K_{ass} can be considered to be only an order-of-magnitude estimate of the value that might be obtained in aqueous solution, its magnitude does indicate that OTA is capable of forming a relatively strong complex with Fe^{3+}, even in the micromolar concentration range.

4.7 Detection of hydroxyl radical formation by ESR and effect of various components on free radical formation

4.7.1 Effect of Fp

The ESR spectrum shown in Fig. 26 has the characteristic 1:2:2:1 4-line spectrum found for DMPO-OH (154). Fig. 26A represents a complete reaction system containing Fe^{3+}, OTA, Fp, NADPH and DMPO. The hyperfine splitting constants were measured from Fig. 26A to be $A_N = A_H$ = 14.9 G, which is identical to that reported by Finkelstein et al. (154). In the absence of NADPH-cytochrome P-450 reductase (Fig. 26B), the amount of DMPO-OH produced is significantly reduced, indicating that the reductase is largely responsible for the production of DMPO-OH.

Figure 26. **A:** **ESR spectrum** recorded at room temperature after Fe^{3+}-OTA (1 mM Fe^{3+}, 3 mM OTA) in Tris buffer (pH 8.5) was incubated for 55 min with NADPH-cytochrome P-450 reductase (7.5 μg protein/ml), NADPH (1 mM) and DMPO (90 mM). The instrument settings were as follows: microwave frequency 9.8 GHz, microwave power 6.3 mW, modulation amplitude 2G, and receiver gain 4 x 105.

B: As in A above, but in the absence of the reductase.

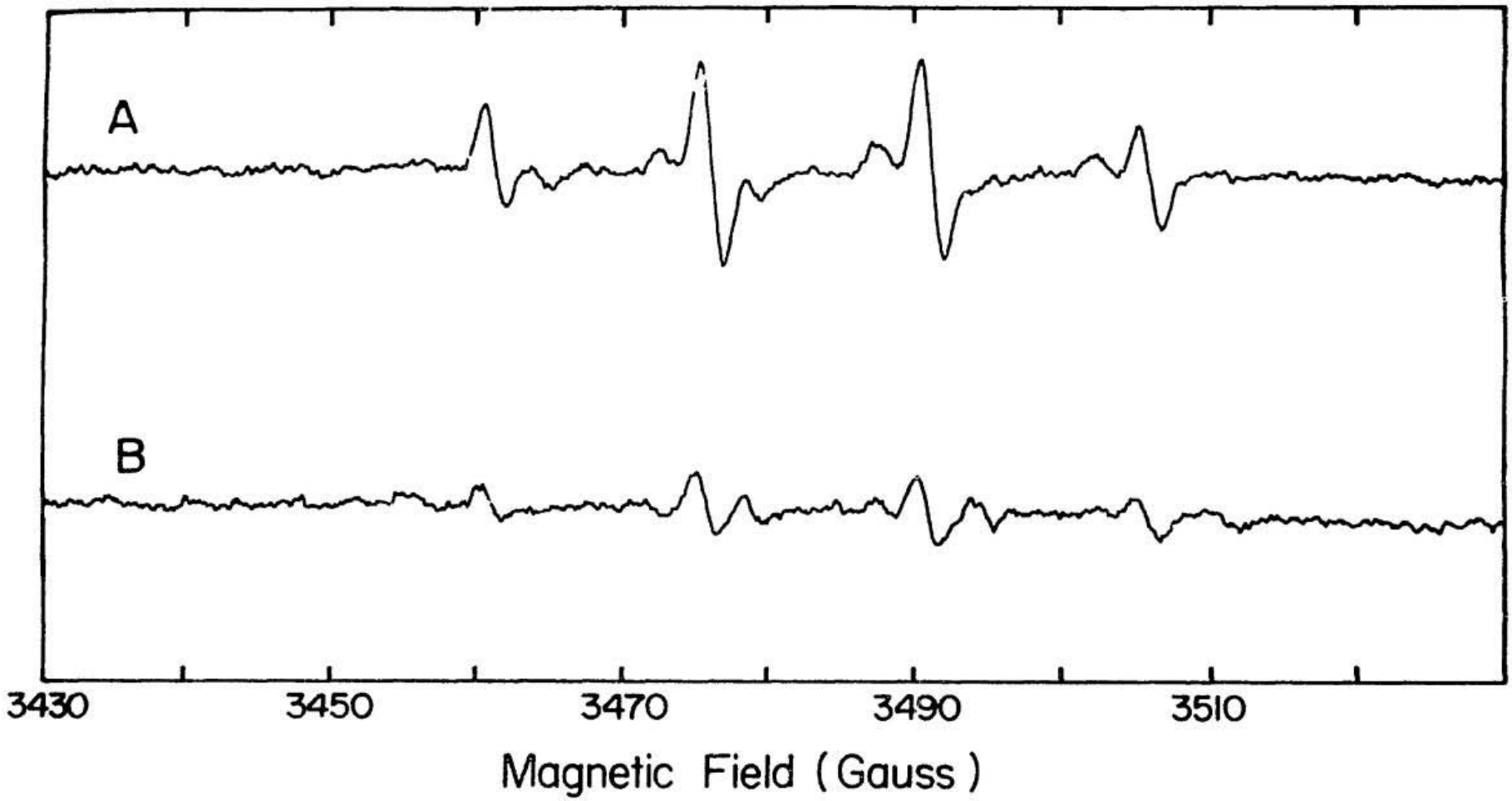
A
B
3430
3450
3470
3490
3510
Magnetic Field (Gauss)

4.7.2 Effect of ethanol

While the 4-line spectrum shown in Fig. 26A of DMPO-OH is known to be produced from the reaction of hydroxyl radical wi: DMPO, it is also known that DMPO-$O_2^{\cdot -}$, formed from the reaction of O_2 with DMPO, decays rapidly to DMPO-$OH^{\cdot}$ (154). Thus, in order to distinguish hydroxyl radical production from $O_2^{\cdot -}$ production, experiments were also carried out in the presence of the hydroxyl radical scavenger ethanol. The hydroxyl radical rapidly reacts with ethanol to form an alkoxyl radical, which then reacts with DMPO to form a 1:1:1:1:1:1 6-line spectrum produced by the carbon-centered DMPO-CH(OH)-CH_3 adduct (154). As shown in Fig. 27 (A, B and C), when the concentration of ethanol is increased (0%, 3% and 5% (v/v), respectively), the 4-line DMPO-OH spectrum is gradually replaced by increasing amounts of a 6-line spectrum which demonstrates that the 6-line spectrum is ethanol-derived. The hyperfine splitting constants of the 6-line spectrum were measured to be A_N = 15.9 G and A_H = 23.1 G which are very close to previously reported values (154-156) for the carbon-centered DMPO-CH(OH)-CH_3 radical. The results shown in Figs. 26 and 27 thus confirm the production of hydroxyl radicals in the reaction system.

Figure 27. **ESR spectra** recorded after 20 min in the presence of increasing amounts of ethanol. A: No added ethanol; B: 3% (v/v) ethanol; C: 5% (v/v) ethanol. Except as noted above, the reaction mixture and the instrument settings were identical to those in Figure 26A.

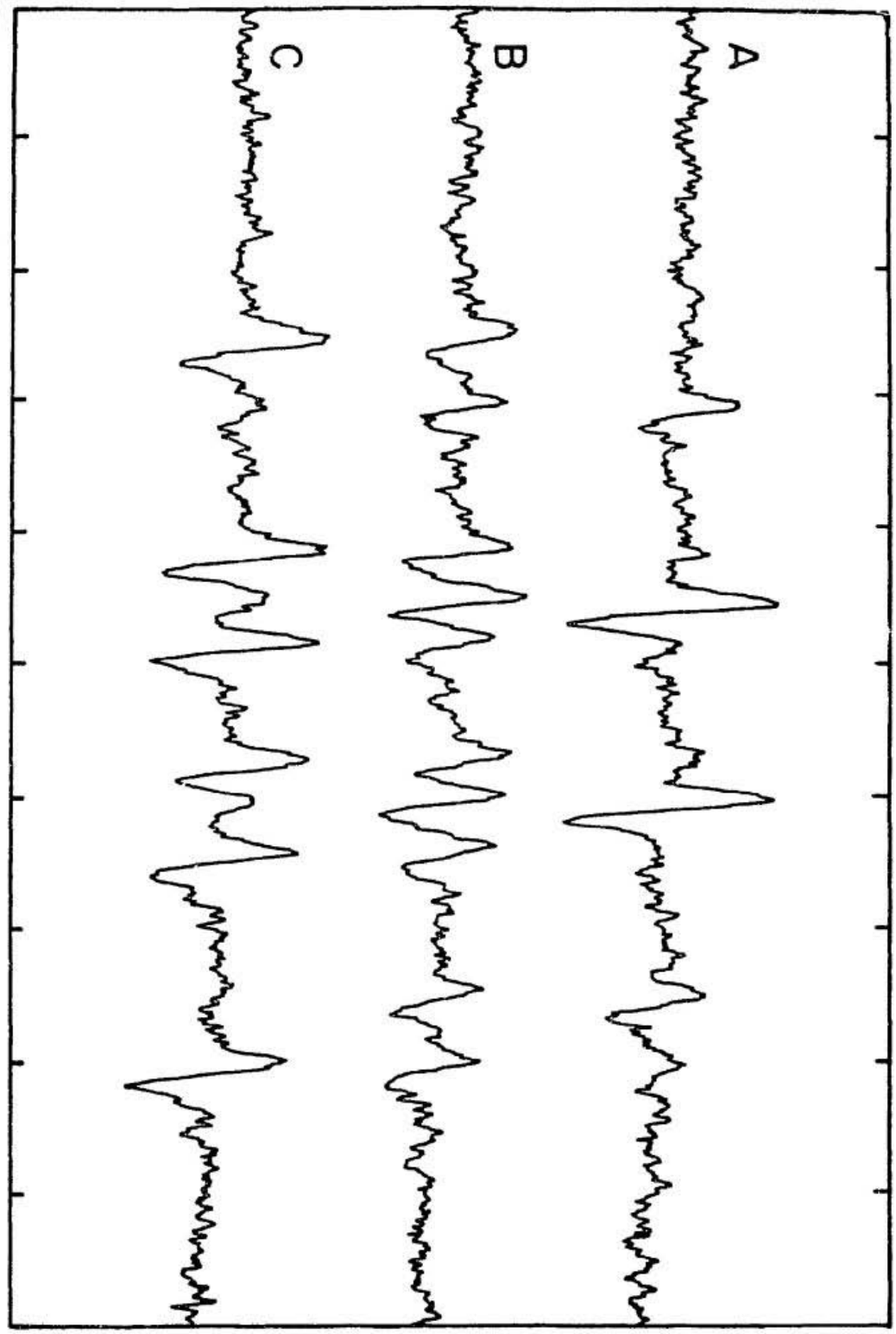
A
B
C
3430
3450
3470
3490
3510
Magnetic Field (Gauss)

4.7.3 Effect of OTA, Fe^{3+} and catalase

Fig. 28A shows the 6-line spectrum for a complete reaction system containing Fe^{3+}, OTA, Fp, NADPH and DMPO, in addition to 5% (v/v) ethanol. As shown in Fig. 28B in the absence of either any added Fe^{3+} or OTA, a significant amount of 4-line spectrum due to DMPO-OH· is produced. Since the NADPH-cytochrome P-450 reductase system is known to produce O_2^- on its own (157,158), the DMPO-OH· is likely being produced either from decomposition of DMPO-O_2^- or from DMPO-OH· (154), or from both. The addition of catalase (which catalyzes the decomposition of H_2O_2 to O_2 and H_2O) to the complete reaction system almost completely abolished the production of the hydroxyl-radical derived 6-line spectrum (Fig. 28C). In fact, upon the addition of catalase, a visible evolution of a gas which was assumed to be O_2 occurred. These results indicate that H_2O_2 is required for the production of hydroxyl radical. When OTA was omitted from the complete system (Fig. 28D) in a control experiment, very little 6-line spectrum was observed. This result demonstrates that complexation of Fe^{3+} by OTA is necessary for hydroxyl radical production.

4.8 Structure-activity relationship studies

Different OTA analogues were tested for their ability

Figure 28. **ESR spectra** recorded after a 20 min incubation of the reaction system described in the caption to Figure 27C except as noted: A. complete reaction system; B. absence of added Fe^{3+} or OTA: C. added catalase at a final concentration of 0.1 mg/ml; D. absence of OTA.

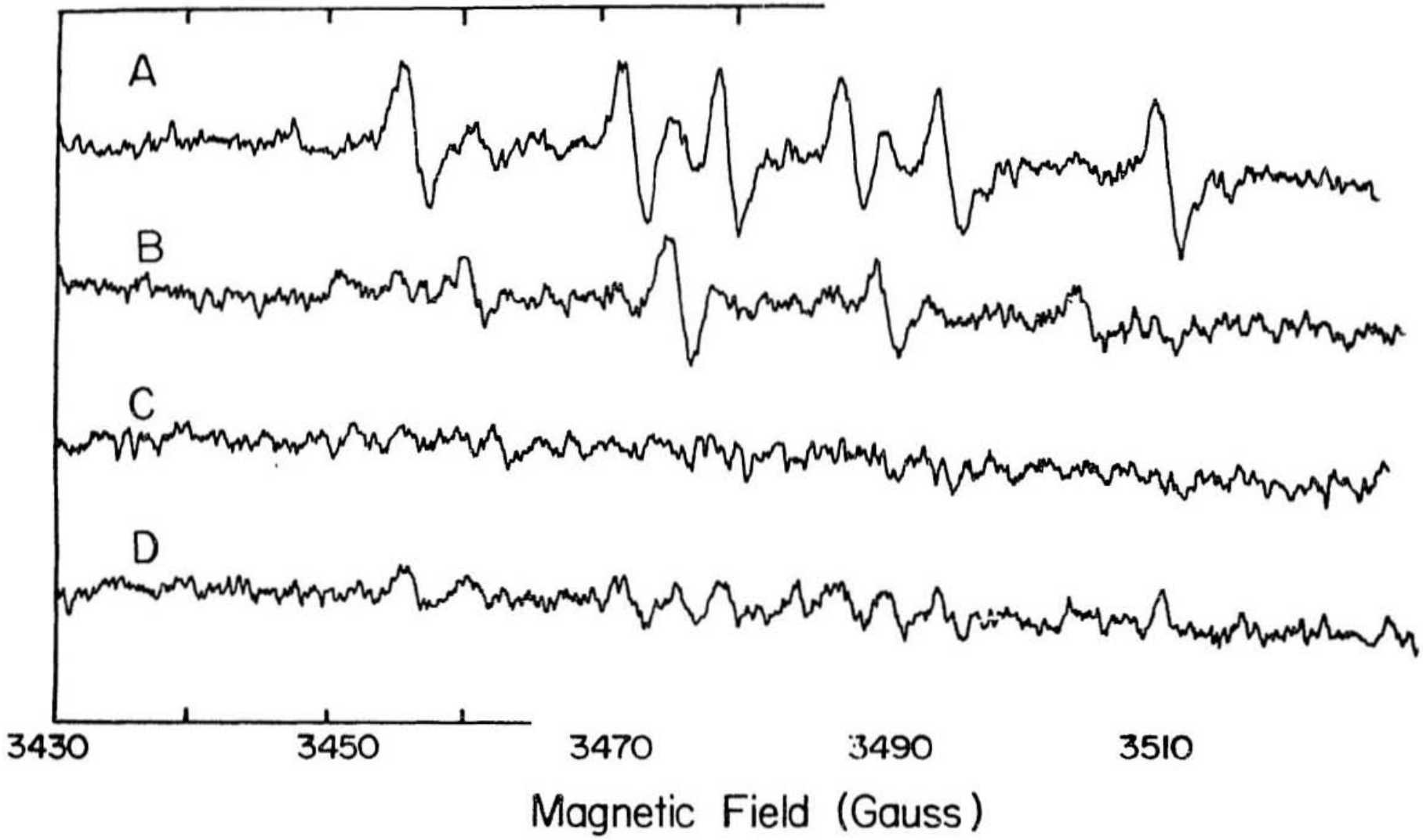
A
B
C
D
3430
3450
3470
3490
3510
Magnetic Field (Gauss)

to stimulate lipid peroxidation in the reconstituted system. Besides OTA, ochratoxin B (OB), ochratoxin C (OC) and ochratoxin α (Oα) were used to characterize the importance of the chlorine atom, the free carboxyl group and the Phe moiety, respectively (Fig. 29). In addition, the L-Phe moiety was replaced by different amino acids (L-Ser, L-Pro and L-Glu) for further characterization of the importance of the L-Phe moiety (Fig. 29). Fig. 30 shows the effect of OTA, OB, OC, Oα (all at 250 μM) on the rate of lipid peroxidation measured as MDA formation. As expected OTA gave the highest stimulation of lipid peroxidation (about 9 nmol MDA/hr); this was followed by OC (about 4.5 nmol MDA/hr). Oα and OB were the least effective (about 2.3 and 1.3 nmol MDA/hr, respectively), while the lack of any added toxin resulted in virtually no lipid peroxidation.

The rate of ferric reduction was also measured in the presence of each of these compounds (OTA, OB, OC and Oα, all 250 μM) (Fig. 31). The highest reduction rate was achieved in the presence of OTA (~ 13.0 nmol Fe^{2+} formed/min). In the presence of OB or OC the reduction rate of Fe^{3+} was 5.8 and 4.7 nmol/min, respectively. Oα resulted in a Fe^{3+} reduction rate of 1.7 nmol/min which is even slower than control (3.5 nmol/min with no added toxin). As expected, in the absence of the reductant NADPH no reduction was seen.

In Fig. 32 the results obtained with Ser-Oα, Pro-Oα, Glu-Oα and Oα are compared to OTA (500 μM each). OTA was

the most effective of all (about 18 nmol MDA formed in 1 hr), while the rest of the tested compounds resulted in the formation of MDA in the range between about 3.5 to 5.5 nmol in 1 hr.

Figure 29. Structures of OTA analogues

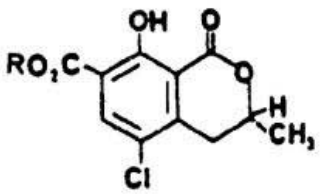

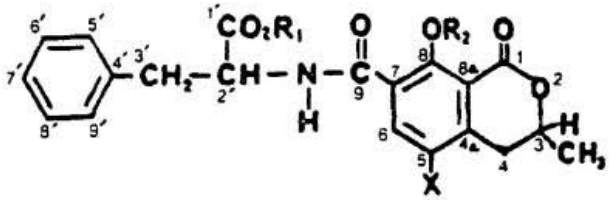

Ochratoxin A: X = Cl; $R_1 = R_2 = H$

Ochratoxin B: X = H; $R_1 = R_2 = H$

Ochratoxin C: X = Cl; $R_1 = CH_3$; $R_2 = H$

Ochratoxin α (Oα): R = H

Serine-Oα: R = L-Serine

Proline-Oα: R = L-Proline

Glutamic Acid-Oα: R = L-Glutamic Acid

Figure 30. **Effect of various ochratoxins on MDA formation.**

Incubations were carried out at 37°C for 20, 40 & 60 min in 0.25 M Tris-HCl buffer, pH 6.8/0.25 M NaCl and contained per ml: phospholipid vesicles (1 μmol P), 177 ng Fp (3.2 units), various toxins (OTA, OC, OB, Oα and no toxin; all toxins were used at a concentration of 250 μM), 25 nmol EDTA, 110 nmol Fe^{3+} and 200 nmol NADPH. Each point represents the mean ± SD of duplicate incubations from one experiment typical of two.

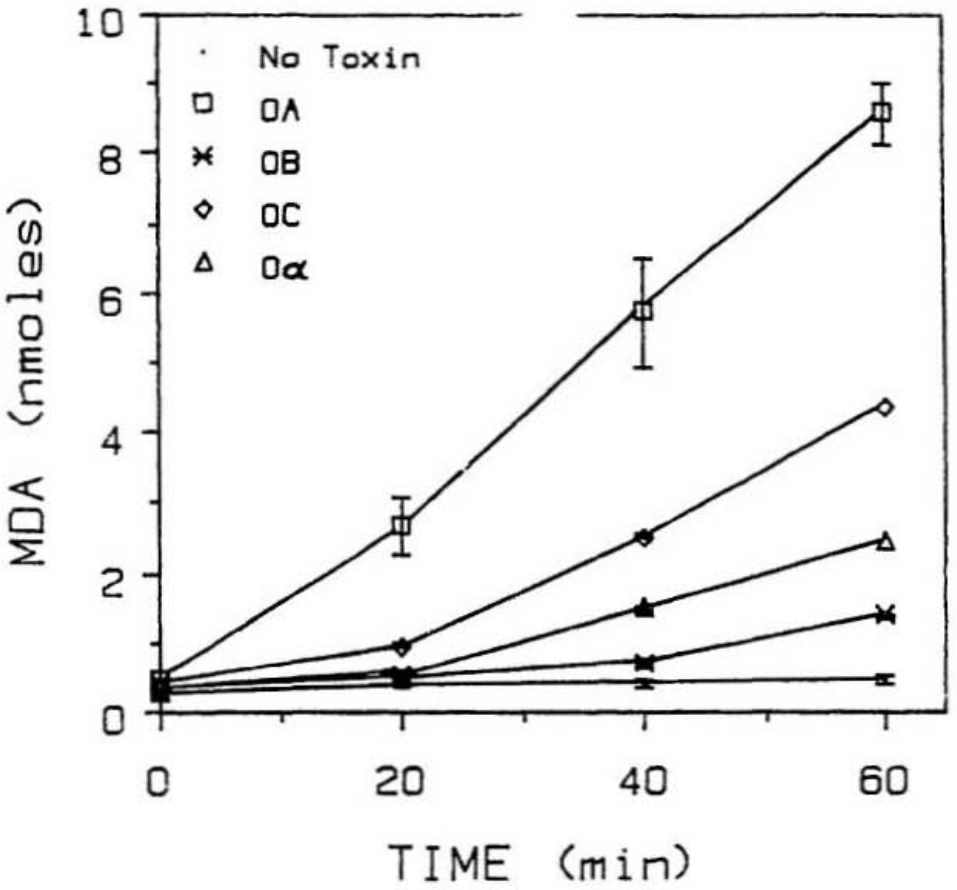
10
8
6
4
2
0
MDA (nmoles)
No Toxin
OA
OB
OC
Oα
0
20
40
60
TIME (min)

Figure 31. Effect of various ochratoxins on iron reduction.

Incubations were carried out at 37°C in 0.25 M Tris-HCl buffer, pH 6.8/0.25 M NaCl in a 3 ml spectrophotometer cuvette and contained per ml: 250 nmol of various toxins (OTA, OB, OC, Oα or no toxin), 110 nmol Fe^{3+}, 177 ng Fp (3.2 units), 10 nmol EDTA, 400 nmol bathophenanthroline-disulfonic acid and 200 nmol NADPH. The results represent one experiment typical of two.

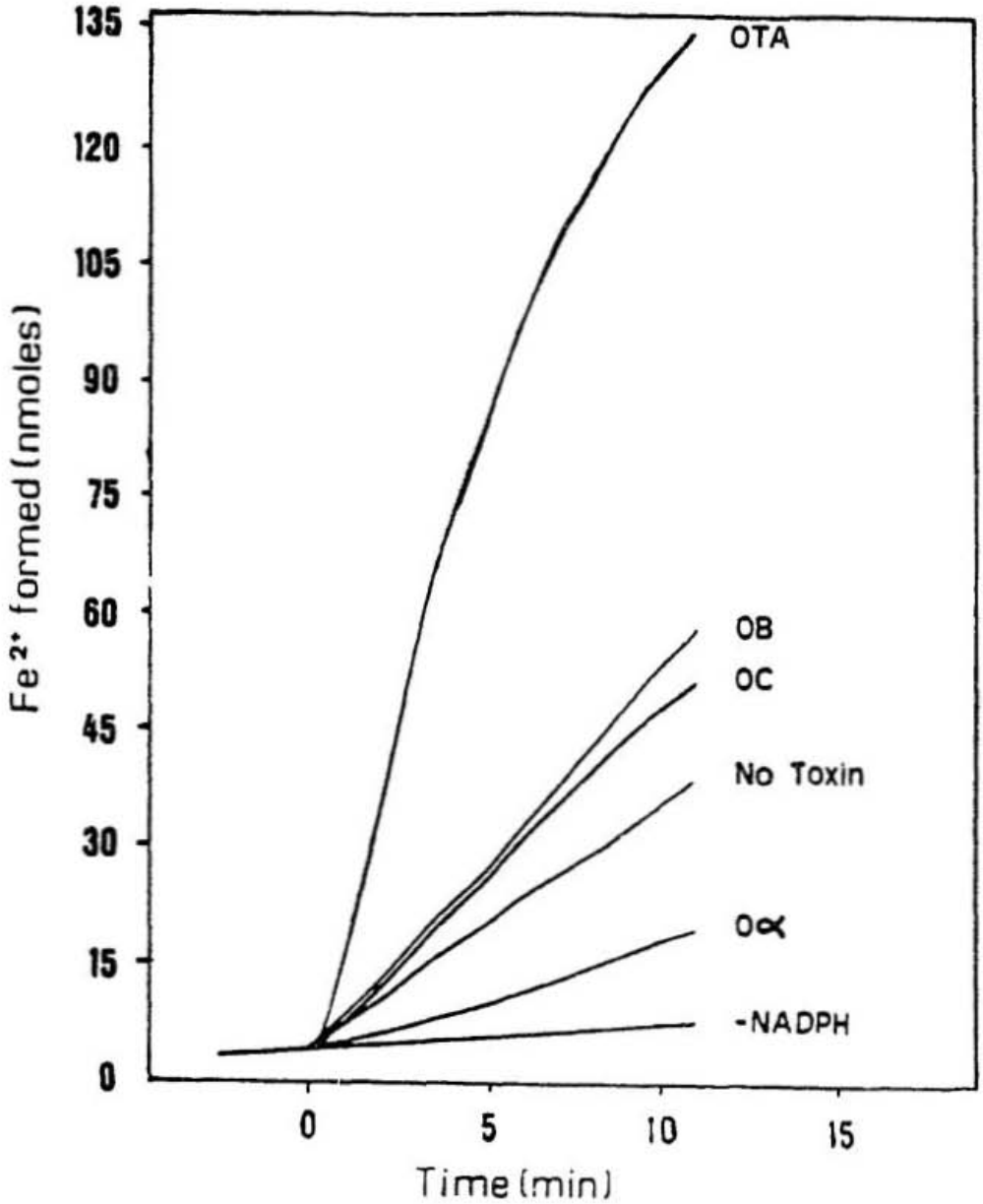
135
120
105
90
75
60
45
30
15
0
Fe²⁺ formed (nmoles)
0
5
10
15
Time (min)
OTA
OB
OC
No Toxin
Oα
-NADPH

Figure 32. **Effect of various OTA analogues on MDA formation.**

Incubations were carried out at 37°C for 0, 20, 40 & 60 min in 0.25 M Tris-HCl buffer, pH 6.8/0.25 M NaCl and contained per ml: phospholipid vesicles (1 μmol P), 177 ng Fp (3.2 units), various toxins (OTA, Oα, Ser-Oα, Glu-Oα , Pro-Oα or no toxin, all at a concentration of 500 μM), 25 nmol EDTA, 110 nmol Fe^{3+} and 200 nmol NADPH. Each point represents the mean ± SD of duplicate incubations from one experiment typical of two.

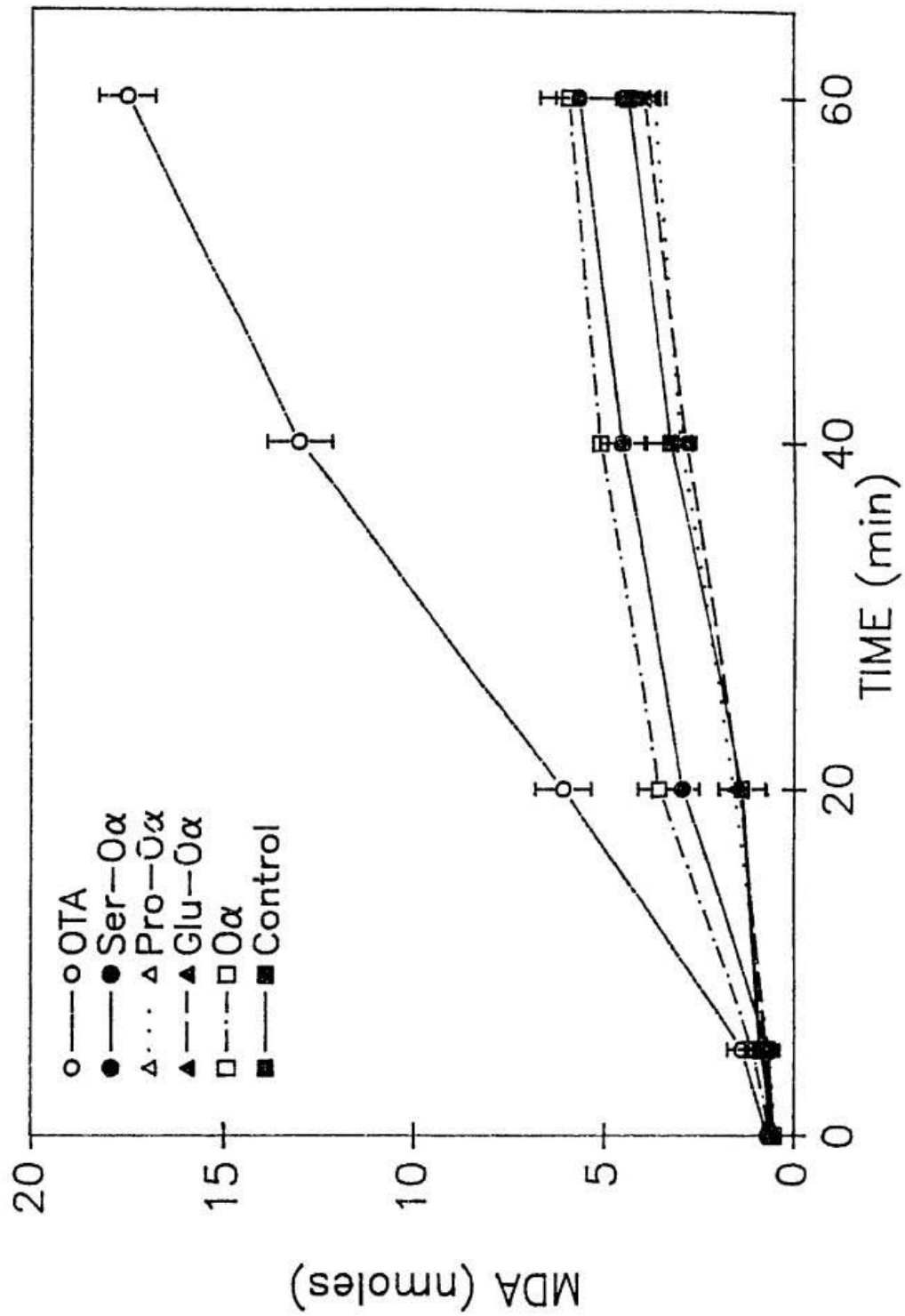
MDA (nmoles)
20
15
10
5
0
0
20
40
60
TIME (min)
OTA
Ser—Oα
Pro—Oα
Glu—Oα
Oα
Control

CHAPTER 5

DISCUSSION

Membrane lipid peroxidation is an important part of oxidative tissue injury and can be an effect as well as a cause of reactions culminating in cytotoxicity (160). A wide and ever-increasing range of compounds have been shown to induce lipid peroxidation both *in vitro* and *in vivo* (134,135 for reviews). Xenobiotics may enhance lipid peroxidation in one of several ways. Haloalkanes such as carbon tetrachloride initiate lipid peroxidation subsequent to cytochrome P-450-dependent reductive activation to the trichloromethyl radical (161). A variety of other agents such as paraquat (162), mitomycin c and nitrofurantoin (163) can redox cycle, resulting in oxygen radical formation which can stimulate lipid peroxidation. Yet other compounds such as acetaminophen and bromobenzene initiate lipid peroxidation through depletion of cellular glutathione (164). Finally, compounds such as ADP can chelate iron, and the resulting ADP-iron complex can undergo enhanced redox cycling thus stimulating lipid peroxidation (67). By using a reconstituted system, I was able to show that OTA stimulates lipid peroxidation by the last mentioned mechanism. Consistent with this is the observation that HPLC analysis did not reveal any appreciable biotransformation of OTA.

The data clearly indicate that a reconstituted system consisting of phospholipid vesicles, purified reductase, OTA, EDTA, Fe^{3+} and NADPH is efficient in carrying out lipid peroxidation, measured either as MDA formation (Fig. 12) or by oxygen uptake (Fig. 14). Omission of OTA gave rise to very little peroxidation (< 10%) while deletion of EDTA reduced the extent of MDA formation by 70% (Fig. 12). Pederson and Aust (69) first characterized such a lipid peroxidation system using ADP instead of the OTA used here. In their reconstituted system, EDTA was required as well since no peroxidation occurred in its absence (69). Fe^{3+} ions rapidly precipitate out of neutral aerobic solutions to form insoluble ferric hydroxides and it was recognized some time ago that complexing iron with ligands such as ADP and EDTA overcame this problem (67). OTA could thus be playing a similar role. Spectrophotometric and fluorometric evidence for the formation of an Fe^{3+}-OTA complex is in support of this (Figs. 23-25).

It is generally accepted (67,134,135) that reduction of the various Fe^{3+} chelates capable of initiating lipid peroxidation proceeds via NADPH-cytochrome P-450 reductase (Fp). The ability of Fp to reduce Fe^{3+}-EDTA but not Fe^{3+}-ADP (165) is in agreement with the iron chelate requirements of the reconstituted system used by Pederson and Aust (69). In the present case, EDTA significantly enhanced the rate of OTA dependent lipid peroxidation, but was not absolutely

essential (Fig. 12). This is consistent with the fact that Fp is able to reduce Fe^{3+}-OTA, albeit more slowly, in the absence of Fe^{3+}-EDTA. It has been suggested that in microsomes another carrier could mediate the transfer of electrons from NADPH to Fe^{3+}-ADP (69). This has led to the demonstration that in a reconstituted system, cytochrome P-450 (normally present in liver endoplasmic reticulum) can replace Fe^{3+}-EDTA in stimulating lipid peroxidation (71,166). OTA-stimulated microsomal lipid peroxidation also does not require EDTA (133), and so cytochrome P-450 could play a similar role in the reconstituted system. This was confirmed when purified cytochrome P-450 was shown to effectively replace EDTA in enhancing MDA formation. The rate of MDA formation increased with increasing cytochrome P-450 concentration up to 0.2 nmol/ml (Fig. 19) which is in good agreement with what Aust et al. (71) observed when they used cytochrome P-450 in their ADP-stimulated lipid peroxidation system. Above a cytochrome P-450 concentration of 0.2 nmol/ml, the rate of MDA formation decreased, but the reasons for this are not clear at the moment.

Another piece of evidence for the participation of cytochrome P-450 in microsomal lipid peroxidation <u>in vitro</u> and possibly <u>in vivo</u> comes from the use of microsomes isolated from cobalt protoporphyrin IX-pretreated rats. The rate of MDA formation was decreased by 50% in cobalt protoporphyrin IX microsomes as compared to control

microsomes, even though the former were fortified with purified Fp. This difference is likely due to lower cytochrome P-450 levels in cobalt protoporphyrin IX microsomes. Earlier, Rahimtula et al. (unpublished data) showed that ethane exhalation was drastically reduced in cobalt protoporphyrin IX pretreated rats as compared to controls on OTA administration. Cobalt protoporphyrin IX pretreatment has been shown not to significantly alter the microsomal fatty acid composition (Fig. 20), thus ruling out such a change as the cause of reduced lipid peroxidation.

Data presented in Figs. 23-25 demonstrate the binding of Fe^{3+} to OTA, both in methanol and in aqueous solution. The cardiotoxic anthracyclic quinone antitumor drug doxorubicin also has a phenolic group beta to a carbonyl group, and likewise forms a strong complex with Fe^{3+} (167). An iron-based oxidative stress produced through an enzymatic reductive activation is thought to be partly responsible for doxorubicin-induced cardiotoxicity.

Ernster, Hochstein and co-workers (70) have investigated the role of iron and iron chelators in the initiation of microsomal lipid peroxidation. Their studies showed that in order to enzymatically initiate microsomal lipid peroxidaton an Fe^{3+} chelate has to fulfill three criteria: (i) reducibility by NADPH; (ii) reactivity of the Fe^{2+} chelate with oxygen; and (iii) formation of a relatively stable perferryl radical. They demonstrated

reduction of the various Fe^{3+} chelates by NADPH oxidation. I have shown that Fe^{3+}-OTA is reduced by measuring the formation of Fe^{2+} with bathophenanthroline disulfonate (Fig. 22). They demonstrated with the oxygen electrode both the interaction of the various Fe^{2+} chelates with oxygen, and the formation of relatively stable perferryl chelates (70). These tests were performed in the absence of microsomes, simply by adding Fe^{2+} to the respective chelators in a buffer (0.1 M Tris-HCl, pH 7.5) and recording oxygen consumption. The slow uptake of oxygen (with ADP, ATP, oxalate or malonate) as opposed to no uptake (with cyanide or o-phenanthroline), or instantaneous uptake (with EDTA or pyrophosphate) was interpreted as interaction of the Fe^{2+} chelate with oxygen and the formation of a relatively stable perferryl complex. This experiment was repeated with OTA and Fe^{2+}, and it was found that the chelate interacts slowly with oxygen (Fig. 33). Thus, the Fe^{3+}-OTA fulfills the three criteria set forth by Ernster and coworkers (70).

In my studies, no attempt was made to distinguish between the various species involved in initiating lipid peroxidation. The precise nature of the initiating species is not known and is currently the focus of active research. Several workers (70,98,168) have implicated the perferryl ion as the initiating species, but its ability to extract a methylene hydrogen has been questioned (86). Recently, Koppenol (169) has proposed that the more reactive ferryl

Figure 33. **Autoxidation of ferrous chelates.** Oxygen consumption was measured polarographically with a Clark electrode. The reaction mixture contained 0.1 M Tris-HCl, pH 7.5 and 0.15 M KCl and either EDTA 210 μM, ADP 7 mM or OTA 250 μM. The concentration of EDTA, ADP and FeCl2 were those used by Ernster and coworkers (70). The reaction was started by the addition of 180 nmol of $FeCl_2$.

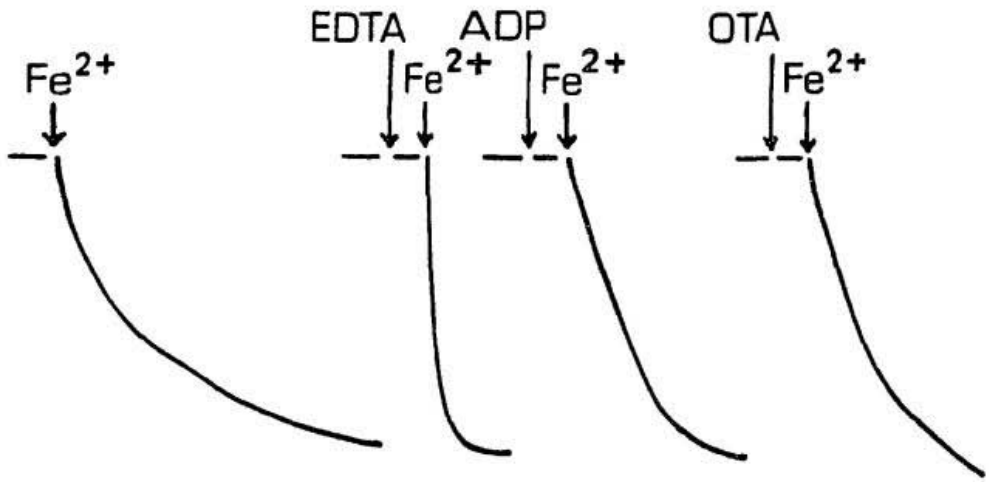
EDTA
ADP
OTA
Fe2+
Fe2+
Fe2+
Fe2+

ion be considered as an alternative. Aust and coworkers (170) have suggested that a Fe^{3+}-O_2-Fe^{2+} complex may be the initiating species but this has recently been disputed (171). Hydroxyl radicals can initiate lipid peroxidation in homogeneous reaction systems (172), but the use of scavengers has unequivocally failed to show any significant involvement of hydroxyl radicals in microsomal or liposomal peroxidation systems (87). My results, showing the lack of inhibitory effect of hydroxyl radical scavengers (Table 2), are consistent with earlier studies (87-90). The slight inhibition observed in the presence of SOD (23 %) could be due to its metal binding ability and/or to its ability to inhibit the superoxide-dependent reduction of the Fe^{3+}-OTA complex.

A variety of toxic compounds, such as doxorubicin, carbon tetrachloride and ethyl hydrazine, have been shown by ESR spin trapping experiments to produce hydroxyl radicals in microsomal systems (155-157,167). The NADPH-cytochrome P-450 reductase system in the presence of iron and EDTA has also been shown by ESR spin-trapping experiments to result in the production of hydroxyl radicals (157). This result was confirmed by us in an experiment conducted as shown in Fig. 28A in which OTA was omitted but which contained 0.25 mM EDTA (157). It therfore seems likely that the hydroxyl radical is produced by an iron-based Fenton-type chemistry in which Fe^{2+}-OTA reduces H_2O_2. Thus, in a mechanism similar

to that described in (157), hydroxyl radical is ultimately produced by the following reactions:

$$E_{ox} + NADPH \longrightarrow E_{red} + NADP^{+} \quad (1)$$

$$E_{red} + O_2 \longrightarrow E_{ox} + O_2^{\cdot -} \quad (2)$$

$$2O_2^{\cdot -} + 2H^{+} \longrightarrow H_2O_2 + O_2 \quad (3)$$

$$Fe^{3+}\text{-OTA} + O_2^{\cdot -} \longrightarrow Fe^{2+}\text{-OTA} + O_2 \quad (4)$$

$$Fe^{2+}\text{-OTA} + H_2O_2 \longrightarrow Fe^{3+}\text{-OTA} + OH^{-} + OH^{\cdot} \quad (5)$$

in which E_{ox} and E_{red} are the oxidized and reduced forms respectively of NADPH-cytochrome P-450 reductase. The direct reduction of Fe^{3+}-OTA by E_{red} may also be occurring simultaneously with reaction [4]. The overall mechanism for the role of OTA in free radical production and stimulation of lipid peroxidation is summarized as a simplified scheme which is given in Fig. 34.

While we have shown that lipid peroxidation induced by OTA is strongly iron dependent (133,174), the lack of any protection offered by catalase and several hydroxyl radical scavengers (Table 2) suggests that hydroxyl radical production through reaction [5] may not be a significant factor in the <u>in vitro</u> lipid peroxidation. On the other hand, it can be argued that catalase is not an effective scavenger of low concentrations of H_2O_2 (93). Similarly, if iron is bound tightly to the membrane, and the hydroxyl radicals are so reactive that they will react almost

Figure 34. **Scheme representing the overall suggested mechanism of OTA stimulated lipid peroxidation.**

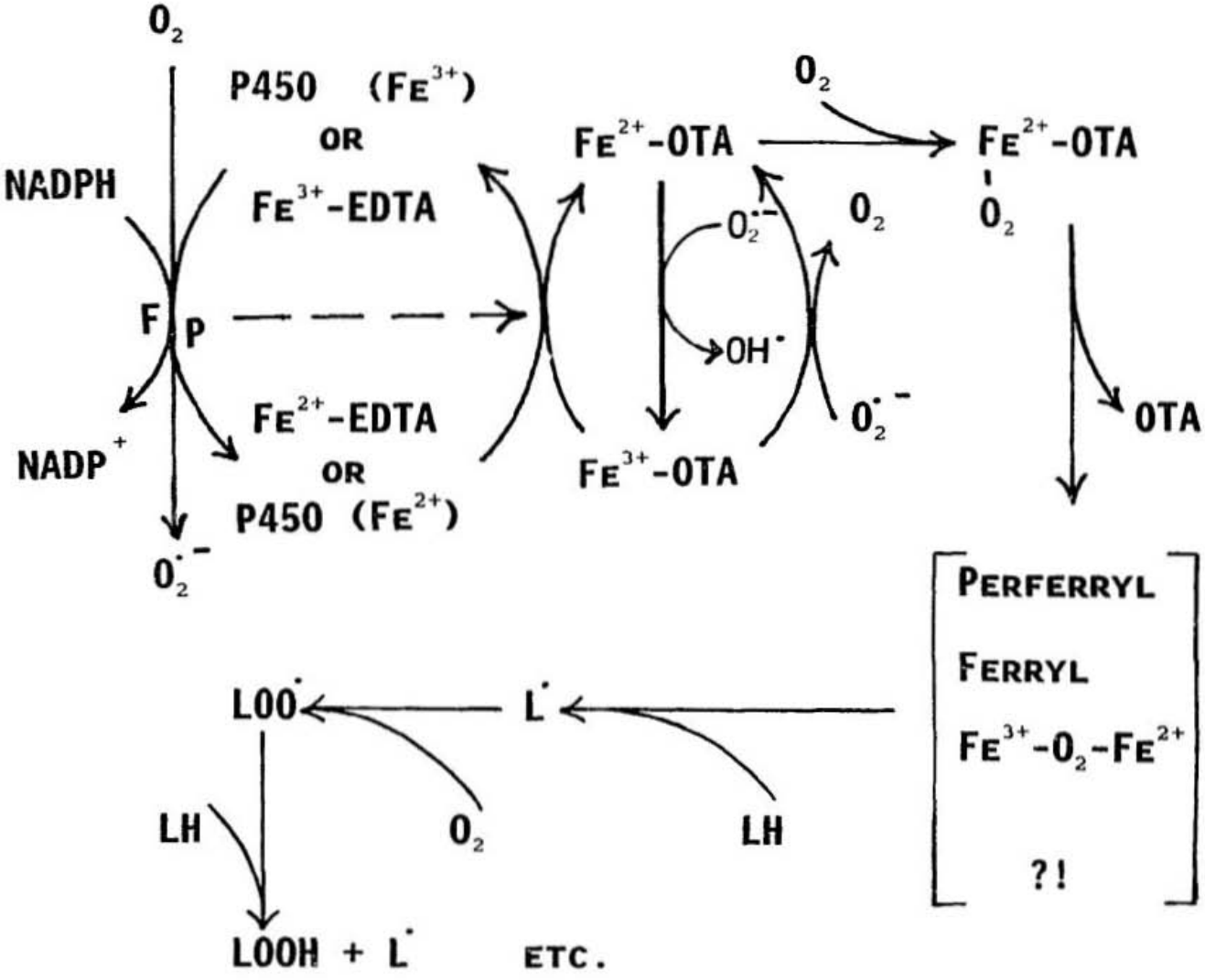
O_2
P450 (Fe^{3+})
OR
Fe^{3+}-EDTA
NADPH
F P
Fe^{2+}-EDTA
OR
P450 (Fe^{2+})
$NADP^+$
$O_2^{\cdot -}$
Fe^{2+}-OTA
Fe^{3+}-OTA
O_2
$O_2^{\cdot -}$
$OH^{\cdot}$
O_2
Fe^{2+}-OTA
O_2
OTA
$O_2^{\cdot -}$
PERFERRYL
FERRYL
Fe^{3+}-O_2-Fe^{2+}
?!
LH
LH
O_2
LOO$^{\cdot}$
L$^{\cdot}$
LOOH + L$^{\cdot}$
ETC.

instantaneously at their point of origin, then water-soluble scavengers such as mannitol, formate and benzoate may not gain access to the hydroxyl radicals and hence may fail to inhibit lipid peroxidation (94). Therefore, these results do not preclude hydroxyl radical production by the Fe^{3+}-OTA complex, as demonstrated by ESR studies, from having an important role in the toxicity of OTA.

Sugioka et al. (173) examined the adriamycin stimulated Fe^{3+}-ADP dependent unsaturated phospholipid decomposition in a model system that included microsomal phospholipid, NADPH and Fp. They provided evidence that a ternary complex of Fe^{2+}-ADP-adriamycin was the active species. It is unlikely that a similar Fe^{2+}-EDTA-OTA ternary complex is formed since the two systems are not comparable. EDTA binds Fe^{3+} many times more strongly that OTA ($K_{EDTA} = 10^{25}$). Thus, the equilibrium for the reaction:

$$Fe^{3+}\text{-OTA} + \text{EDTA} \rightleftharpoons Fe^{3+}\text{-EDTA} + \text{OTA}$$

lies very far to the right. Also, since EDTA is a hexa coordinate ligand, the Fe^{3+}-OTA-EDTA complex is unlikely to form. In contrast, ADP forms a weak complex with Fe^{3+} thus permitting the formation of a Fe^{3+}-ADP-adriamycin complex.

From structure-activity relationship studies (Figs. 30-32), it can be concluded that OTA is the most effective of all the compounds tested in stimulating lipid peroxidation.

OC was next best with about half the activity of OTA (Fig. 30). Oα, OB, L-Ser-Oα, L-Pro-Oα and L-Glu-Oα were very poor in stimulating lipid peroxidation (Figs. 30 and 32). The ability of these compounds to stimulate lipid peroxidation roughly paralleled their ability to reduce Fe^{3+} (Fig. 31). Thus, in addition to OTA, OC may fulfill the criteria outlined by Ernster and coworkers (70) for stimulation of lipid peroxidation. These results are in good agreement with what Rahimtula et al. (133) observed using the microsomal lipid peroxidation system.

From the above studies, it can be inferred that the presence of a free carboxyl group is important since its blockage by esterification, as in OC, substantially reduced the stimulatory effect on lipid peroxidation. The very low potency of OB in stimulating lipid peroxidation is likely due to the absence of the chlorine atom. L-Phe also appears to be important since its replacement by other amino acids (L-Ser, L-Pro or L-Glu) almost abolished the stimulatory effect of lipid peroxidation observed with OTA. Earlier studies had shown an absolute requirement for the free phenolic hydroxyl group on OTA. The correlation between the ability of these compounds to stimulate lipid peroxidation and their toxicity has yet to be determined.

CHAPTER 6

CONCLUSION

The objective of this study was to investigate the mechanism and structural requirements of OTA-stimulated lipid peroxidation. The results indicate the following.

1) OTA stimulates lipid peroxidation by a mechanism that involves the formation of a 1:1 complex with iron. The resulting Fe^{3+}-OTA complex is rapidly reduced to $Fe2^{+}$-OTA which, after binding to molecular oxygen, is transformed to a reactive species that initiates lipid peroxidation.

2) In the reconstituted system, maximum lipid peroxidation was observed in the presence of phospholipid vesicles (liposomes),iron, the flavoprotein NADPH-cytochrome P-450 reductase (Fp), EDTA and NADPH as well as OTA.

3) Purified cytochrome P-450 could effectively replace EDTA suggesting that this hemoprotein could play an important role in OTA-stimulated lipid peroxidation in microsomes, liposomes and possibly also in vivo. However, the role of lipid peroxidation in OTA toxicity remains to be determined.

4) Structure-activity relationship studies indicated that the presence of a free carboxyl group and chlorine atom as well as L-Phe on OTA contributed significantly to the stimulatory effect on lipid peroxidation. Earlier

studies had shown an absolute requirement for the free phenolic hydroxyl group on OTA.

5) ESR studies demonstrated the formation of the highly reactive hydroxyl radicals in the presence of OTA. These hydroxyl radicals appeared not to participate in lipid peroxidation, but they could contribute to the toxic effect of OTA.

REFERENCES

1. Scott De B. Toxigenic fungi isolated from cereal and legume products. *Mycopath Mycol* **25**: pp. 213, 1965.

2. Van Der Merwe K J, Steyn P S and Fourie L. The constitution of ochratoxin A, B and C metabolites of Aspergillus ochraceus Wilh. *J Chem Soc*, 7083-7088, 1965.

3. Steyn P S and Holzapfel C W. The isolation of the methyl and ethyl esters of ochratoxin A and B, metabolites of Aspergillus ochraceus Wilh. *J S Afr Chem Inst* **20**: pp. 186, 1967.

4. Steyn P S, Holzapfel C W and Ferreira N P. Biosynthesis of the ochratoxins, metabolites of Aspergillus ochraceus. *Phytochemistry* **9**: pp. 1977, 1970.

5. Kurata H. Current scope of mycotoxin research from the viewpoint of food mycology. In: *Toxicology, biochemistry and pathology of mycotoxins* (Eds. Uraguchi K and Yamazaki M), pp. 162. Kodansha Ltd., Tokyo, 1978.

6. Ueno Y. The toxicology of mycotoxins. *CRC Crit Rev Toxicol* **14**: 99-132, 1985.

7. Hult K, Hokby E, Gatenbeck S and Rutquist L. Ochratoxin A in blood from slaughter pigs in sweden: use in evaluation of toxic content of consumed feed. *Appl Environ Microbiol* **39**: pp. 828, 1980.

8. Marquardt R R, Frolich A A, Sreemannarayana O, Abramson D and Bernatsky A. Ochratoxin A in blood from slaughter pigs in Western Canada. *Can J Vet Res* **52**: 186-190, 1988.

9. Scott P M, Van Walbeek W, Kennedy B and Anyeti D. Mycotoxins (ochratoxin A, citrinin and stregmatocystin) and toxigenic fungi in grains and other agricultural products. *J Agric Food Chem* **20**: 1103-1109, 1972.

10. Krogh P. Ochratoxins. In: *Mycotoxins in human and animal health* (Eds. Rodricks J V, Hesseltine C W and Mehlman, M A), pp. 489-498. Park Forest South, IL: Pathtox, 1977.

11. Krogh P and Nesheim S. Ochratoxin A, Introduction. In: *Environmental Carcinogens. Selected Methods of Analysis*, Vol. 5, *Some Mycotoxins* (Eds. Stoloff L, Castegnaro M, Scott P, O'Neill I K, and Bartsch H), pp. 247-259. IARC Scientific Publications, No. 44, Lyon, 1982.

12. Krogh P. Mycotoxic porcine nephropathy: A possible model for Balkan endemic nephropathy. In: *Endemic nephropathy* (Eds. Puchlev A, Dinev I V, Milev B and Doichinov D), pp. 266-270. Sofia: Bulgarian Academy of Sciences, 1974.

13. Petkova-Bocharova T and Castegnaro M. Ochratoxin A contamination of cereals in an area of high incidence of Balkan endemic nephropathy in Bulgaria. *Food Addit Contam* **2**: 267-270, 1985.

14. Galtier P, Alvinerie M and Charpenteau J L. The pharmacokinetic profiles of ochratoxin A in pigs, rabbits and chickens. *Food Cosmet Toxicol* **19**: 735-738, 1981.

15. Szczech G M, Carlton W W and Truite J. Ochratoxicosis in beagle dogs. II. Pathology. *Vet Pathol* **10**: 219-231, 1973.

16. Szczech G M, Carlton W W and Caldwell R. Ochratoxin A toxicosis in swine. *Vet Pathol* **10**: 347-364, 1973.

17. Berndt W O, Hayes A W and Phillips R D. Effects of mycotoxins on renal function: Mycotoxic nephropathy. *Kidney Intl* **18**: 656-664, 1980.

18. Berndt W O and Hayes A W. In vivo and in vitro changes in renal function caused by ochratoxin A in the rat. *Toxicology* **12**: 5-17, 1979.

19. Kane A, Creppy E E, Roschenthaler R and Dirheimer G. Changes in urinary and renal tubular enzymes caused by sub-chronic administration of ochratoxin A to rats. *Toxicology* **42**: 233-243, 1986.

20. Meisner H and Selanik P. Inhibition of renal gluconeogenesis in rats by ochratoxin. *Biochem J* **180**: 681-684, 1979.

21. Suzuki S, Satoh T and Yamazaki M. Effect of ochratoxin A on carbohydrate metabolism in rat liver. *Toxicol Appl Pharmacol* **32**: 116-122, 1975.

22. Creppy E E, Roschenthaler R and Dirheimer G. Inhibition of protein synthesis in mice by ochratoxin A and its prevension by phenylalanine. *Food Chem Toxicol* **22**: 883-886, 1984.

23. Moore JH and Truelove B. Ochratoxin A: Inhibition of

mitochondrial respiration. *Science*: **168**, 1102-1103, 1970.

24. Meisner H and Chan S. Ochratoxin A, an inhibitor of mitochondrial transport systems. *Biochemistry* **13**: 2795-2800, 1974.

25. Khan S, Martin M, Bartsch H and Rahimtula A D. Perturbation of liver microsomal calcium homeostasis by ochratoxin A. *Biochem Pharmacol* **38**: 67-72, 1989.

26. Krogh P, Axelsen N H, Elling F, Gyrd-Hansen N, Hald B and Aalund O. Experimental porcine nephropathy: Changes of renal function and structure induced by ochratoxin A contaminated feed. *Acta Path Microbiol Scand A*, Suppl No. **246**: 1-21, 1974.

27. Krogh P, Elling F, Gyrd-Hansen N, Hald B, Larsen A E and Ravnskov U. Experimental porcine nephropathy: Changes of renal function and structure perorally induced by crystalline ochratoxin A. *Acta Path Microbiol Scand. Sect. A*, **84**: 429-434, 1976.

28. Galtier P, Boneu B, Charpenteau J L, Bodin G, Alvinerie M and More J. Physiopathology of haemorrhagic syndrome related to ochratoxin A intoxication in rats. *Food Cosmet Toxicol* **17**: 49-53, 1979.

29. Chang F C, Huff W E and Hamilton P B. A leucocytopenia-induced in chickens by dietary ochratoxin A. *Poultry Sci* **58**: 555-558, 1976.

30. Dwivedi P and Burns R B. Effects of ochratoxin A on immunoglobulins in broiler chickens. *Res Vet Sci* **36**: 117-121, 1984.

31. Boorman G A, Hong H L, Dieter M P, Hayes H T, Pohland A E, Stack M and Luster MI. Myelotoxicity and macrophage alteration in mice exposed to ochratoxin A. *Toxicol Appl Pharmacol* **72**: 304-312, 1984.

32. Hayes A W, Hood R D and Lee H L. Teratogenic effects of ochratoxin A in mice. *Teratology* **9**: 93-99, 1974.

33. Sreemannarayana O, Marquardt R R, Frohlich A A, Abramson D and Phillips G D, Organ weights, liver constituents and serum components in growing chicks fed ochratoxin A. *Arch Environ Contam Toxicol* **18**: 404-410, 1989.

34. Bendele A M, Carlton W W, Krogh P and Lillehoj E B.

Ochratoxin A carcinogenesis in the (C57BL/6J x C3H) F1 mouse. *J Natl Cancer Inst* **75:** 733-739, 1985.

35. Kanesawa M and Suzuki S. Induction of renal and hepatic tumors in mice by ochratoxin A, a mycotoxin. *Gann* **69:** 599-600, 1978.

36. Umeda T M, Tsutsui T and Saito M. Mutagenicity and inducibility of single-strand breaks and chromosome aberrations by various mycotoxins. *Gann* **58:** 619-625, 1977.

37. Wehner F C, Theil P G, Van Rensberg S J and Demasius I P. Mutagenicity to Salmonella typhimurium of some Aspergillus and Penicillium mycotoxins. *Mut Res* **58:** 193-203, 1978.

38. Kane A, Creppy E E, Roth A, Roschenthaler R and D[illegible]eimer G. Distribution of the tritium label from low dose of radioactive ochratoxin A ingested by rats and evidence for DNA single-strand breaks caused in liver and kidneys. *Arch Toxicol* **58:** 219-224, 1986.

39. Kumagai S and Aibara K. Intestinal absorption and secretion of ochratoxin A in the rat. *Toxicol Appl Pharmacol* **64:** 94-102, 1982.

40. Lee S C, Berry J T and Chu F S. Immunohistochemical fate of ochratoxin A in mice. *Toxicol Appl Pharmacol* **72:** 218-227, 1984.

41. Miller E C and Miller J A. Searches for ultimate chemical carcinogens and their relations with cellular macromolecules. *Cancer* **47:** 2327-2345, 1981.

42. Stormer F C, Hansen C E, Pederson J I, Hvistendahl G and Aasen A J. Formation of (4R)-and(4S)-4-hydroxyochratoxin A from ochratoxin A by liver microsomes from various species. *Appl Environ Microbiol* **42:** 1051-1056, 1981.

43. Stormer F C, Storen O, Hansen C E, Pederson J I and Aasen A J. Formation of (4R)-and(4S)-4-hydroxyochratoxin A and 10-hydroxyochratoxin A from ochratoxin A by rabbit liver microsomes. *Appl Environ Microbiol* **45:** 1183-1187, 1983.

44. Storen O, Holm H and Stormer F C. Metabolism of ochratoxin A by rats. *Appl Environ Microbiol* **44:** 785-789, 1982.

45. Dahle L K, Hill E G and Holman R T. The thiobarbituric

acid reaction and the autoxidation of polyunsaturated fatty acid methyl esters. *Arch Biochem Biophys* **98:** 253-261, 1962.

46. Dillard C J, Dumelin E E and Tappel A L. Effect of dietary vitamin E on expiration of pentane and ethane by the rat. *Lipids* **12:** 109-114, 1977.

47. Hafeman D G and Hoekstra W G. Protection against carbon tetrachloride-induced lipid peroxidation in the rat by dietary vitamin E, Selenium and methionine as measured by ethane evolution. *J Nutr* **107:** 656-665, 1977.

48. Benedetti A, Comporti M and Esterbauer H. Identification of 4-hydroxynonenal as a cytotoxic product originating from the peroxidation of liver microsomal lipids. *Biochem Biophys Acta* **620:** 281-296, 1980.

49. Recknagel R O, Glende E A, Jr. Spectrophotometric detection of lipid conjugated dienes. *Methods in Enzymology*, Vol. **105:** 331-337 (Packer L, Ed.), Academic Press, New York, 1984.

50. May H E and Reed D J. A kinetic assay of TPNH-dependent microsomal lipid peroxidation by changes in different spectra. *Anal Biochem* **55:** 331-337, 1973.

51. Corongiu F P and Milia A, An improved and simple method for determining diene conjugation in autoxidized polyunsaturated fatty acids. *Chem Biol Interact* **44:** 289-297, 1983.

52. Pryor W A and Castle L. Chemical methods for the detection of lipid hydroperoxides. In: *Methods in Enzymology*, Vol **105: 293-299** (Packer L, Ed.), Academic Press, New York, 1984.

53. Catheart R, Schwiers E and Ames BN. Detection of picomole levels of hydroperoxides using a fluorescent dichlorofluorescein assay. *Anal Biochem* **134:** 111-116, 1983.

54. Niehaus W G and Samuelsson B. Formation of malondialdehyde from phospholipid arachidonate during microsomal lipid peroxidation. *Eur J Biochem* **6:** 126-130, 1968.

55. Frankel E N and Neff W E. Formation of malondialdehyde from lipid oxidation products. *Biochem Biophys Acta* **754:** 264-270, 1983.

56. May H E and McCay P B. Reduced diphosphopyridine nucleotide oxidase-catalyzed alterations of membrane phospholipids. *J Biol Chem* **243**: 2296-2305, 1968.

57. Csallany A S, Dergvan M, Manwaring J D and Addis P B. Free malondialdehyde determination in tissues by high performance liquid chromatography. *Anal Biochem* **142**: 277-283, 1984.

58. Kunert K J and Tappel A L. The effect of vitamin C on in vivo lipid peroxidation in Guinea pigs as measured by pentane and ethane production. *Lipids* **18**: 271-274, 1983.

59. Muller A and Sies H. Assay of ethane and pentane from isolated organs and cells. In: *Methods in Enzymology*, Vol. **105**: 311-319 (Packer L, Ed.), Academic Press, New York, 1984.

60. Lawrence G D and Cohen G. Ethane exhalation as an index of in vivo lipid peroxidation: Concentrating ethane from a breath collection chamber. *Anal Biochem* **122**: 283-290, 1982.

61. Kappus H and Muliawan H. Alkane formation during liver microsomal lipid peroxidation. *Biochem Pharmacol* **31**: 597-600, 1982.

62. Crawford D L, Yu T C and Sinnhuber R O. Reaction of malondialdehyde with glycin. *J Agri Food Chem* **14**: 182-184, 1966.

63. Bird R P Hung S O, Hadley M and Draper H H. Determination of malondialdehyde in biological materials by High Pressure Liquid Chromatography. *Anal Biochem* **128**: 240-244, 1983.

64. Tappel A L. Measurement of and protection from in vivo lipid peroxidation. In: *Free radicals in biology* (Ed. Pryor WA) **4**: 1-45. Academic Press, New York and London, 1980.

65. Yagi K (Ed.). *Lipid peroxides in biology and medicine*. Academic Press, New York and London, 1982.

66. Pompella A, Maellaro E, Casini A F, Ferrali M, Ciccoli L and Comporti M. Measurement of lipid peroxidation in vivo: A comparison of different procedures. *Lipids* **22**: 206-211, 1987.

67. Hochstein P and Ernster L. ADP-activated lipid

peroxidation coupled to the TPNH oxidase system of microsomes. *Biochem Biophys Res Commun* **12**: 388-394, 1963.

68. Hochstein P, Nordenbrand K and Ernster L. Evidence for the involvement of iron in the ADP activated peroxidation of lipids in microsomes and mitochondria. *Biochem Biophys Res Commun* **14**: 323-328, 1964.

69. Pederson T C and Aust S D. NADPH-dependent lipid peroxidation catalyzed by purified NADPH-cytochrome c reductase from rat liver microsomes. *Biochem Biophys Res Commun* **48**: 789-795, 1972.

70. Ursini F, Maiorino M, Hochstein P and Ernster L. Microsomal lipid peroxidation: Mechanisms of initiation. The role of iron and iron chelators. *Free Rad Biol Med* **6**: 31-36, 1989.

71. Morehouse L A and Aust S D. Reconstituted microsomal lipid peroxidation: ADP-Fe^{3+}-dependent peroxidation of phospholipid vesicles containing NADPH-cytochrome P-450 reductase and cytochrome P-450. *Free Rad Biol Med* **4**: 269-277, 1988.

72. Aisen P and Listowsky I. Iron transport and storage proteins. In: *Annual Review of Biochemistry* (Snell E, Boyer P D, Meister A and Richardson C C, Eds.), **49**: 357-393, Palo Alto: Annual Reviews, Inc., 1980.

73. Theil E C. Ferritin: Structure, function and regulation. In: *Iron binding proteins without cofactors or sulfur clusters* (Theil E C, Eichhorn G L and Marzili L G, Eds.), Vol. **5**: 1-38, New York, Elsevier, 1983.

74. Aisen P, Iron metabolism. *CIBA Found Symp No. 51*. Elsevier/Excerpta Medica/North-Holland, Amsterdam, 1977, 1.

75. Jacobs A, Iron metabolism. *CIBA Found Symp No. 51*. Elsevier/Excerpta Medica/North-Holland, Amsterdam, 1977, 91.

76. Gutteridge J M C. Iron promoters of the Fenton reaction and lipid peroxidation can be released from haemoglobin by peroxides. *FEBS Lett* **201**: 291-295, 1986.

77. Comporti M. Biology of disease, lipid peroxidation and cellular damage in toxic liver injury. *Lab Invest* **53**: 599-623, 1985.

78. Poli G, Albano E and Dianzani M V. The role of lipid

peroxidation in liver damage. *Chem Phys Lipids* **45**: 117-142, 1987.

79. Sies H (Ed.). *Oxidative Stress*, Academic Press, London, 1985.

80. Anbar M, Ross F and Ross B R. *National Bureau of Standards NSRDS* **59**, 1977.

81. Fridovich I. Superoxide dismutase. *In: Molecular Mechanisms of Oxygen Activation* (Hayaishi O, Ed.), 453, Academic Press, New York, 1974.

82. Mishin V, Pokrovsky A and Lyakovich V V. Interaction of some acceptors with superoxide anion radicals formed by the NADPH specific flavoprotein in rat liver microsomal fraction. *Biochem J* **154**: pp. 307, 1976.

83. Chance B, Sies H and Boveris A. Hydroperoxide metabolism in mammalian organs. *Physiol Rev* **59**: pp. 527, 1979.

84. Svingen B A, O'Neal F O and Aust S D. The role of superoxide and singlet oxygen in lipid peroxidation. *Photochem Photobiol* **28**: pp. 803, 1978.

85. Aust S D and Svingen B A. The role of iron in enzymatic lipid peroxidation. In: *Free Radicals in Biology*, Vol. **5** (Pryor W A, Ed.), 1-28, Academic Press, New York, 1982.

86. Halliwell B and Gutteridge J M C. The importance of free radicals and catalytic metal ions in human disease. *Mol Aspects Med* **8**: 89-193, 1985.

87. Gutteridge J M C. The role of superoxide and hydroxyl radicals in phospholipid peroxidation catalysed by iron salts. *FEBS Lett* **150**: 454-458, 1982.

88. Morehouse L A, Tieng M, Bucher J R and Aust S D. Effect of hydrogen peroxide on the initiation of microsomal lipid peroxidation. *Biochem Pharmacol* **32**: 123-127, 1983.

89. Gutteridge J M C. Ferrous-EDTA-stimulated phospholipid peroxidation. A reaction changing from alkoxyl-radical to hydroxyl-radical dependent initiation. *Biochem J* **224**: 697-701, 1984.

90. Beloqui O and Cederbaum A I. Prevention of microsomal products of hydroxyl radicals, but not lipid

peroxidation, by the glutathione-glutathione peroxidase system. *Biochem Pharmacol* **35**: 2663-2669, 1986.

91. Barber D J W and Thomas J K. Reactions of radicals with lecithin bilayers. *Radiation Res* **74**: 51-65, 1978.

92. O'Connell M J and Garner A. Radiation-induced generation and properties of lipid hydroperoxide in liposomes. *Int J Radiation Biol* **44**: 615-625, 1983.

93. Misra H P. Generation of superoxide free radicals during the autoxidation of thiols. *J Biol Chem* **249**: 2151-2155, 1974.

94. Fong K-L, McCay P B, Poyer J L, Misra H P and Keele B B. Evidence for superoxide-dependent reduction of Fe3+ and its role in enzyme generated hydroxyl radical formation. *Chem Biol Interact* **15**: 77-89, 1976.

95. Fee J A. Is superoxide toxic and are superoxide dismutases essential for aerobic life. In: *Oxygen and Oxy-Radicals in Chemistry and Biology* (Rodgers M A J and Powers E L, Eds.), 205-221, Academic Press, New York, 1981.

96. Koppenol W H. The physiological role of the charge distribution on superoxide dismutase. In: *Oxygen and Oxy-Radicals in Chemistry and Biology* (Rodgers M A J and Powers E L, Eds.), 671-673, Academic Press, New York, 1981.

97. Gutteridge J M C. The protective action of superoxide dismutase on metal ion catalyzed peroxidation of phospholipids. *Biochem Biophys Res Commun* **77**: 379-386, 1977.

98. Tien M, Svingen B A and Aust S D. Initiation of lipid peroxidation by perferryl complexes. In: *Oxygen and Oxy-Radicals in Chemistry and Biology* (Rodgers M A J and Powell E L, Eds.), 147-152. Academic Press, New York, 1981.

99. Minotti G and Aust S D. The role of iron in the initiation of lipid peroxidation. *Chem Phys Lipids* **44**: 191-208, 1987.

100. Minotti G and Aust S D. The requirement of Iron (III) in the initiation of lipid peroxidation by Iron (II) and hydrogen peroxide. *J Biol Chem* **262**: 1098-1104, 1987.

101. Aust S D. Sources of iron for lipid peroxidation in

biological systems. In: *Oxygen Radical and Tissue Injury; Proceedings of an Upjohn Symposium* (Halliwell B, Ed.), 27-33, Allen Press, Kansas, 1988.

102. Braughler J M, Duncan L A and Chase P L. The involvement of iron in lipid peroxidation. Importance of ferric to ferrous ratios in initiation. *J Biol Chem* **261:** 10282-10289, 1986.

103. Slater T F (Ed.). *Free Radical Mechanisms in Tissue Injury*, Pion Press Ltd., London, 1972.

104. Comporti M, Saccocci C and Dianzani M U. Effect of CCl_4 in vitro and in vivo on lipid peroxidation of rat liver homogenates and subcellular fractions. *Enzymologia* **29:** 185-204, 1965.

105. Ghoshal A K and Recknagel R O. On the mechanism of carbon tetrachloride hepatotoxicity: Co-incidence of loss of glucose-6-phosphatase activity with peroxidation of microsomal lipid. *Life Sci* **4:** 2195-2209, 1965.

106. Slater T F. Activation of carbon tetrachloride: Chemical principles and biological significance. In: *Free Radicals, Lipid Peroxidation and Cancer* (McBrien D C H and Slater T F, Eds.), 243-274, Academic Press, London, 1982.

107. Ekstrom T and Hogberg J. Chloroform induced glutathione depletion and toxicity in freshly prepared hepatocytes. *Biochem Pharmacol* **29:** 3059-3065, 1980.

108. Albano E, Poli G, Tomasi A, Bini A, Vannini V and Dianzani M U. Toxicity of 1,2-dibromo-methane in isolated hepatocytes: Role of lipid peroxidation. *Chem Biol Interact* **50:** 255-265, 1984.

109. Tomasi A, Billings S, Garner A, Stier A, Slater T F and Albano E. The metabolism of halothane by hepatocytes: A comparison between free radical spin trapping and lipid peroxidation in relation to cell damage. *Chem Biol Interact* **46:** 353-368, 1983.

110. Wendel A and Feuerstein S. Drug induced lipid peroxidation in mice -I: Modulation of mono-oxygenase activity, glutathione and selenium status. *Biochem Pharmacol* **30:** 2513-2520, 1981.

111. Casini A F, Pompella A and Comporti M. Liver glutathione depletion induced by bromobenzene,

iodobenzene and diethyl maleate poisoning and its relation to lipid peroxidation and necrosis. *Am J Pathol* **118**: 225-237, 1985.

112. Halliwell B. Free radicals, oxygen toxicity and aging. In: *Age pigments* (Sohal R S, Ed.), 1-62, Elsevier/North Holland Biomedical Press, Amsterdam, 1981.

113. Sandy M S, Moldeus P, Ross D and Smith M. Role of redox cycling and lipid peroxidation in bipyridyl herbicide cytotoxicity. Studies with a compromised isolated hepatocyte model system. *Biochem Pharmacol* **35**: 3095-3101, 1986.

114. Jaeschke H, Kleinwaechter C and Wendel A. The role of acrolein in allyl alcohol induced lipid peroxidation and liver cell damage in mice. *Biochem Pharmacol* **36**: 51-57, 1987.

115. Dianzani M U and Torrielli M V. Lipid peroxidation in ethanol-induced liver damage. The problem of its possible relevance in both acute and chronic alcoholism. *Med Biol Environ* **9**: 177-190, 1981.

116. Dianzani M U. Lipid peroxidation in ethanol poisoning: A critical reconsideration. *Alcohol and alcoholism* **20**: 161-173, 1985.

117. Dianzani M U and Ugazio G. Lipid peroxidation. In: *Biochemical Mechanisms of Liver Injury* (Slater T F, Ed.), 669-707, Academic Press, London, 1978.

118. Vladimirov Y A, Olenev V I, Suslova T B and Cheremisina Z P. Lipid peroxidation in mitochondrial membrane. In: *Advances in Lipid Research* (Paoletti R and Kritchevsky D, Eds.), Vol. **7**, 173-249, Academic Press, New York, 1980.

119. Recknagel R O, Glende E A, Waller R L and Lowrey K. Lipid peroxidation: Biochemistry, measurement, and significance in liver cell injury. In: *Toxicology of the Liver* (Plaa G and Hewitt W R, Eds.), 213-241, Raven Press, New York, 1982.

120. Curtis M T, Gilfor D and Farber J L. Lipid peroxidation increases the molecular order microsomal membranes. *Arch Biochem Biophys* **235**: 644-649, 1984.

121. Bruch R C and Thayer W S. Differential effect of lipid peroxidation on membrane fluidity as determined by electron spin resonance probes. *Biochem Biophys Acta* **733**: 216-222, 1983.

122. Eichenberg K, Bohni P, Winterhalter K H, Kawato S and Richter C. Microsomal lipid peroxidation causes an increase in the order of the membrane lipid domain. *FEBS Lett* **142**: 59-62, 1982.

123. Hogberg J, Bergstrand A and Jakobasson S V. Lipid peroxidation of rat liver microsomes: Its effect on the microsomal membrane and some membrane bound microsomal enzymes. *Eur J Biochem* **37**: pp. 51-59, 1973.

124. de Groot H, Noll T and Toll T. Loss of latent activity of liver microsomal enzymes evoked by lipid peroxidation. Studies of nucleoside diphosphatase, glucose-6-phosphatase, and UDP glucosyl transferase. *Biochem Biophys Acta* **815**: pp. 91-96, 1985.

125. Ferrali M, Fulceri R, Benedetti A and Comporti M. Effects of carbonyl compounds (4-hydroxyalkenals) originating from the peroxidation of liver microsomal lipids on microsomal enzyme system of the liver. *Res Commun Chem Pathol Pharmacol* **30**: pp. 99, 1980.

126. Jones D P, Thor H, Smith M T, Jewell S A and Orrenius S. Inhibition of ATP-dependent microsomal Ca^{2+} sequestration during oxidative stress and its prevention by glutathione. *J Biol Chem* **258**: 6390-6393, 1983.

127. Palmer D N, Rabin B R and Williams D J. A subpopulation of rat liver membrane-bound ribosomes that are detached in vitro by carcinogens and centrifugation. *Biochem J* **176**: 9-14, 1978.

128. Hunter F E, Jr., Gebicki J M, Hoffsten P I, Weinstein J and Scott A. Swelling and lysis of rat liver mitochondria induced by ferrous ions. *J Biol Chem* **238**: pp. 828-835, 1963.

129. Narabayashi H, Takeshige K and Minakami S. Alterations of inner-membrane components and damage to electron-transfer activity of bovine heart submitochondrial particles by NADPH-dependent lipid peroxidation. *Biochem J* **202**: pp. 97-105, 1982.

130. Fong K-L, McCay P B, Poyer J L, Keele B B and Misra H. Evidence that peroxidation of lysosomal membranes is initiated by hydroxyl radicals produced during flavin enzyme activity. *J Biol Chem* **248**: 7792-7797, 1973.

131. Wills E D and Wilkinson A E. Release of enzymes from

lysosomes by irradiation and the relation of lipid peroxide formation to enzymic release. *Biochem J* **99**: pp. 657-666, 1966.

132. Brownlee N R, Hunter J J, Panganamala R V and Cornwell D C. Role of Vitamin E in glutathione induced oxidatative stress: Methemoglobin, lipid peroxidation, and hemolysis. *J Lipid Res* **18**: pp. 635-644, 1977.

133. Rahimtula A D, Bereziat J-C, Bussacchini-Griot V and Bartsch H. Lipid peroxidation as a possible cause of ochratoxin A toxicity. *Biochem Pharmacol* **37**: 4469-4477, 1988.

134. Kappus H. Lipid peroxidation: Mechanisms, analysis, enzymology and biological relevance. In: *Oxidative Stress* (Ed. Sies H), pp. 273-310. Academic Press, Florida, 1985.

135. Horton A A and Fairhurst S. Lipid peroxidation and mechanisms of toxicity. *CRC Crit Rev Toxicol* **18**: 27-9, 1987.

136. David N S, Searcy J W and Diener U L. Production of ochratoxin A by Aspergillus ochraceus in a semi-synthetic medium. *Appl Microbiol* **17**: 742-744, 1969.

137. Wei Ru-Dong, Strong F M and Smalley E B. Incorporation of ^{36}Cl into ochratoxin A. *Appl Microbiol* **22**: 276-277, 1971.

138. Nesheim S. Isolation and purification of ochratoxin A and B and production of their methyl and ethyl esters. *J Assoc Off Anal Chem* **52**: 975-979, 1969.

139. Pohland A E, Schuller P L and Steyn P S. Physicochemical data for some selected mycotoxins. *Pure Appl Chem* **54**: 2219-2284, 1982.

140. Murray Ardies C, Lasker J M, Bloswick B P and Lieber C S. Purification of NADPH:cytochrome c (cytochrome P-450) reductase from hamster liver microsomes by detergent extraction and affinity chromatography. *Anal Biochem* **162**: 39-46, 1987.

141. Lowry O H, Rosebrough N J, Farr A L and Randall R J. Protein measurement with the Folin phenol reagent. *J Biol Chem* **193**: pp. 265, 1951.

142. Lake B G, Preparation and characterization of microsomal fractions for studies on xenobiotic

metabolism. In: *Biochemical Toxicology* (Eds. Snell K and Mulloch B), 183-215. IRL Press Ltd, 1987.

143. Guengerich F P. Microsomal enzymes involved in toxicology-Analysis and separation. In: *Principles and Methods of Toxicology* (Hayes AW, Ed.), 609-634, Raven Press, New York, 1982.

144. Steyn P S and Holzapfel C W. The synthesis of ochratoxin A and B, metabolites of Aspergillus ochraceus Wilh. *Tetrahedron* **23**: 4449-4461, 1967.

145. Steyn P S, Vleggaar R, Du Preez N P, Blyth A A and Seegers J L. The in vitro toxicity of analogs of ochratoxin A in monkey kidney epithelial cells. *Toxicol Appl Pharmacol* **32**: 198-203, 1975.

146. Folch J, Lees M and Stanley G H. A simple method for isolation and purification of total lipids from animal tissues. *J Biol Chem* **226**: 497-509, 1956.

147. Bartlett G R. Phosphorus assay in column chromatography. *J Biol Chem* **234**: 466-468, 1959.

148. Marinetti G V. Chromatographic separation, identification and analysis of phosphatides. *J Lipid Res* **3** (1): 1-20, 1962.

149. Pederson T C, Buege J A and Aust S D. Microsomal electron transport. The role of NADPH-cytochrome c reductase in liver microsomal lipid peroxidation. *J Biol Chem* **248**: 7134-7141, 1973.

150. Sinnhuber R O, Yu T C and Yu T C. Characterization of the red pigment formed in 2-thiobarbituric acid determination of oxidative rancidity. *Food Res* **23**: 620-633, 1958.

151. Cheng K L, Ueno K and Imamura T. (Eds.). Bipyridine and other ferroin reagents. In: *CRC Handbook of Organic Analytical Reagents*, 309-321. CRC Press, Boca Raton, 1982.

152. Khan S, Rahman A M, Payne J F and Rahimtula A D. Mechanisms of petroleum hydrocarbon toxicity: Studies on the response of rat liver mitochondria to Prudhoe Bay Crude Oil and its aliphatic, aromatic and heterocyclic fractions. *Toxicology* **42**: 131-142, 1986.

153. Green M J and Hill H A O. Chemistry of dioxygen. In: *Methods in Enzymology*, Vol. **105**: 3-22 (Packer L, Ed.),

Academic Press, New York, 1984.

154. Finkelstein E, Rosen G M and Rauckman E J. Spin trapping of superoxide and hydroxyl radical: Practical aspects. *Arch Biochem Biophys* **200**: 1-16, 1980.

155. Myers C E, Muindi J R F, Zweier J and Sinha B K. 5-Iminodaunomycin: An anthracyclin with unique properties. *J Biol Chem* **262**: 11571-11577, 1987.

156. Buettner G R. *Spin trapping: ESR parameters of spin adducts. Free Rad Biol Med* **3**: 259-303, 1987.

157. Lai C S, Grover T A and Piette L H. Hydroxyl radical production in a purified NADPH-cytochrome c (P-450) reductase system. *Arch Biochem Biophys* **193**: 373-378, 1979.

158. Rosen G M, Finkelstein E and Rauckman E J. A method for the detection of superoxide in biological systems. *Arch Biochem Biophys* **215**: 367-378, 1982.

159. Chu F S, Noh I and Chong C C. Structural requirements for ochratoxin intoxication. *Life Sci.* **11**: 503-508, 1972.

160. Halliwell B and Gutteridge J M C. Oxygen free radicals and iron in relation to biology and medicine: Some problems and concepts. *Arch Biochem Biophys* **246**: 501-514, 1986.

161. Albano E, Lott K A K, Slater T F, Stier A, Symons M C R and Tomasi A. Spin-trapping studies of the free-radical products formed by metabolic activation of carbon tetrachloride in rat liver microsomal fractions isolated from hepatocytes and in vivo in the rat. *Biochem J* **204**: 593-603, 1982.

162. Bus J S, Aust S D and Gibson J E. Paraquat toxicity: Mechanism of action involving lipid peroxidation. *Environ Health Persp* **16**: 139-146, 1976.

163. Trush M A, Mimnaugh E G, Ginsburg E and Gram T E. Studies on the in vitro interaction of mitomycin, nitrofurantoin and paraquat with pulmonary microsomes. *Biochem Pharmacol* **31**: 805-814, 1982.

164. Comporti M. Glutathione depleting agents and lipid peroxidation. *Chem Phys Lipids* **45**: 143-169, 1987.

165. Morehouse L A, Thomas C E and Aust S D. Superoxide

generation by NADPH-cytochrome P-450 reductase: The effect of iron chelators and the role of superoxide in microsomal lipid peroxidation. *Arch Biochem Biophys* **232**: 366-377, 1984.

166. Elkstrom G and Ingelman-Sundberg M. Cytochrome P-450 dependent lipid peroxidation in reconstituted membrane vesicles. *Biochem Pharmacol* **33**: 2523-2525, 1984.

167. Gianni L and Myers C E. The biochemical basis of anthracycline toxicity and antitumor activity. In: *Reviews in Biochemical Toxicology* (Eds. Hodgson E, Bend J R and Philpot R M), **5**: 1-82. Elsevier, New York, 1983.

168. Sugioka K, Nakano H, Nakano M, Tero-Kubota S and Ikegami Y. Generation of hydroxyl radicals during the enzymatic reductions of the Fe^{3}+-ADP-phosphate-adriamycin and Fe^{3}+-ADP-EDTA systems: Less involvement of hydroxyl radical and a great importance of proposed perferryl ion complexes in lipid peroxidation. *Biochim Biophys Acta* **753**: 411-421, 1983.

169. Koppenol W H. The reaction of ferrous EDTA with hydrogen peroxide: Evidence against hydroxyl radical formation. *Free Rad Biol Med* **1**: 281-285, 1985.

170. Bachur J R, Ming T and Aust S D. Requirement for ferric in initiation of lipid peroxidation by chelated ferrous iron. *Biochem Biophys Res Commun* **111**: 777-784, 1983.

171. Aruoma O I, Halliwell B, Laughton M J, Quinlan G J and Gutteridge J M C. The mechanism of initiation of lipid peroxidation: Evidence against a requirement for an iron (II)-iron (III)-complex. *Biochem J* **258**: 617-620, 1989.

172. Hasegawa K and Patterson L K. Pulse radiolysis studies in model lipid systems: Formation and behavior of peroxy radicals in fatty acids. *Photochem Photobiol* **28**: 817-823, 1978.

173. Sugioka K, Nakano H, Noguchi T, Tuchuga J and Nakano M. Decomposition of unsaturated phospholipid by iron-ADP-adriamycin co-ordination complex. *Biochem Biophys Res Commun* **100**: 1251-1258, 1981.

174. Omar R F, Hasinoff B B, Mejilla F and Rahimtula A D. Mechanism of ochratoxin A-stimulated lipid peroxidation. *Biochem Pharmacol*, 1990 (in press).

175. Smith J E and Moss M O (Eds.). Structure and formation of mycotoxins. In: *Mycotoxins: Formation, Analysis and Significance*, 31-49, 1985.

176. Horton A A and Fairhurst S. Lipid peroxidation and mechanisms of toxicity. *CRC Critical Reviews in Toxicology* **18**: 27-79, 1987.

177. Gutteridge J M C. Lipid peroxidation: Some problems and concepts. In: *Oxygen Radical and Tissue Injury; Proceedings of an Upjohn Symposium* (Halliwell B, Ed.), 9-19, Allen Press, Kansas, 1988.

178. Silverblatt F, Turck M and Bulger R. Nephrotoxicity due to cephaloridine: A light- and electron-microscopic study in rabbits. *J Infect Dis* **122**:33-44, 1970.

179. Atkinson R M, Currie J P, Davis B, Pratt D A H; Sharpe H M and Tomich E G. Acute toxicity of cephaloridine, an antibiotic derived from cephalosporin C. *Toxicol Appl Pharmacol* **8**: 398-406, 1966.

180. Tune B M and Fravert D. Mechanisms of cephaloridine nephrotoxicity, A comparison of cephaloridine and cephaloglycin. *Kidney Int* **18**: 591-600, 1980.

181. Kuo C-H, Maita K, Sleight S D and Hook J B. Lipid peroxidation: A possible mechanism of cephaloridine-induced nephrotoxicity. *Toxicol Appl Pharmacol* **67**: 78-88, 1983.

182. Goldstein R S, Pasino D A, Hewitt W R and Hook J B. Biochemical mechanisms of cephaloridine nephrotoxicity: Time and concentration dependence of peroxidative injury. *Toxicol Appl Pharmacol* **83**: 261-270, 1986.

183. Cojocel C, Hannemann J and Baumann K. Cephaloridine-induced lipid peroxidation initiated by reactive oxygen species as a possible mechanism of cephaloridine nephrotoxicity. *Biochem Biophys Acta* **834**: 402-410, 1985.

184. Cojocel C, Laeschke K H, Inselmann G and Baumann K. Inhibition of cephaloridine-induced lipid peroxidation. *Toxicology* **35**: 295-305, 1985.

185. Bligh EG and Dyer WJ. A rapid method of total lipid extraction and purification. *Can J Biochem* **37**: 911-917, 1959.

186. Boorman G. NTP technical report on the toxicology and carcinogenesis studies of ochratoxin A. NTP TR358, NIH

publication No. 88-2813, 1988.

187. Drummond GS and and Kappas A. The cytochrome P-450 depleted animals: An experimental model for in vivo studies in chemical biology. *Proc Natl Acad Sci* **79**: 2384-2388, 1982.

APPENDIX

OTA analogues were analyzed by TLC and HPLC in comparison to OTA. The R_f values obtained differ a little in absolute values from those published by Steyn et al. (145). However, the order of the R_f values is the same. Difference in R_f values are presumably due to the different TLC plates used.

The various analogues were also checked for their purity by HPLC. Ser-Oα, Pro-Oα and Glu-Oα were judged to be 96.0%, 97.5% and 91.5% pure.

Table A1: R_f value of OTA and its analogues

Sample*	R_f value
OTA	0.55
Oα	0.16
Ser-Oα	0.12
Pro-Oα	0.34
Glu-Oα	0.26

* Samples (5 μl of 25 mM) were applied on TLC plates with fluorescent indicator.

Figure A1. **The HPLC profile of OTA and its analogues.**

A. OTA (2.5 mM) B. Oα (25 mM)

C. Ser-Oα (25 mM) D. Pro-Oα (7 mM)

E. Glu-Oα (7 mM)

All samples were injected in methanol (5 μl of each indicated concentration) into a Perkin Elmer Series 4 Liquid Chromatograph. The column used was Partisil 10 ODS-2. The solvent system consisted of a mixture of a) acetonitrile: methanol (500:500, v/v) 55% and b) 5 mM sodium acetate:acetic acid (500:14, v/v) 45%. The flow rate was 1.5 ml/min and the spectrophotometric detection was performed at 332 nm.

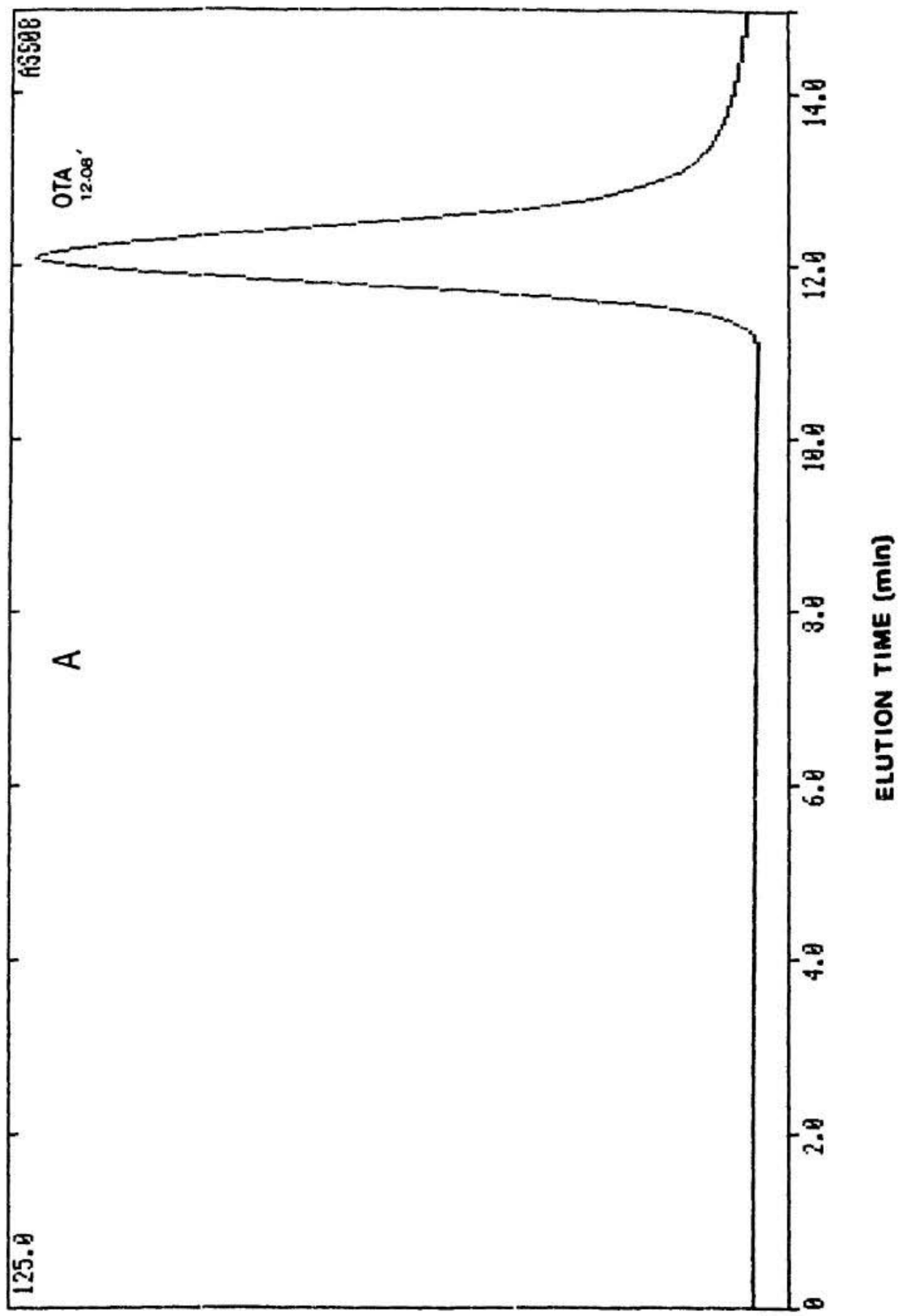
A
OTA
12.08'
125.0
0
2.0
4.0
6.0
8.0
10.0
12.0
14.0
ELUTION TIME (min)
DETECTOR RESPONSE [mvits]

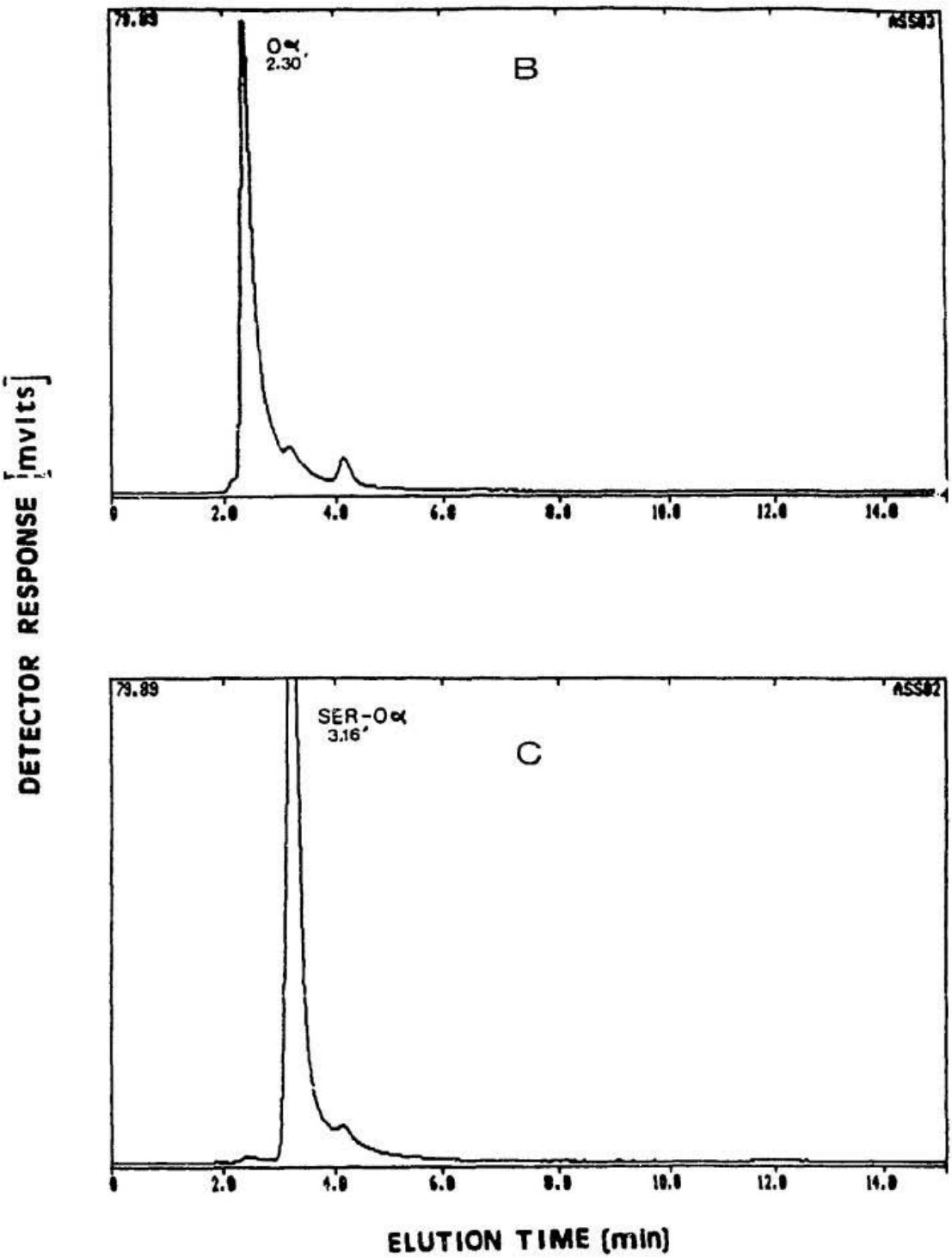
79.89
Oα
2.30'
B
79.89
SER-Oα
3.16'
C
2.0
4.0
6.0
8.0
10.0
12.0
14.0
DETECTOR RESPONSE [mVlts]
ELUTION TIME (min)

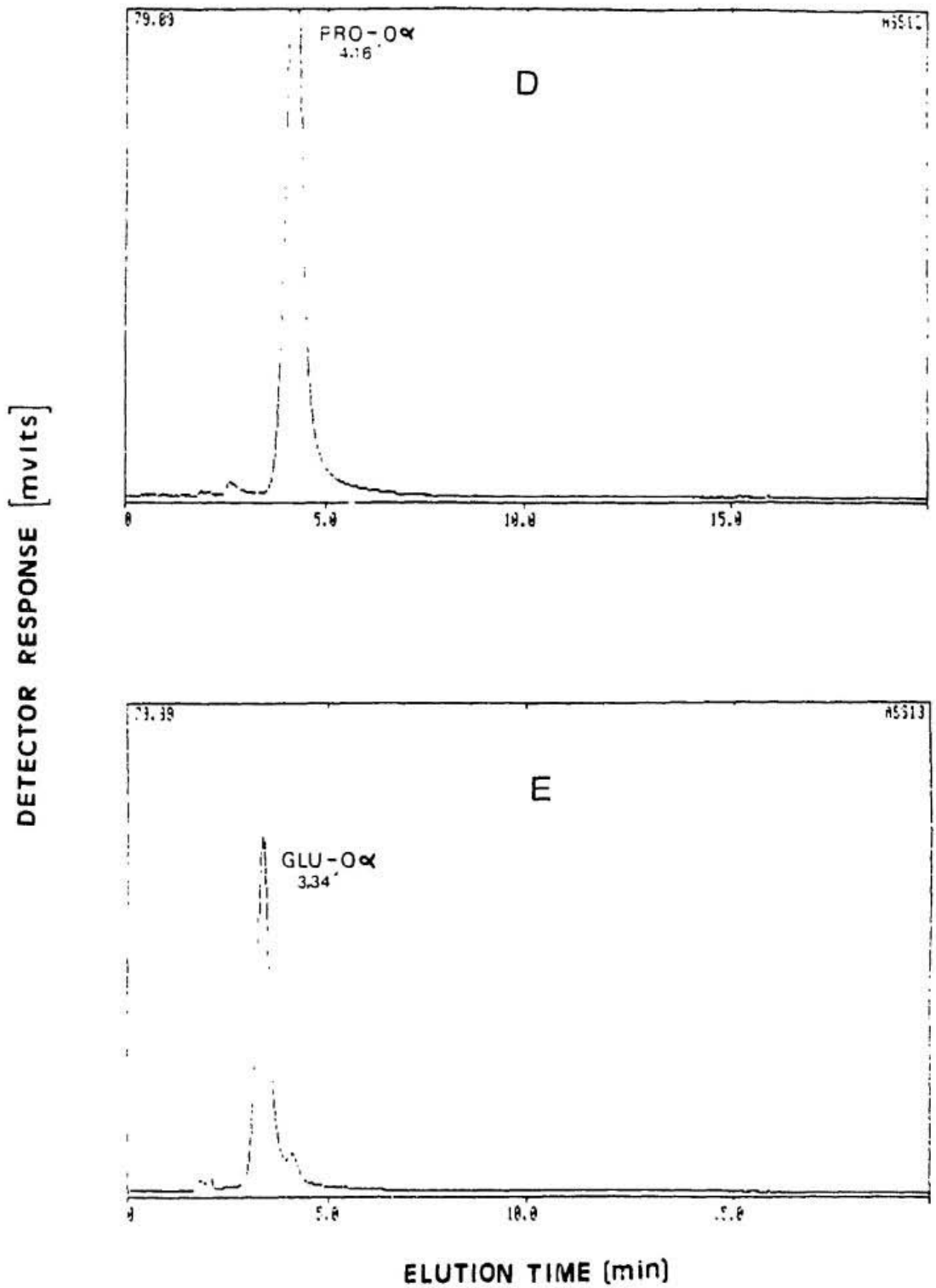
PRO-Oα
4.16
D
E
GLU-Oα
3.34
DETECTOR RESPONSE [mvlts]
ELUTION TIME (min)